

**SELECTIVE FRUCTOSE DEHYDRATION TO  
5-HYDROXYMETHYLFURFURAL BY  
HETEROGENEOUS SULFATED  
CATALYSTS IN DIFFERENT SOLVENTS**

**A Thesis Submitted to  
the Graduate School of Engineering and Sciences of  
İzmir Institute of Technology  
in Partial Fulfillment of the Requirements for the Degree of**

**DOCTOR OF PHILOSOPHY**

**in Chemical Engineering**

**by  
Emre KILIÇ**

**July 2016  
İZMİR**

## ACKNOWLEDGEMENTS

I would like to express my sincere gratitude to my advisor Prof. Dr. Selahattin Yılmaz for his supervision, support and confidence during my studies. Moreover, I would like to thank him for his guidance that broadened my vision and helped me to develop my own perspective. I would like to thank to Dr. T.J. Alexander Nijhuis from Technical University of Eindhoven for his warm hospitality, invaluable collaborations and supervisions during research in Eindhoven. I also would like to thank to Dr. Muhsin Çiftçiođlu for his help and support during my PhD.

I would like to thank to research specialists Rukiye Çiftçiođlu, Nesrin Tatlıdil, Nesrin Gaffarođulları, Özlem Duvarcı, Gülnihal Yelken for the characterization studies presented in this study. I would like to thank the technical staff Ahmet Kurul, Nazil Karaca and Ahmet Köken for their friendship and help during the laboratory works.

I am also grateful to my special friends Mert Tunçer, Hüsnu Arda Yurtsever, Metin Uz, Özgün Deliismail, Okan Akın, Vahide Nuran Mutlu, Dildare Metin, Emre Demirkaya, Sedef Tamburacı, Hasan Örtün for their friendship, understanding, help and supports.

My special thanks go to my wife Hülya AÇAR KILIÇ and my family for their endless support, tolerance and understanding during my PhD.

# ABSTRACT

## SELECTIVE FRUCTOSE DEHYDRATION TO 5-HYDROXYMETHYLFURFURAL BY HETEROGENEOUS SULFATED CATALYSTS IN DIFFERENT SOLVENTS

In the present study, different sulfated ( $\text{SO}_4/\text{ZrO}_2$ ,  $\text{SO}_4/\text{SiO}_2$ ,  $\text{SO}_4/\text{AC}$ ,  $\text{SO}_4/\text{TiO}_2\text{SiO}_2$  and  $\text{SO}_4/\text{Ti-SBA-15}$ ) and zirconium sulfate loaded ( $\text{ZrSO}_4/\text{SiO}_2$  and  $\text{ZrSO}_4/\text{AC}$ ) catalysts were prepared and characterized. Effect of sulfur content (2.5, 3.0 and 3.5 wt. %) in  $\text{SO}_4/\text{ZrO}_2$ , effect of Ti content (2 and 6 wt. %) in  $\text{SO}_4/\text{TiO}_2\text{SiO}_2$  and  $\text{SO}_4/\text{Ti-SBA-15}$ , also La incorporation in to  $\text{SO}_4/\text{TiO}_2\text{SiO}_2$  and  $\text{SO}_4/\text{Ti-SBA-15}$  were investigated.

Prepared catalysts were tested in fructose dehydration using dimethylsulfoxide (DMSO), water and biphasic aqueous solvents which were water-MIBK and water-MIBK-butanol. Effect of reaction temperature (110, 160 and 200 °C) and effect of fructose/catalyst weight ratio ( $W_{\text{Fr}}/W_{\text{cat}} = 0.5, 1.0$  and  $2.0$ ) on activity and selectivity were investigated. Activity tests were performed in a batch reactor under  $\text{N}_2$  atmosphere. Reusability tests were carried out up to 4 times.

Sulfated catalysts showed different activities. However, there was sulfur leaching in all of them except  $\text{SO}_4/\text{TiO}_2\text{SiO}_2$  and  $\text{SO}_4/\text{Ti-SBA-15}$ . This was due to chelating bidentate bond formation between S, Ti and S. Sulfur leaching was also observed over zirconium sulfate loaded catalysts. Acidity of the catalysts increased with sulfur and Ti content; and also La addition. Sulfation created Brønsted acid sites.

The most active, selective and stable catalyst was found to be  $\text{SO}_4/\text{La-TS-6}$  (95 % HMF selectivity at 58 % fructose conversion at 110 °C) in DMSO. Testing of this catalyst in water gave high amount of byproducts. Introducing second phase (MIBK) to water, improved HMF selectivity significantly (up to 78 %) and reduced conversion (by 7 %). Fructose dehydration kinetics was also investigated over this catalyst in water-MIBK-butanol (the most selective environmental benign solvent). Selectivity to HMF increased with reaction temperature up to 160 °C, above which it dropped. Increase in  $W_{\text{Fr}}/W_{\text{cat}}$  from 0.5 to 2.0, reduced the selectivity to HMF from 98 to 82 % at high fructose conversions (~90 %). Reaction was found to be 1<sup>st</sup> order in fructose concentration.

## ÖZET

### FRUKTOZ'UN FARKLI ÇÖZÜCÜLER İÇİNDE 5-HİDROKSİMETİLFURFURAL'A SÜLFATLANMIŞ HETEROJEN KATALİZÖRLERLE SEÇİCİ DEHİDRASYONU

Bu çalışmada, farklı sülfatlanmış ( $\text{SO}_4/\text{ZrO}_2$ ,  $\text{SO}_4/\text{SiO}_2$ ,  $\text{SO}_4/\text{AC}$ ,  $\text{SO}_4/\text{TiO}_2\text{SiO}_2$  ve  $\text{SO}_4/\text{Ti-SBA-15}$ ) ve zirkonyum sülfat yüklenmiş ( $\text{ZrSO}_4/\text{SiO}_2$  ve  $\text{ZrSO}_4/\text{AC}$ ) katalizörler hazırlanmış ve karakterizasyonları yapılmıştır.  $\text{SO}_4/\text{ZrO}_2$  içindeki sülfür miktarının (2.5, 3.0 ve 3.5 ağırlık %),  $\text{SO}_4/\text{TiO}_2\text{SiO}_2$  ve  $\text{SO}_4/\text{Ti-SBA-15}$  içindeki Ti miktarının (2 ve 6 ağırlık %), ayrıca  $\text{SO}_4/\text{TiO}_2\text{SiO}_2$  ve  $\text{SO}_4/\text{Ti-SBA-15}$  içine La eklenmesinin etkisi incelenmiştir.

Hazırlanan katalizörler fruktoz dehidrasyonunda dimetilsülfoksit (DMSO), su ve çift fazlı sulu çözücüler (su-MIBK ve su-MIBK-bütanol) kullanılarak test edilmiştir. Reaksiyon sıcaklığının (110, 160 ve 200 °C) ve fruktoz/katalizör ağırlık oranının ( $W_{\text{Fr}}/W_{\text{cat}} = 0.5, 1.0$  ve  $2.0$ ) aktivite ve seçicilik üzerine etkisi incelenmiştir. Aktivite testleri kesikli reaktör içinde azot ortamında gerçekleştirilmiştir. Tekrar kullanılabilirlik testleri 4 kereye kadar yapılmıştır.

Sülfatlanmış katalizörler farklı aktivite sonuçları göstermiştir. Ancak,  $\text{SO}_4/\text{TiO}_2\text{SiO}_2$  ve  $\text{SO}_4/\text{Ti-SBA-15}$  dışındaki tüm sülfatlanmış katalizörlerde sülfür liçi görülmüştür. Elde edilen bu sonuç şelatlayıcı bidentate bağların oluşumuna bağlanmıştır. Zirkonyum sülfat yüklü katalizörlerde de sülfür liçi gözlemlenmiştir. Katalizörlerin asitliği sülfür, Ti miktarı ve La eklemesiyle artmıştır. Sülfatlama işlemi Brønsted tipi asit merkezleri oluşturmuştur.

DMSO içinde 110 °C'de en aktif, seçici ve kararlı katalizör  $\text{SO}_4/\text{La-TS-6}$  (% 58 fruktoz dönüşümü ve % 95 HMF seçiciliği) olarak bulunmuştur. Bu katalizör ile su içinde yapılan testlerde yüksek miktarda yan ürün oluşumu gözlemlenmiştir. Su çözücüsüne ikinci fazın (MIBK) eklenmesi seçiciliği önemli derecede (%78'e kadar) arttırmış; aktivitede ise az miktarda (7 %) düşüşe neden olmuştur. Fruktoz dehidrasyon kinetiği su-MIBK-bütanol (en seçici ve çevre dostu çözücü) içinde gerçekleştirilmiştir. Sıcaklığın 160 °C'ye çıkarılması seçiciliği arttırmıştır.  $W_{\text{Fr}}/W_{\text{cat}}$  oranının 0,5'ten 2.0'a çıkarılması HMF' ye seçiciliğini yüksek fruktoz dönüşümlerinde (~%90) % 98'den % 82'ye düşürmüştür. Reaksiyon derecesi birinci derece olarak belirlenmiştir.

# TABLE OF CONTENTS

LIST OF FIGURES.....	ix
LIST OF TABLES.....	xiii
CHAPTER 1. INTRODUCTION.....	1
CHAPTER 2. FRUCTOSE DEHYDRATION TO 5-HYDROXYMETHYLFURFURAL.....	4
2.1. Biomass.....	4
2.2. Reaction Mechanism of Fructose Dehydration to HMF.....	7
2.3. Kinetics of Fructose Dehydration.....	11
CHAPTER 3. FRUCTOSE DEHYDRATION STUDIES.....	13
3.1. Homogeneous Catalysts.....	13
3.2. Heterogeneous Catalysts.....	14
3.2.1. Phosphated Oxides, Sulfated Oxides and Mixed Oxides.....	14
3.2.2. Sulfated and ZrSO <sub>4</sub> Loaded Mesoporous Supports.....	19
3.2.3. Resin Catalysts.....	21
3.2.4. Heteropoly Acids.....	21
3.3. Solvent Effects.....	23
3.3.1. Single Phase Solvents.....	23
3.3.2. Multiphase Solvents.....	25
3.4. Effect of Reaction Parameters.....	26
3.5. Literature Outcomes and Statement of Work.....	28
CHAPTER 4. EXPERIMENTAL STUDY.....	31
4.1. Materials.....	31

4.2. Catalyst Preparation.....	32
4.2.1. Sulfated Zirconia, Silica and AC Preparation.....	32
4.2.2. Silica and AC Supported Zirconium Sulfate Preparation.....	33
4.2.3. Titania-Silicate and Sulfated Titania-Silicate Preparation.....	34
4.2.4. Ti-SBA-15 and Sulfated Ti-SBA-15 Preparation.....	35
4.2.5. Homogeneous Catalysts Studied.....	35
4.3. Characterization of the Catalysts Prepared.....	36
4.3.1. X-Ray Diffraction (XRD).....	36
4.3.2. N <sub>2</sub> Adsorption/Desorption Tests (BET).....	36
4.3.3. Temperature Program Desorption (TPD).....	36
4.3.4. Fourier Transform Infrared Spectroscopy (FT-IR).....	37
4.3.5. X-Ray Fluorence Spectroscopy (XRF).....	37
4.4. Fructose Dehydration Tests.....	37
 CHAPTER 5. RESULTS AND DISSCUSSIONS.....	 39
5.1. Homogeneous Catalysts.....	39
5.1.1. Activities of Homogeneous Catalysts in DMSO.....	40
5.2. Sulfated Zirconia Catalysts.....	44
5.2.1. Characterization of the Sulfated Zirconia Catalysts.....	44
5.2.2. Activities of the Sulfated Zirconia Catalysts in DMSO.....	47
5.3. Sulfated and Zirconium Sulfate Loaded Catalysts.....	52
5.3.1. Characterization of Sulfated and Zirconium Sulfated Loaded Catalysts.....	52
5.3.2. Activities of the Zirconium Sulfate Loaded Catalysts in DMSO.....	54
5.3.3. Activities of the Different Sulfated Catalysts in DMSO.....	58
5.4. Titania-Silicate Based Catalysts.....	63
5.4.1. Characterization of Titania-Silicate Based Catalysts.....	63
5.4.2. Activities of Titania-Silicate Based Catalysts in DMSO.....	66
5.5. Sulfated Ti-SBA-15 Based Catalysts.....	73

5.5.1. Characterization of Sulfated Ti-SBA-15 Based Catalysts.....	73
5.5.2. Activities of Sulfated Ti-SBA-15 Based Catalysts in DMSO.....	75
5.6. Activities of SO <sub>4</sub> /La-TS-6 in Water and Water-MIBK.....	80
5.7. Fructose Dehydration Kinetics over SO <sub>4</sub> /La-TS-6 in Water-Butanol-MIBK.....	84
5.7.1. Effect of Reaction Temperature.....	84
5.7.2. Effect of Fructose/Catalysts Ratio.....	88
CHAPTER 6. CONCLUSIONS.....	94
REFERENCES.....	96

# LIST OF FIGURES

<u>Figure</u>	<u>Page</u>
Figure 2.1. Transesterification of triglycerides with methanol for FAME production.....	4
Figure 2.2. Molecular structure of the two main components of starch.....	5
Figure 2.3. Lignocellulosic biomass conversion to monosaccharides and valuable chemicals.....	5
Figure 2.4. Structural units of lignin.....	6
Figure 2.5. Structure of cellulose.....	6
Figure 2.6. Valuable chemicals from HMF.....	7
Figure 2.7. Possible reaction mechanisms and pathways for biomass conversion to HMF.....	8
Figure 2.8. Proposed reaction mechanism for fructose dehydration to HMF in DMSO.....	9
Figure 2.9. Forms of the fructose.....	10
Figure 2.10. Distribution of fructose tautomers in different solvents.....	11
Figure 2.11. Proposed reaction pathway for fructose dehydration.....	12
Figure 3.1. Chelating bidentate bonds in titania-silicates.....	17
Figure 3.2. Keggin structure in heteropoly acids.....	22
Figure 3.3. Structural analogies of DMSO and acetone.....	26
Figure 5.1. Product distribution without using a catalyst at 110 °C in DMSO.....	40
Figure 5.2. Product distribution over homogeneous H <sub>2</sub> SO <sub>4</sub> at 110 °C in DMSO.....	41
Figure 5.3. Product distribution over homogeneous H <sub>3</sub> PO <sub>4</sub> at 110 °C in DMSO.....	41
Figure 5.4. Product distribution over homogeneous HCl at 110 °C in DMSO.....	42
Figure 5.5. Fructose conversions over homogeneous catalysts and without a catalyst at 110 °C in DMSO.....	43
Figure 5.6. HMF selectivities over homogeneous catalysts and without a catalyst at 110 °C in DMSO.....	43
Figure 5.7. XRD patterns of different sulfated zirconia catalysts.....	45
Figure 5.8. NH <sub>3</sub> -TPD profiles of the sulfated zirconia catalysts.....	46
Figure 5.9. FT-IR spectra of the sulfated zirconia catalysts after pyridine adsorption.....	47
Figure 5.10. Product distribution obtained over SO <sub>4</sub> /ZrO <sub>2</sub> -2.5 at 110 °C in DMSO.....	48

Figure 5.11. Product distribution obtained over SO <sub>4</sub> /ZrO <sub>2</sub> -3.0 at 110 °C in DMSO.....	48
Figure 5.12. Product distribution obtained over SO <sub>4</sub> /ZrO <sub>2</sub> -3.5 at 110 °C in DMSO.....	49
Figure 5.13. Fructose conversions over sulfated zirconia catalysts in DMSO at 110 °C.....	50
Figure 5.14. HMF selectivities over sulfated zirconia catalysts in DMSO at 110 °C.....	50
Figure 5.15. Reusability of sulfated zirconia catalysts.....	51
Figure 5.16. NH <sub>3</sub> -TPD profiles of sulfated catalysts.....	53
Figure 5.17. FT-IR spectra of sulfated catalysts after pyridine adsorption.....	54
Figure 5.18. Product distribution obtained over ZS/AC at 110 °C in DMSO.....	55
Figure 5.19. Product distribution obtained over ZS/SiO <sub>2</sub> at 110 °C in DMSO.....	55
Figure 5.20. Fructose conversions over ZS/SiO <sub>2</sub> and ZS/AC at 110 °C in DMSO.....	56
Figure 5.21. HMF selectivities over ZS/SiO <sub>2</sub> and ZS/AC at 110 °C in DMSO.....	56
Figure 5.22. Reusability of zirconium sulfate loaded catalysts.....	57
Figure 5.23. Product distribution obtained over SO <sub>4</sub> /TS-6 at 110 °C in DMSO.....	58
Figure 5.24. Product distribution obtained over SO <sub>4</sub> /Ti-SBA-6 at 110 °C in DMSO.....	59
Figure 5.25. Product distribution obtained over SO <sub>4</sub> /SiO <sub>2</sub> at 110 °C in DMSO.....	59
Figure 5.26. Product distribution obtained over SO <sub>4</sub> /AC at 110 °C in DMSO.....	60
Figure 5.27. Fructose conversions over different sulfated catalysts at 110 °C in DMSO.....	61
Figure 5.28. HMF selectivities over different sulfated catalysts at 110 °C in DMSO.....	61
Figure 5.29. Reusability results of sulfated catalysts.....	63
Figure 5.30. NH <sub>3</sub> -TPD profiles of titania-silicate based catalysts.....	65
Figure 5.31. FT-IR spectra of titania silica catalysts after pyridine adsorption.....	66
Figure 5.32. Product distribution of over TS-2 at 110 °C in DMSO.....	67
Figure 5.33. Product distribution of over TS-6 at 110 °C in DMSO.....	67
Figure 5.34. Product distribution of over SO <sub>4</sub> /TS-2 at 110 °C in DMSO.....	68
Figure 5.35. Product distribution of over SO <sub>4</sub> /TS-6 at 110 °C in DMSO.....	68
Figure 5.36. Product distribution of over SO <sub>4</sub> /La-TS-6 at 110 °C in DMSO.....	69
Figure 5.37. Fructose conversions over titania silicates at 110 °C in DMSO.....	70

Figure 5.38. HMF selectivities over titania silicates in DMSO at 110 °C.....	71
Figure 5.39. Reusability tests of titania silicates.....	72
Figure 5.40. NH <sub>3</sub> -TPD profiles of the sulfated Ti-SBA-15 catalysts.....	74
Figure 5.41. FT-IR spectra of sulfated Ti-SBA-15 catalysts after pyridine adsorption.....	75
Figure 5.42. Product distribution over SO <sub>4</sub> /Ti-SBA-2.....	76
Figure 5.43. Product distribution over SO <sub>4</sub> /Ti-SBA-6.....	76
Figure 5.44. Product distribution over SO <sub>4</sub> /La-Ti-SBA-6.....	77
Figure 5.45. Fructose conversions over sulfated Ti-SBA-15 catalysts at 110 °C in DMSO.....	78
Figure 5.46. Selectivities to HMF over sulfated Ti-SBA catalysts at 110 °C in DMSO.....	79
Figure 5.47. Reusability tests of sulfated Ti-SBA-15 catalysts.....	80
Figure 5.48. Product distribution over SO <sub>4</sub> /La-TS-6 at 110 °C in water.....	81
Figure 5.49. Product distribution over SO <sub>4</sub> /La-TS-6 at 110 °C in water-MIBK.....	81
Figure 5.50. Product distribution over SO <sub>4</sub> /La-TS-6 at 110 °C in water-MIBK-butanol.....	82
Figure 5.51. Fructose conversions in different solvents over SO <sub>4</sub> /La-TS-6 at 110 °C.....	83
Figure 5.52. Selectivities to HMF in different solvents over La-SO <sub>4</sub> /TS-6 at 110 °C.....	84
Figure 5.53. Product distribution at 110 °C over SO <sub>4</sub> /La-TS-6 in water-MIBK-butanol.....	85
Figure 5.54. Product distribution at 160 °C over SO <sub>4</sub> /La-TS-6 in water-MIBK-butanol.....	85
Figure 5.55. Product distribution at 200 °C over SO <sub>4</sub> /La-TS-6 in water-MIBK-butanol.....	86
Figure 5.56. Fructose conversions at 110, 160 and 200 °C over SO <sub>4</sub> /La-TS-6 in water-butanol- MIBK .....	87
Figure 5.57. Selectivities to HMF at 110, 160 and 200 °C over SO <sub>4</sub> /La-TS-6 in water-butanol- MIBK.....	87
Figure 5.58. Reusability of the SO <sub>4</sub> /La-TS-6 in water-butanol-MIBK at 160 °C with fructose/catalyst ratio: 1 .....	88
Figure 5.59. Product distribution of SO <sub>4</sub> /La-TS-6 in water-butanol-MIBK at 160 °C for W <sub>Fr</sub> /W <sub>cat</sub> :0.5.....	89

Figure 5.60. Product distribution of SO <sub>4</sub> /La-TS-6 in water-butanol-MIBK at 160 °C for W <sub>Fr</sub> /W <sub>cat</sub> :1.....	89
Figure 5.61. Product distribution of SO <sub>4</sub> /La-TS-6 in water-butanol-MIBK at 160 °C for W <sub>Fr</sub> /W <sub>cat</sub> :2.....	90
Figure 5.62. Fructose conversions for W <sub>Fr</sub> /W <sub>cat</sub> : 0.5, 1 and 2 over SO <sub>4</sub> /La-TS-6 in water-butanol-MIBK at 160 °C.....	91
Figure 5.63. Selectivities to HMF for W <sub>Fr</sub> /W <sub>cat</sub> : 0.5, 1 and 2 over SO <sub>4</sub> /La-TS-6 in water-butanol-MIBK at 160 °C.....	91
Figure 5.64. HMF yield over SO <sub>4</sub> /La-TS-6 in water-butanol-MIBK at 160 °C with fructose/catalyst for W <sub>Fr</sub> /W <sub>cat</sub> : 0.5, 1, 2.....	92
Figure 5.65. Logarithmic change of fructose concentrations with reaction time at 110 and 200 °C over SO <sub>4</sub> /La-TS-6 in water-butanol-MIBK at W <sub>Fr</sub> /W <sub>cat</sub> :1.....	93

## LIST OF TABLES

<b><u>Table</u></b>	<b><u>Page</u></b>
Table 2.1. Estimated reaction rate constants for fructose dehydration.....	12
Table 4.1. List of the chemicals used.....	31
Table 4.2. The labels of the sulfated zirconia catalysts.....	33
Table 4.3. The labels of the zirconium sulfate loaded catalysts.....	33
Table 4.4. The labels of different titania silicate catalysts prepared.....	34
Table 4.5. Different sulfated Ti-SBA-15 catalysts prepared.....	35
Table 5.1. Different sulfated catalysts prepared.....	39
Table 5.2. Textural properties of sulfated zirconia catalysts.....	45
Table 5.3. Sulfur leaching from sulfated zirconia catalysts.....	51
Table 5.4. Textural properties of sulfated catalysts.....	52
Table 5.5. Sulfur leaching from zirconium sulfate loaded catalysts.....	57
Table 5.6. Sulfur leaching from different sulfated catalysts.....	62
Table 5.7. Textural properties of titania silica catalysts.....	64
Table 5.8. Optimum HMF yields over the catalysts prepared.....	71
Table 5.9. Sulfur leaching from titania-silicates.....	72
Table 5.10. Textural properties of sulfated catalysts.....	73
Table 5.11. Sulfur leaching from sulfated Ti-SBA-15 catalysts.....	79
Table 5.12. Kinetic parameters of fructose dehydration.....	92

# CHAPTER 1

## INTRODUCTION

Increase in energy demand around the world, diminishing fossil fuel reserves, and CO<sub>2</sub> emission problems force people to find alternative and sustainable resources to produce valuable chemicals. Production of these chemicals from biomass is alternative and environmentally friendly process compared to petroleum based process. 5-hydroxymethylfurfural (HMF) is known as “Top Value Added Chemicals” in the US Department of Energy and top building-block chemicals. It is the key intermediate in order to convert the biomass to valuable chemicals such as polymers, bio-fuels, bulk chemicals (Tong et al., 2011; Guo et al., 2012). Its production by dehydration of sugars is considered to be the most promising way (Yang et al., 2010; Wang et al., 2011; Tong et al., 2010; Cao et al., 2011). Sugars such as xylose, glucose and fructose have been investigated and it has been found that HMF production from fructose and glucose is the most economical and effective way.

Glucose is cheaper but provides lower HMF yields than fructose due to its stable ring structure. Besides, glucose conversion to HMF includes two different steps, such as; isomerization to fructose over basic sites and dehydration to HMF over acid sites (Rosatella et al., 2011). Fructose dehydration is also reported as 40 times faster than glucose dehydration (Tong et al., 2011; Guo et al., 2012, Juan et al., 2007; Caratzoulas et al., 2011; Cao et al., 2011).

Fructose dehydration occurs on the acid sites of the catalyst. Nature, concentration and strength of the acid sites of the catalyst affect the product distribution significantly. It is also reported that Lewis acid sites are responsible for fructose conversion where Brønsted sites are responsible for HMF formation (Weingarten et al., 2011).

Various acid catalysts were investigated for fructose dehydration from homogeneous (ionic liquids, mineral and organic acids) to the different heterogeneous ones. Due to the product contamination, difficulties in separation and recovery problems, heterogeneous catalyst are generally preferred (Carniti et al., 2011; Wang et al., 2011). Heterogeneous solid acid catalysts used in fructose dehydration include resins, metal

sulfates, metal phosphates, heteropolyacids, zeolites and niobic acid based catalysts and etc. However, solid acid catalysts did not provide satisfactory yields in aqueous solvents. Some of heterogeneous catalysts have low stabilities due to leaching & some of them are not selective and promote side product formation such as formic acid and levulinic acid. Thus, researchers are trying to find a stable, active and selective catalyst for fructose dehydration to HMF. (Wang et al., 2011; Qi et al., 2009; Carniti et al., 2011; Guo et al., 2012; Ordonsky et al., 2012; Fan et al., 2011).

Sulfur containing catalysts have been found to be very active for fructose dehydration (Qi et al., 2009; Wang et al., 2011; Guo et al., 2012). As sulfur ions and sulfate groups create Brønsted and strong acid sites when loaded on support. The supports used include such as iron oxide, alumina, titania and zirconia. Zirconia is known as the good support for sulfates as it strongly interacts with sulfur ions.

Sulfated zirconia is known as a very acidic catalyst for many reactions. It has Brønsted sites which are selective sites for fructose dehydration (Qi et al., 2009). However, low surface area of the sulfated zirconia limits its activity. Surface area may be enhanced by loading them on to mesoporous support. Sulfate ions may also be loaded onto a carbon based support. Sulfated catalysts are very active and can be used without leaching problems in polar aprotic solvents, such as DMSO, acetone and dimethylamide (Guo et al., 2012). On the other hand, sulfates were leached in alcohols or in water (Yadav et al., 2004; Juan et al., 2007).

In recent years, mixed oxides, especially titania-silicates became important as acidic catalyst. They are prepared by several methods such as sol-gel technique, precipitation and impregnation. Sol-gel synthesized titania-silicates have very stable structure, super acidic centers and regular mesopores. However, they have merely Lewis acid sites. Brønsted sites which are selective sites for HMF formation are created by sulfation of these titania silicates. Ti in these mixed oxides prevents the leaching of sulfur in alcohol and water as well. (Li et al., 2013; Sharma et al., 2012).

HMF yield is also affected by the solvent type. Solvents ranging from environmentally benign alcohols and water to the high boiling point polar aprotic solvents (DMSO, dimethylamide) have been investigated. High yields of HMF have been achieved by using high boiling point solvents such as DMSO and DMA. (Guo et al., 2012). Nevertheless, these group solvents require high energy consumption during separation. Aqueous solvents are cheaper but increase the rehydration of HMF to

levulinic and formic acids. Biphasic solvent composed of organic-aqueous phases can be used to reduce rehydration rate. HMF formed is transferred to organic phase before rehydrated (Ordonsky et al., 2012).

Under the view of above discussions, in this study, it was aimed to prepare sulfated heterogeneous catalysts including  $\text{SO}_4/\text{ZrO}_2$ ,  $\text{SO}_4/\text{AC}$ ,  $\text{SO}_4/\text{SiO}_2$ ,  $\text{ZrSO}_4/\text{AC}$ ,  $\text{ZrSO}_4/\text{SiO}_2$ ,  $\text{SO}_4/\text{TiO}_2\text{-SiO}_2$  and  $\text{SO}_4/\text{Ti-SBA-15}$ . And also effects of different titania content and La incorporation to  $\text{SO}_4/\text{TiO}_2\text{-SiO}_2$  catalyst were investigated. In addition, non-sulfated catalysts ( $\text{TiO}_2\text{-SiO}_2$ ) with different titania contents were tested to evaluate role of catalyst acidity nature on the reaction. Homogeneous catalysts ( $\text{HCl}$ ,  $\text{H}_3\text{PO}_4$ , and  $\text{H}_2\text{SO}_4$ ) were also tested for comparison purpose.

Moreover, the role of solvent on dehydration for the most active, selective and stable catalyst was investigated. Solvents studied were water and DMSO. Different biphasic solvents systems (Water-MIBK and Water-MIBK-butanol) were also studied to investigate the effects of extracting phase addition.

The activities and selectivities obtained for the prepared catalysts were compared. Stability tests were also pursued.

The reaction kinetics was studied by varying the reaction temperature (110, 160 and 200 °C) and fructose/catalyst weight ratio (0.5, 1 and 2).

## CHAPTER 2

### FRUCTOSE DEHYDRATION TO 5-HYDROXYMETHYLFURFURAL

#### 2.1. Biomass

Biomass is a renewable raw material on the earth; include vegetable oils, starches and sugars from plants. Vegetable oils are triglyceride esters of fatty acids, can be used for the production of fuels. They can be converted to fatty acid methyl esters (bio-diesel) from transesterification with alcohols (Perego et al., 2011). The general reaction scheme of transesterification of triglycerides with methanol is given in Figure 2.1.

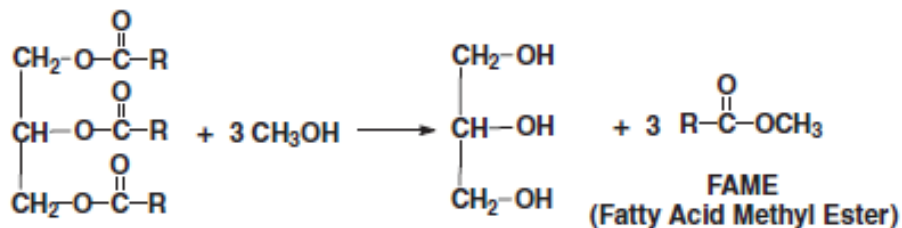


Figure 2.1. Transesterification of triglycerides with methanol for FAME production  
(Source: Perego et al., 2011).

Starch is one of the most abundant polysaccharides in nature; also obtained from plants. It includes two main components: amylose and amylopectin; and their amounts change depending on the starch source. Starches contain commonly 15-35 % amylose. Amylose is linear unbranched chains of glucopyranosyl units, where amylopectin includes branched glucan units (Perego et al., 2011). The molecular structures of starch components are given in Figure 2.2.

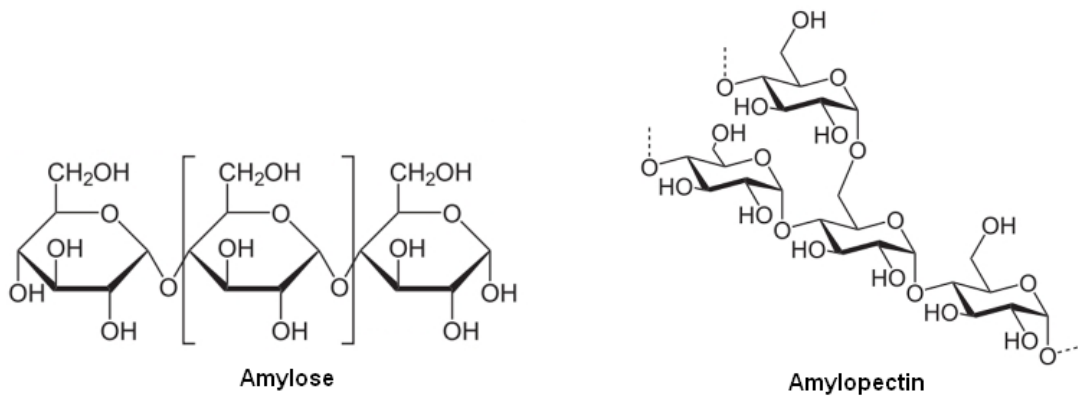


Figure 2.2. Molecular structure of the two main components of starch.

Sugar based biomass consist of lignin, cellulose and hemicelluloses which are converted to hexoses and pentoses, and subsequently to bio-fuels and alcohols (Figure 2.3).

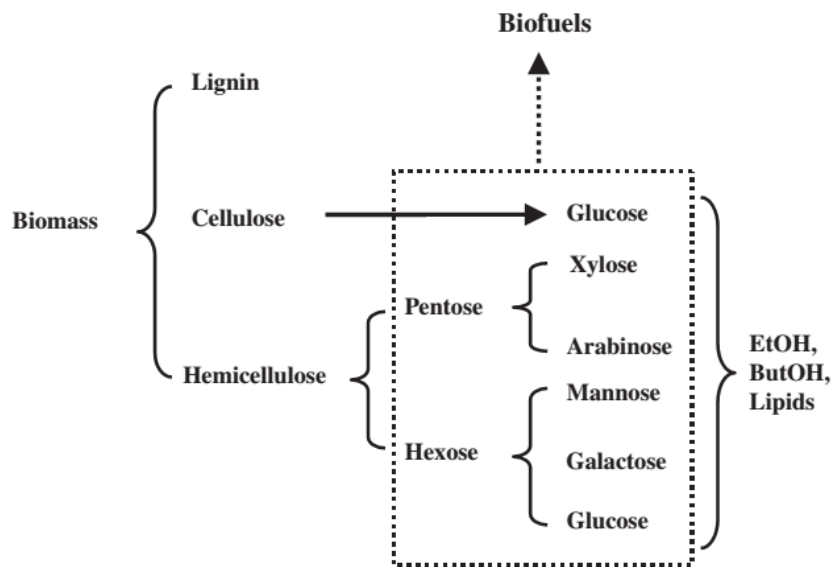


Figure 2.3. Lignocellulosic biomass conversion to monosaccharides and valuable chemicals (Source: Perego et al., 2011).

Generally, 10-25 wt. % of biomass is composed of lignin. Lignin is an organic heteropolymer consists of different alcohol monomers which are coniferyl alcohol, sinapyl alcohol and coumparyl alcohol. It is formed by the polymerization of these monomers. Typical structural units of lignin are given in Figure 2.4.

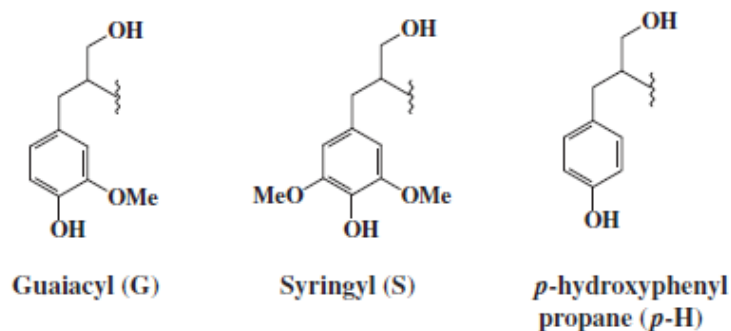


Figure 2.4. Structural units of lignin  
(Source: Perego et al., 2011).

Cellulose (Figure 2.5) is a crystalline unbranched linear polysaccharide. It includes  $\beta$ -1,4-linkages of glucopyranose monomers and it is commonly formed by 5000-7000 sugar units. The general molecular formula of cellulose is reported as:  $(C_6H_{10}O_5)_n$ . Its structure is given in Fig. 5. Cellulose is obtained from wood and cotton. It can be converted to valuable chemicals via hydrolysis, and to the glucose at high temperatures and low pH values. Glucose could be also used as a starting material to produce its isomer fructose. On the other hand, hemicellulose is branched amorphous heteropolymer. It can be broken down to several sugars such as xylose, glucose and galactose. Hemicellulose was reported to have shorter chains than cellulose (~200 sugar units), thus they are hydrolyzed to monosaccharides, easier than cellulose (Perego et al., 2011).

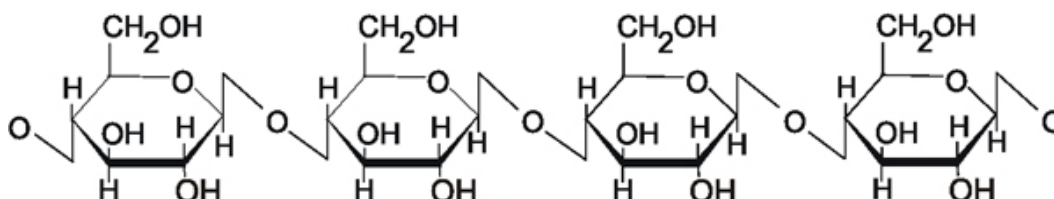


Figure 2.5. Structure of cellulose.

Monosaccharides in nature generally include six-carboned monosaccharides (hexoses). Among the hexoses transformation of fructose and glucose are the most convenient way for the production of valuable chemicals. They can be converted into furan derivatives in many steps, such as hydrolysis, dehydration, isomerization, hydrogenation and oxidation (Chedda et al., 2007). These derivatives include HMF, 2,5-diformylfuran (2,5-DFF), 2,5-furandicarboxylic acid (2,5-FDCA), 2,5-bis(hydroxymethyl)-furan (2,5-BHF) and 2,5-DMF. These furanic products are used for the production of valuable chemicals. Among these furans, HMF produces from the

dehydration of glucose and fructose, are called as one of the most important renewable platform chemical (Tong et al., 2010). It is also used as a starting material to produce some bulk chemicals, monomers and solvents as given in Figure 2.6.

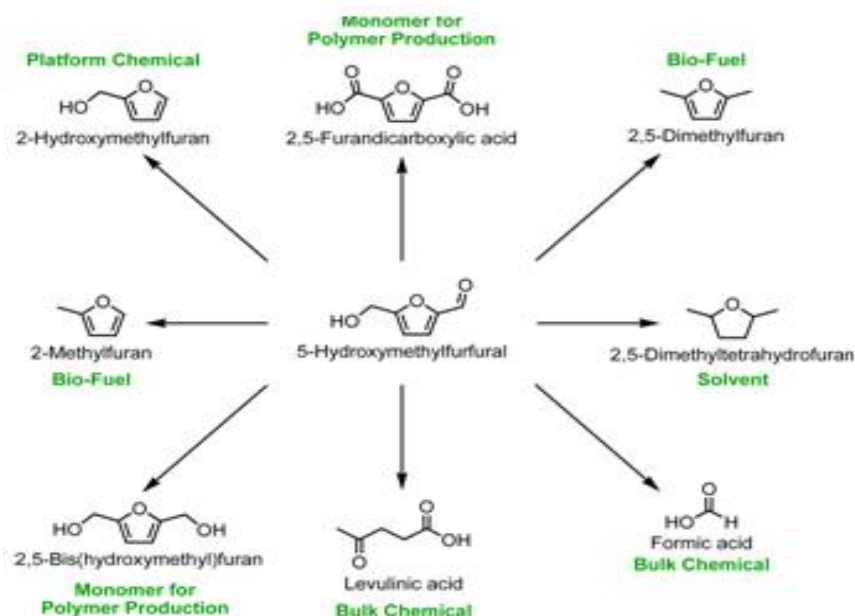


Figure 2.6. Valuable chemicals from HMF.

## 2.2. Reaction Mechanism of Fructose Dehydration to HMF

The general reaction pathway and mechanism for HMF production from polysaccharides is given in Figure 2.7. Biomass conversion starts with acid hydrolysis of polysaccharides to monosaccharides as seen in Figure 2.7. Parallel and series reactions, isomerization reactions between glucose and fructose, dehydration of fructose to HMF are also shown in Figure 2.7. According to the many authors (Li et al., 2010; Antal et al., 1990; Amarasekara et al., 2005), dehydration of fructose carries out through one of two possible pathways. One of them is acyclic route including reaction between open chain molecules. The other one is cyclic route, in which only cyclic forms of the fructose and intermediates play a role in the reaction (transformation of ring).

Cyclic and acyclic pathways include three dehydration steps and finally HMF forms. In each step, hydrogen bonded OH ions (water molecules) in the fructose are protonated by acidic reaction medium, and then water molecules leave the structure of the sugar (Chedda et al., 2007).

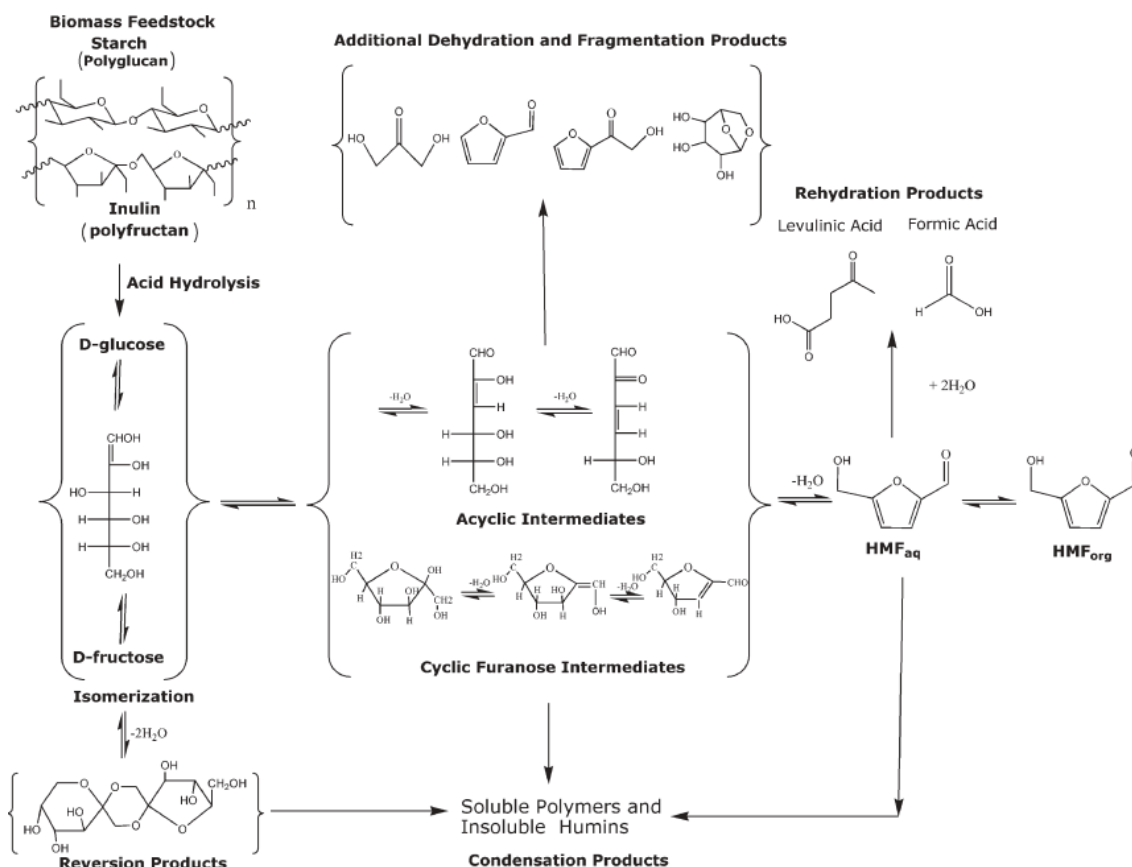


Figure 2.7. Possible reaction mechanisms and pathways for biomass conversion to HMF (Source: Chedda et al., 2007).

Caratzoulas et al. (2011) stated that fructose dehydration proceeds mostly through cyclic pathway since acyclic route involves extremely higher activation barriers than cyclic one. Antal et al. (1990) also experimentally proved the impossibility of the acyclic mechanism. They showed that 5-HMF formation proceeds completely via cyclic intermediates. This was attributed to lower activation energy of cyclic pathway and the facile conversion of intermediate enol (2,5-anhydro-dmannose) to HMF.

Three different side reaction pathway was proposed by Qi et al. (2009) which are (1) Rehydration of HMF to levulinic acid and formic acid from the reaction of HMF with water in the medium, (2) HMF ethers may be formed over the basic sites and unselective sites, (3) Self and cross polymerization of HMF into soluble polymers and insoluble humins (Reaction between fructose and HMF or fructose collisions).

Two different type of acid sites are responsible for HMF formation mechanism. These are Brønsted and Lewis acid sites (Asghari et al., 2006; Qi et al., 2009; Weingarten et al., 2009). Brønsted acid sites belong to hydroxyl groups and they have proton donor properties. So, reaction on the Brønsted sites usually occur by proton

transfer. On the other side, Lewis acid sites have electron acceptor properties on which reactions occur via electron transfer or electron sharing by forming covalent bonds (Asghari et al., 2006).

Weingarten et al. (2009) proved in his study that, fructose conversion to intermediates from fructofuranoses was carried out on the Lewis sites whereas Brønsted sites were responsible for the HMF formation from these intermediates. So, fructose conversion was related to the Lewis, HMF selectivity is related to the Brønsted sites (Weingarten et al., 2009). Then, selectivity to HMF could be attributed to the Brønsted/Lewis ratio which is directly proportional with HMF selectivity.

Amarasekara et al. (2008) proposed a mechanism and investigated the role of dimethylsulfoxide (DMSO) solvent (without catalyst at 150 °C) in fructose dehydration (Figure 2.8). DMSO acted as both solvent and catalyst in reaction. Dehydration also occurred in three steps. In each step, covalent bonds were formed by electron sharing between DMSO and OH groups of fructose, and hydrogen bonded hydroxides (water) were separated from fructose. It was also found that anomeric composition of fructose (forms of fructose) affect the product distribution. They obtained that maximum percentage of the furanoid forms of fructose phases are present at 150 °C in DMSO.

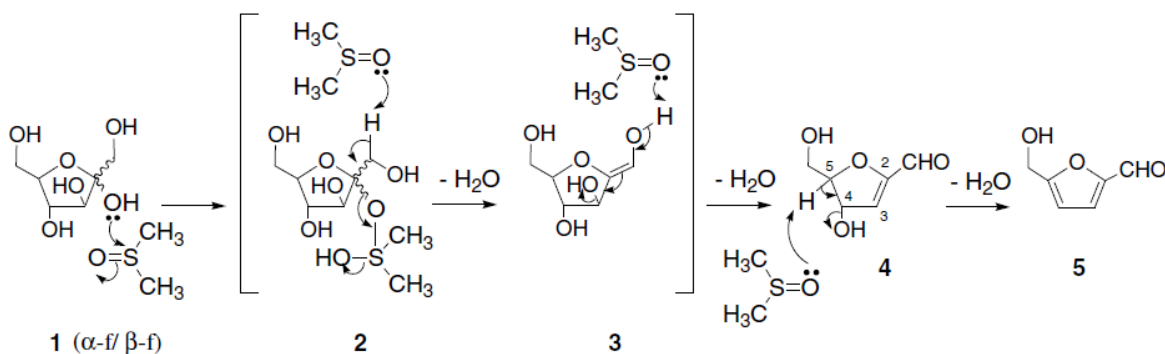


Figure 2.8. Proposed reaction mechanism for fructose dehydration to HMF in DMSO (Source: Amarasekara et al., 2008).

Possible fructose forms (tautomers) existing in a solution are given in Figure 2.9. There are five different forms of fructose ( $\alpha$ -pyranoid,  $\beta$ -pyranoid,  $\alpha$ -furanoid,  $\beta$ -furanoid and open chain). Composition of these forms change depending on the solvent.

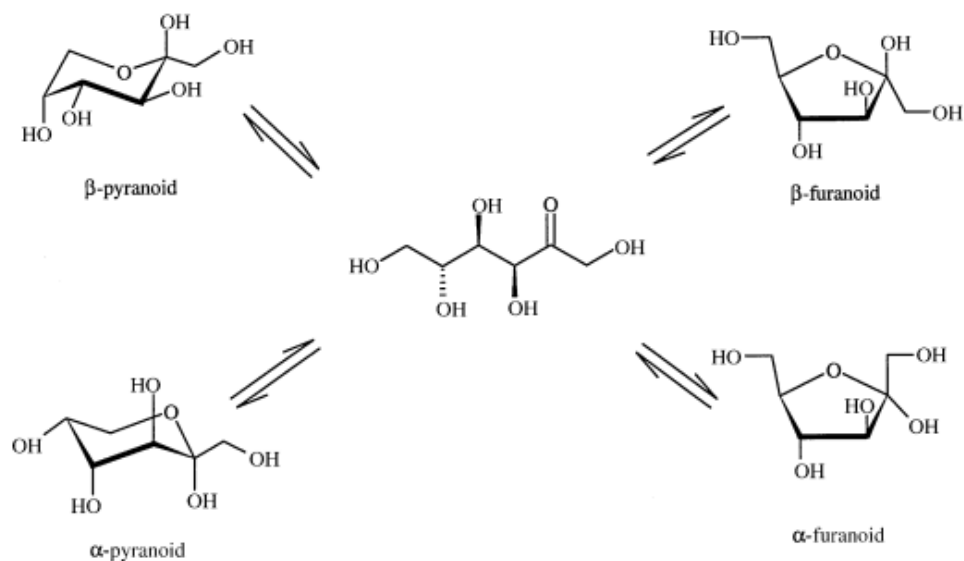


Figure 2.9. Forms of the fructose  
(Source: Bicker et al., 2005).

It was stated in the literature that (Antal et al., 1990; Bicker et al., 2005) presence of the furanoid forms of the fructose favor the HMF formation; because three moles of water molecules were eliminated from  $\alpha$ -furanoid or  $\beta$ -furanoid forms of fructose to form 5-HMF.

Bicker et al. (2005) investigated the effect of the solvent type on the distribution of fructose tautomers in solution (Figure 2.10). It was obtained that furanoid forms of fructose were least favored in aqueous based solvents. On the other hand, they were much favored in organic solvents (acetone, DMSO). The highest concentration of furanoid forms were obtained in DMSO. Water in the reaction medium also causes rehydration of HMF to levulinic and formic acids (Ordonsky et al., 2012).

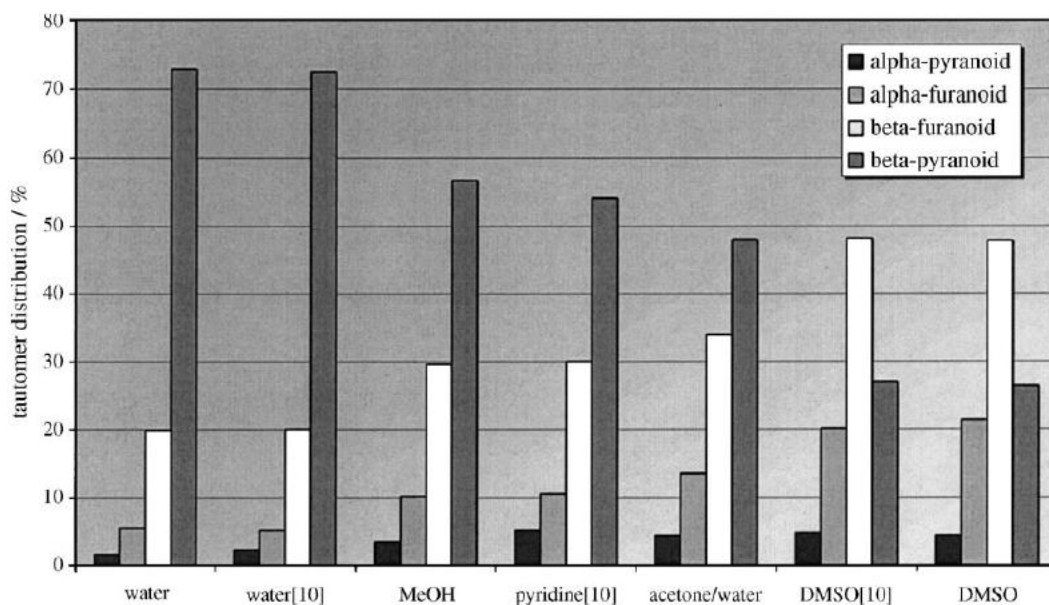


Figure 2.10. Distribution of fructose tautomers in different solvents  
(Source: Bicker et al., 2005).

### 2.3. Kinetics of Fructose Dehydration

In order to determine the optimum conditions and initial concentrations, it is substantial to understand the kinetics of fructose dehydration and the reaction pathway. Specific reaction rate provide informations about the optimum conditons that should be. Few studies about the kinetics of fructose dehydration to HMF is present in literature. One of the kinetic model for fructose dehydration to HMF was proposed by Asghari et al. (2007) in water by using HCl catalyst. Proposed reaction pathway is shown in Figure 2.11. In this reaction scheme, F refers to fructose, SP1, SP2, 2FA resfers to polymeric products, LA and FA refers to levulinic acid and formic acid respectively. They matched the proposed model and experimental data to obtain the rate constants in Table 2.1. Two different starting material; fructose and HMF were used. Some basic assumptions were made before using this model. All the reactions were treated as 1<sup>st</sup> order, irreversibe and it was assumed that formic acid and polymers did not undergo any decomposition.

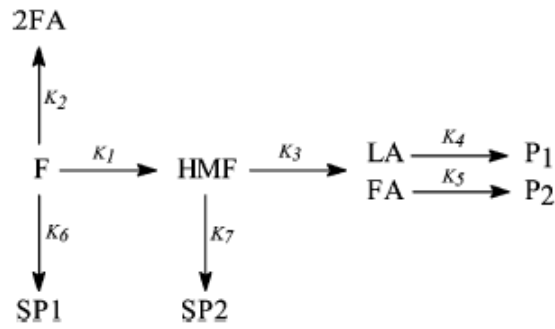


Figure 2.11. Proposed reaction pathway for fructose dehydration  
(Source: Ashgari et al., 2007).

Rate constants were calculated. It is known from the Arrhenius equation that, rate constants are highly temperature sensitive. Except  $k_6$ , the highest rate constant was  $k_1$ . Thus, at high temperatures, reaction rate of fructose to HMF may be improved if fructose to SP1 reaction is prevented. Higher concentration of fructose cause collisions of fructose molecules. Then SP1 is formed. If fructose concentration is adjusted as optimum, SP1 formation can be inhibited.

Table 2.1. Estimated reaction rate constants for fructose dehydration  
(Source: Ashgari et al., 2007).

temp. (K)	substrate					
	F	(s <sup>-1</sup> )	HMF	(s <sup>-1</sup> )	LA and/or FA	(s <sup>-1</sup> )
483	$k_1$	$4.53 \times 10^{-3}$				
	$k_2$	$5.12 \times 10^{-4}$				
	$k_3$	$3.01 \times 10^{-3}$	$k_3$	$3.32 \times 10^{-3}$		
	$k_4$	$3.18 \times 10^{-5}$	$k_4$	$3.18 \times 10^{-5}$	$k_4$	$3.18 \times 10^{-5}$
	$k_5$	$8.30 \times 10^{-5}$	$k_5$	$8.30 \times 10^{-5}$	$k_5$	$8.30 \times 10^{-5}$
	$k_6$	$1.02 \times 10^{-1}$				
	$k_7$	$5.03 \times 10^{-5}$	$k_7$	$5.03 \times 10^{-5}$		
513	$k_1$	$9.05 \times 10^{-2}$				
	$k_2$	$4.83 \times 10^{-3}$				
	$k_3$	$9.90 \times 10^{-3}$	$k_3$	$9.81 \times 10^{-3}$		
	$k_4$	$1.78 \times 10^{-4}$	$k_4$	$1.78 \times 10^{-4}$	$k_4$	$1.78 \times 10^{-4}$
	$k_5$	$5.09 \times 10^{-4}$	$k_5$	$5.09 \times 10^{-4}$	$k_5$	$5.09 \times 10^{-4}$
	$k_6$	$3.06 \times 10^{-1}$				
	$k_7$	$2.68 \times 10^{-4}$	$k_7$	$2.68 \times 10^{-4}$		
543	$k_1$	$3.63 \times 10^{-1}$				
	$k_2$	$1.95 \times 10^{-2}$				
	$k_3$	$4.42 \times 10^{-2}$	$k_3$	$4.46 \times 10^{-2}$		
	$k_4$	$6.07 \times 10^{-4}$	$k_4$	$6.07 \times 10^{-4}$	$k_4$	$6.07 \times 10^{-4}$
	$k_5$	$9.07 \times 10^{-4}$	$k_5$	$9.07 \times 10^{-4}$	$k_5$	$9.07 \times 10^{-4}$
	$k_6$	1.77				
	$k_7$	$1.91 \times 10^{-3}$	$k_7$	$1.91 \times 10^{-3}$		

## CHAPTER 3

### FRUCTOSE DEHYDRATION STUDIES

#### 3.1. Homogeneous Catalysts

Homogeneous catalysts include liquid mineral acid catalysts (e.g. hydrochloric acid, nitric acid, sulfuric acid) and ionic liquids. Although very high selectivities can be obtained by using these catalysts, they have very important drawbacks. Some of these problems are equipment corrosion, high cost, significant energy input, difficulties in separation and catalyst recovery (Benvenuti et al., 2000; Shimizu et al., 2009). However, in many studies homogeneous catalysts are used with heterogeneous ones for comparison purpose or to understand the role of acids in the reaction (Huang et al., 2009; Leshkov et al., 2006).

Qi et al. (2009) investigated the effect of the type of the mineral acid on the catalytic activity in fructose dehydration at 80 °C in acetone-DMSO solvent. It was reported that H<sub>3</sub>PO<sub>4</sub> and HCl had weak acidity among the homogeneous catalysts thus lower yield values (61 and 69 %) were obtained. However, H<sub>2</sub>SO<sub>4</sub> was found as the most active homogeneous mineral acid and it was found to give the highest selectivity to HMF.

In the study of Leshkov et al. (2006) fructose dehydration was carried out at 180 °C using HCl vs H<sub>2</sub>SO<sub>4</sub> catalysts in biphasic solvents (Water-DMSO and Water-Butanol-MIBK). Second phase was used to prevent the rehydration of HMF. Conversion and selectivity were found to be very close to each other for both catalysts. Fructose conversions and HMF selectivities were 85 and 71 % for H<sub>2</sub>SO<sub>4</sub>, 80 % and 75 % for HCl respectively. Higher selectivity results were attributed to the high acid strength of these catalysts.

Moreau et al. (2006) used ionic liquid (1-H-3-methyl imidazolium chloride, (HMIM<sup>+</sup>Cl<sup>-</sup>)) in fructose dehydration which acted as both solvent and catalyst. The reaction was carried out at 90 °C for 30 min. HMF formation rate was promoted by ionic liquids since its activation energy in ionic liquid was very low. High yield of HMF (86 %) was obtained at 90 % conversion. No decomposition of HMF was observed and

yield was almost same after 5 reuse. On the other hand, high cost of ionic liquids force people to find an alternative solvent and catalyst.

Homogeneous iron salts including metal chlorides and bromides ( $\text{FeCl}_3\text{-LiCl}$ ,  $\text{FeCl}_3\text{-NaCl}$ ,  $\text{FeCl}_3\text{-KCl}$ ,  $\text{FeCl}_3\text{-LiBr}$ ,  $\text{FeCl}_3\text{-NaBr}$ ,  $\text{FeCl}_3\text{-KBr}$  and  $\text{FeCl}_3\text{-NH}_4\text{Br}$ ) were used in fructose dehydration by Tong et al. (2011). Reaction was carried out at 90 °C by using N-methylpyrrolidone solvent. The highest HMF yield (75 %) was achieved by using the  $\text{FeCl}_3\text{-NH}_4\text{Br}$  catalyst. This was attributed to the superior activity of bromide ion when it was coupled with ammonium cation. On the other hand, reusability of these chlorides was found very low.

## **3.2. Heterogeneous Catalysts**

Because of the difficulties in using the homogeneous catalysts, people are trying to find a selective, active and stable heterogeneous catalyst for fructose dehydration. These type of catalysts have many advantages such as easy separation, reusability and green processes. Heterogeneous catalysts investigated are grouped under the following topics.

### **3.2.1. Phosphated Oxides, Sulfated Oxides and Mixed Oxides**

Metals have active and strong acidic properties for many reactions and also dehydration reactions. However, monometal oxides have only Lewis acid sites, some of them also include basic sites that are correlated with side product formation and HMF decomposition (Yan et al., 2009). The most effective method to create OH groups (Brønsted sites) on metal surfaces is modifying the metals with functional groups. Most effective functional groups for fructose dehydration were found as phosphates and sulfates (Qi et al., 2009; Benevuti et al., 2000).

Dutta et al. (2011) investigated the effect of mesoporous  $\text{TiO}_2$  nanoparticles on HMF yield. This catalyst was prepared via sol-gel method. Surface area of the  $\text{TiO}_2$  particles was 326  $\text{m}^2/\text{g}$ . Different metal oxides including commercial  $\text{TiO}_2$ ,  $\text{CeO}_2$ ,  $\text{Al}_2\text{O}_3$ , and  $\text{SiO}_2$  were also tested for comparison. Reactions were carried out under microwave heating at 120 °C in water and DMSO solvents. HMF yields of 34 % in water and 56 %

in DMSO were obtained. Yields were remained same up to 4 reuse. These obtained yields were much higher than the other oxides ( $\text{CeO}_2$ ,  $\text{Al}_2\text{O}_3$ , and  $\text{SiO}_2$ ). This was attributed to mesoporosity, strong surface acidity and Lewis nature of  $\text{TiO}_2$ .

Most researchers have been investigating the effect of the sulfation on metals acidity or generation of Brønsted acid sites with sulfur ions (Qi et al., 2009; Guo et al., 2012; Farcasiu et al., 1997). Among the many metals, the most selective and active ones are titanium and zirconium. The oxides of them have very strong Lewis sites and form Brønsted sites when interact with sulfate ions. Strong interaction between these metals and sulfurs can give satisfactory results for dehydration reactions.

Zirconia has two different phases in its crystal structure which are tetragonal (acidic) and monoclinic (basic) phases (Farcasiu et al., 1997; Chareolimkun et al., 2010; Qi et al., 2009). Tetragonal phases are selective phases and responsible for HMF formation from fructose intermediates; whereas monoclinic phases are unselective and cause rehydration of HMF to side products and humin formation (Chareolimkun et al., 2010; Qi et al., 2009). After the sulfation, most of monoclinic phases convert to the tetragonal phases and also sulfur ions make the tetragonal phases stable. Sulfation also enhances the surface area of the catalyst. The distribution of these phases depends on the sulfur content in the sulfated zirconia and also depends on the calcination temperature. Sulfur content in a range of 2.5-3.5 % makes the most of the crystal phase tetragonal (Farcasiu et al., 1997). Higher sulfate loadings ( $> 3.5$  %) cause migration of sulfates from surface to the bulk phase which creates monoclinic phases and unselective sites. Farcasiu et al. (1997) stated that maximum capacity of sulfur to be loaded on zirconia is 3.5 % when sulfuric acid was used as sulfating agent. On the other hand, Yadav et al. (2004) proved that this capacity could be increased by using chlorosulfonic acid as a sulfating agent. Moreover, this agent forms strong acid sites and bonds on zirconia, also increases the amount of acid sites and tetragonal phases more than sulfuric acid. Tetragonal phases transform into monoclinic phases at calcination temperature higher than  $650$  °C. The highest amount of tetragonal phases occurs at calcination temperature between  $540$  and  $600$  °C.

Preparation of the  $\text{SO}_4^{2-}/\text{ZrO}_2$  using  $\text{ZrO}(\text{OH})_2$  instead of  $\text{Zr}(\text{OH})_4$  make the catalyst consisting entirely tetragonal form (Farcasiu et al., 1997). So, to obtain  $\text{ZrO}(\text{OH})_2$  instead of the  $\text{Zr}(\text{OH})_4$ ,  $\text{ZrCl}_4$  was precipitated at the basic medium (pH=9-9.5), although point of zero charge of  $\text{ZrCl}_4$  is pH=5-6 (Qi et al., 2009).

In spite of the high activity of the sulfated zirconia, significant deactivation in water was observed due to the  $\text{SO}_4^{2-}$  leaching (Chareonlimkun et al., 2010). Qi et al. (2009) investigated the activity of the sulfated zirconia on HMF yield. Sulfate ions were impregnated on zirconia. Zirconium sulfate exhibited lower activity when water was used as solvent. The reason was leaching of  $\text{SO}_4^{2-}$  ions in water. On the other hand, sulfated zirconia was very active and selective (91.3 % fructose conversion and 71.9 % HMF yield) in non-aqueous organic solvents such as acetone–DMSO mixtures at 160 °C and 20 min. Catalytic activity was directly attributed to the amount of acid sites. The higher yield is from the higher amount of Brønsted/Lewis site ratio.

The activity of sulfated oxides was satisfactory in organic solvents such as DMSO and acetone. On the other hand, stability of these types of catalysts was also very low in aqueous or alcohol based solvents (Li et al., 2013; Qi et al., 2009). Sulfur atoms in the structure leach easily due to the weak interaction of single metal oxide and sulfur. Using mixed metal oxides, bimetallic catalysts combined with promoters may be an alternative to overcome this situation. Mixed oxides are reported as the best catalyst for many acid catalyzed reactions since they have better acidity and thermal stability than single oxides. Among the many mixed oxides, titania-silicates seems to be very effective catalyst and they attracted much attention in recent years (Li et al., 2013; Shao et al., 2012; Shao et al., 2013, Sharma et al., 2012).

More acid sites were generated by the combination of  $\text{TiO}_2$  and  $\text{SiO}_2$  with respect to other mixed oxides (Yang et al., 2003, Shao et al., 2013). Acid sites on this mixed oxide were formed by excess positive charge of Ti atoms in the  $\text{TiO}_2$ . Interaction of  $\text{TiO}_2$  with  $\text{SiO}_2$  increased the number of acid sites due to the well dispersion of Ti atoms on  $\text{SiO}_2$ . Acid sites in the  $\text{TiO}_2$ - $\text{SiO}_2$  are obviously Lewis acids because of the Ti. The strong and Brønsted acidity are related to the sulfur atoms and sulfate ions. High electronegativity of sulfur could induce polarization of the neighboring OH groups. Thus, Brønsted acidity was created by the sulfation of  $\text{TiO}_2$ - $\text{SiO}_2$  (Li et al., 2013; Yang et al., 2003). It was observed that both Brønsted acid and Lewis acid sites exist on the surface of  $\text{SO}_4^{2-}/\text{TiO}_2$ - $\text{SiO}_2$ , but mostly Brønsted sites were present (Li et al., 2013).  $\text{SO}_4^{2-}/\text{TiO}_2$ - $\text{SiO}_2$ , is called as superacid catalyst due to its higher acidity than sulfuric acid ( $\text{pK}_A > 3.2$ ) and exhibited high activity for many reactions (alkylation, cracking). Besides, no one used this catalyst in fructose dehydration to HMF. Preparation of  $\text{TiO}_2$ - $\text{SiO}_2$  instead of solely  $\text{TiO}_2$  prevents the surface sulfur leaching, enhances the stability

by creation of strong chelating bonds as shown in Figure 3.1. These bonds are strong Brønsted sites and form at calcination temperature around 400- 450 °C. It was indicated that calcination temperature has a crucial role on acid sites formation, the maximum interaction of sulfur species also forms at 450 °C. At calcination temperature higher than 540 °C, some Brønsted sites were removed due to the decomposition of SO<sub>4</sub> ions (Li et al., 2013, Yang et al., 2003). It may be deduced that calcination temperature should be between 450 - 540 °C to protect the strong Brønsted sites.

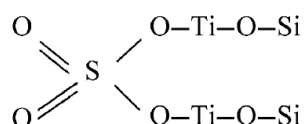


Figure 3.1. Chelating bitentate bonds in titania-silicates  
(Source: Yang et al., 2003).

Shao et al. (2013) prepared TiO<sub>2</sub>-SiO<sub>2</sub> mixed oxide by sol-gel method at 80 °C. Sol-gel formed very strong Si-O-Ti bonds so this method was considered as the best method to prepare TiO<sub>2</sub>-SiO<sub>2</sub> mixed oxide. More stable catalysts were obtained via sol-gel due to its matrix. Sulfuric acid was impregnated on a TiO<sub>2</sub>-SiO<sub>2</sub> support to obtain SO<sub>4</sub>/TiO<sub>2</sub>-SiO<sub>2</sub>. Three different calcination temperatures (450 °C, 550 °C, 650 °C and 800 °C) were investigated. Calcination temperature was reported as the important criteria for sulfur content, pore structure and surface area. The highest surface (457 m<sup>2</sup>/g), largest pore volume (0.28 cm<sup>3</sup>/g) and the most amount of sulfur (5.37 %) were observed in catalyst calcined at 450 °C. Prepared SO<sub>4</sub>/TiO<sub>2</sub>-SiO<sub>2</sub> catalyst was used in esterification of waste oil and oleic acid at 120 °C. The highest conversion (77 %) was obtained with the catalyst calcined at 450 °C. SO<sub>4</sub>/TiO<sub>2</sub>-SiO<sub>2</sub> (calcined at 450 °C) was regenerated and reused. Only 2 % activity loss was observed.

Li et al. (2013) investigated the effect of the addition of La<sup>+3</sup> into SO<sub>4</sub>/TiO<sub>2</sub>-SiO<sub>2</sub> on esterification of itaconic acid. No diffraction patterns of La and Si was observed which demonstrated that La and Si were well dispersed. It was reported that esterification of itaconic acid reaction occurs on the strong acid sites of the catalysts like fructose dehydration. Without La<sup>+3</sup> addition, pure SO<sub>4</sub><sup>-2</sup>/TiO<sub>2</sub>-SiO<sub>2</sub> catalyst exhibited very high activity because of the strong acidity of the catalyst. But addition of La<sup>+3</sup> enhanced the SO<sub>4</sub>/TiO<sub>2</sub>-SiO<sub>2</sub> stability and sulfur capture significantly by increasing the yield and conversion slightly. Improvement in yield was attributed to the increase in the

number of acid sites. Activity remained constant up to 8 times reuse although methanol was used as solvent which indicated the prevention of surface sulfur leaching by La addition.

Sharma et al. (2012) synthesized Ti incorporated mesoporous SBA-15 (Ti-SBA-15). Hydrothermal preparation method was applied for crystallization process. Ti-SBA-15 was sulfated by using chlorosulfonic acid agent. More sulfates were loaded with this agent compared to sulfuric acid. Super acid sites were observed by  $\text{NH}_3$ -TPD analysis. It was reported that super acidity was caused by chlorosulfonic acid. This was attributed to the generation of Lewis acid sites on surface of Ti-SBA-15, then catalyst become superacid. Different Si/Ti ratios (10, 20, 40 and 80) were studied. It was also found that the amount of sulfur in structure increased with the increase in Ti content. The highest amount of sulfur (2.1 %) and the highest amount of acid sites were obtained at Si/Ti = 10. Prepared  $\text{SO}_4/\text{Ti-SBA-15}$  was tested in liquid phase oxidation of benzyl alcohol to benzaldehyde at 60 °C. The highest benzyl alcohol conversion (70 %) and the highest benzaldehyde selectivity (90 %) was also achieved over catalyst having Si/Ti = 10.

Chareonlimkun et al. (2010) investigated the effect of different metal oxides ( $\text{TiO}_2$ ,  $\text{ZrO}_2$  and mixed-oxide  $\text{TiO}_2\text{-ZrO}_2$ ) on HMF yield in the reaction of sugar-based biomass (sugarcane bagasse) dehydration to HMF. Three different calcination temperatures (773, 873 and 973 K) and three different Ti/Zr ratio (3/1, 1/1 and 1/3) were also investigated. Reactions were carried out under nitrogen atmosphere in water at 523 K. The highest HMF yield (8.8 %) was obtained over  $\text{TiO}_2\text{-ZrO}_2$  mixed oxide with Ti/Zr ratio of 3/1 at calcination temperature of 873 K. This was attributed to the higher acidity and reactivity of  $\text{TiO}_2\text{-ZrO}_2$  than single oxides  $\text{TiO}_2$  and  $\text{ZrO}_2$ . It was also found that higher acid sites could be obtained at higher ratio of anatase/rutile for  $\text{TiO}_2$  and tetragonal/monoclinic for  $\text{ZrO}_2$ .

Phosphated metals (zirconium phosphates, vanadium phosphates, titanium phosphates) were also investigated for fructose dehydration since phosphate groups create Brønsted sites when they were loaded on metals (Benvenuti et al., 2000). High selectivity results were obtained by using metal phosphates, (99.8 % of HMF selectivity in fructose dehydration was achieved with zirconium phosphates). But it was observed that these types of the catalysts deactivate quickly especially in aqueous solvents and reusability of metal phosphates are lower than other catalysts. In addition, geminal groups ( $\text{P-OH}$ ,  $\text{P}=(\text{OH})_2$ ) are formed when phosphates loaded on metals which are

responsible for the formation of polymeric compounds and side reactions. Geminal groups also cause rehydration and so reduce the selectivity to HMF ((Benvenuti et al., 2000).

Asghari et al. (2006) prepared mesoporous zirconium phosphate catalyst for fructose dehydration in subcritical water at 240 °C. It was observed that zirconium phosphate had both Brønsted and Lewis acid sites. At 80 % of fructose conversion 61 % of selectivity to HMF was achieved. On the other hand, humin formation was observed. Lower selectivity results and observed humin formation was attributed to the unselective geminal sites on the metal phosphates which was reported in the study of Benvenuti et al. (2000).

Carlini et al. (2004) investigated the effect of different metals incorporation ( $\text{Fe}^{3+}$ ,  $\text{Cr}^{3+}$ ,  $\text{Ga}^{3+}$ ,  $\text{Mn}^{3+}$ ,  $\text{Al}^{3+}$ ) into vanadium phosphate support on selectivity to HMF and fructose conversion. The reaction was carried out at 80 °C in water. It was observed that activity of these catalysts were very low (30-40 % conversion) although HMF selectivity was high (~90 %). Reusability of these vanadium phosphates were presumed to be low because of the easy leaching of phosphates in aqueous medium.

### **3.2.2. Sulfated and $\text{ZrSO}_4$ Loaded Mesoporous Supports**

Although modified metals gave good results for fructose dehydration, these catalysts have low surface area. Thus, these catalysts may be loaded on to a support to enhance the active sites distribution and surface area. Many supports, from mesoporous silicas to activated carbons are investigated in literature (Zhao et al., 1998; Guo et al., 2012). Mesopore supports increase the rate of fructose diffusion from the reaction medium in to the pores. In micropores, large size of the fructose molecules cause pore blockage. Then humin formation is observed due to the collision of fructose molecules.

Guo et al. (2012) prepared functionalized mesoporous catalyst (SBA-15- $\text{SO}_3\text{H}$ ). Functionalization was performed by loading propyl sulfonic acid group ( $\text{SO}_3\text{H}$ ) on SBA-15 support by co-condensation. 3-mercaptopropyltrimethoxysilane (MPTMS) was used as propyl sulfonic acid agent and Tetraethylorthosilicate (TEOS) was used as silica source. Different amounts of propyl sulfonic acid groups (MPTMS / (MPTMS + TEOS) = 5, 10, 15 and 20) were studied. It was observed that functionalization of SBA-15 did

not change the crystal structure of SBA-15, only surface area reduced slightly. This catalyst was tested in fructose dehydration at 120 °C in an ionic liquid solvent (BmimCl). H<sub>2</sub>SO<sub>4</sub> was used as homogeneous catalyst for comparison. Without functionalization, pure SBA-15 catalyst exhibited 41.9 % of HMF yield. It was reported that SBA-15 had no acid sites; thus, yield was related to the acidic ionic liquid BmimCl which was both solvent and catalyst. HMF yield over SBA-15-SO<sub>3</sub>H was obtained as 81 % at complete conversion of fructose which was almost same with H<sub>2</sub>SO<sub>4</sub> (82 %). Amount of propyl sulfonic acid affected the activity and selectivity slightly. The high yields were attributed to the Brønsted acidity of this catalysts and inhibition of rehydration (No levulinic acid and formic acid was observed).

In literature, MCM-41 was also investigated as supports in many studies (Wang et al., 2008; Chen et al., 2001; Sun et al., 2002). It was observed that using MCM-41 as support give large surface area and better dispersion but its thermal stability in aqueous systems was found very low although it had high thermal stability in organic solvents and gas phase systems (Juan et al., 2007). Activity with MCM-41 supported catalysts was also found lower when compared with other supports (Zeolite beta, SBA-15) (Leshkov et al., 2011; Juan et al., 2007). The acidic strength of sulfated zirconia loaded MCM-41 was found also much weaker than that of SBA-15 (Sun, 2002).

Juan et al. (2008) prepared hexagonal mesoporous silica (HMS) by sol-gel and loaded zirconium sulfate onto this support by impregnation. Zirconium sulfate (ZS) was well dispersed on to HMS. Mesopore structure was observed having pore diameter 4 nm. High amounts of Brønsted and Lewis sites were also obtained after impregnation. This catalyst was tested in esterification of oleic acid with n-butanol at 120 °C. Different zeolites (H-ZSM-5, H-Y, H-Beta and H-Mordenite) were also tested for comparison purpose. Zirconium sulfate loaded HMS was more active (98 % oleic acid conversion) than zeolites (the highest conversion among zeolites was found 42 %). This was attributed to the smaller pores in zeolites and higher acidity of the ZS/HMS catalyst. Reusability tests indicated that ZS/HMS exhibited same activity 4 times reuse.

Activated carbon (AC) supported catalysts are also used for many reactions such as; esterification and dehydration. Satisfactory results were obtained by the interaction of sulfate groups with AC support (Juan et al., 2007; Khayoon et al., 2011; Feng et al., 2006). Juan et al. (2007) prepared zirconium sulfate loaded activated carbon catalyst (ZS/AC). Zirconium sulfate (ZS) loaded by impregnation was found as well dispersed

on AC support. Micropore diameter and volume were slightly reduced after 10 % of ZS loading. ZS/AC was tested in esterification of oleic acid with n-butanol at 120 °C. Oleic acid conversion over ZS/AC was observed as 91 %. On the other hand, conversion reduced to 80 % after second reuse and remained almost same upto 4 reuse.

### **3.2.3. Resin Catalysts**

Resins are natural hydrocarbons which are secretion of the plants. They are found in nature. Most resins are Brønsted acid catalysts having high ion exchange capacity. They are also giving very high selectivity results (Moreau et al (2006): 92 % of HMF yield, Takagaki et al (2009): 76 % yield) especially with Amberlyst-15. Nevertheless, resins are not stable and reusability of these types of catalysts is very low.

Thermal stability of sulfonated resins was also found low. They can be used up to 130 °C, after that temperature they are deactivated easily. They have also low stability and activity in water (Moreau, et al., 1996; Qi et al., 2009).

Takagaki et al. (2009) investigated the activity of Amberlyst-15 resin in fructose conversion and HMF yield. Reaction was carried out at 100 °C using dimethylamide (DMA) solvent. Glucose conversion was also investigated. HMF yield of 76 % was achieved at complete conversion of fructose. On the other hand, adsorption of the water to the active sites due to the hydrophilicity of Amberlyst-15 was observed. High glucose conversion (69 %) by using Amberlyst-15 was the indication of presence of basic sites which are responsible for the glucose conversion. These basic sites also caused side product formation in fructose dehydration.

### **3.2.4. Heteropoly Acids**

Heteropoly acids are materials which composed of hydrogen and oxygen around a central metal atom. They are known as strong acidic and thermally stable catalysts. Heteropolyacids have special structure called as Keggin structure (shown in Figure 3.2) which creates strong Brønsted acid sites by bonding OH groups to the central metal atoms. The most used heteropoly acids are tungstophosphoric and tungstomolybdic acids. Besides their many advantages such as high acidity, they have some important

drawbacks. They are highly soluble in organic based solvents and alcohols. They may also be leached in aqueous based solvents and lose its activity easily. An alternative route to use heteropoly acids is, loading them onto a support.

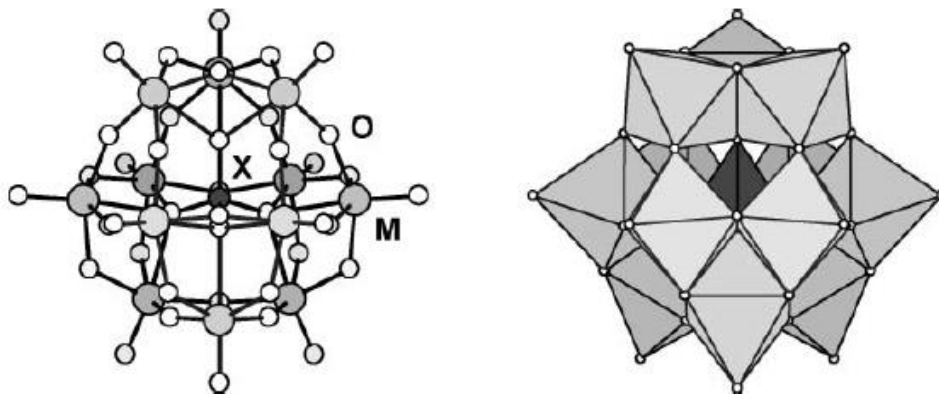


Figure 3.2. Keggin structure in heteropoly acids (X: P, B; M: W, Mo, Cu, Ni)  
(Source: Ninomiya et al., 2009).

Patel et al. (2003) loaded 12-tungstophosphoric acid (HPW) onto zirconia by impregnation to improve its stability. Different amounts of HPW loadings (20–70 % HPW) were studied. After impregnation HPW retained its Keggin type structure for all loading amounts. Acidity of the catalysts was correlated with ion exchange capacity. The highest ion exchange capacity as well as acidity was observed in 30 % HPW loaded zirconia. Surface area of this catalyst was found as 146 m<sup>2</sup>/g. All the catalysts were tested in esterification of cyclohexanol to cyclohexyl acetate. The highest cyclohexyl acetate yield (68 %) was obtained with 30 % HPW loaded zirconia. This was attributed to the highest acidity at this loading.

Jin et al. (2005) synthesized tungstovanadogermanic acid loaded SBA-15. Prior to the heteropoly acid (HPA) loading, prepared SBA-15 support was silylated with  $\gamma$ -aminopropyltriethoxysilane. Tungstovanadogermanic acid was then loaded on to SBA-15 by impregnation. Obtain catalysts had 284 m<sup>2</sup>/g surface area and 5.1 nm of mesopores. HPA clusters were found as well dispersed on SBA-15 support. It was reported that silylation made the surface bonds much stronger since amino groups interacted strongly with HPA.

Brahmkatri et al. (2011) prepared 12-tungstophosphoric (TPA) acid loaded SBA-15. The loading amount was changed from 10 to 30 %. Acidity of the catalyst increased with the TPA loading. At 30 % TPA loading 1.82 mmol/g acidity was

obtained. Catalysts were tested in esterification of oleic acid at 40 °C. The highest turnover frequency (TOF) and oleic acid conversion achieved were 9.3 min<sup>-1</sup> and 90 %, respectively over 30 % TPA loaded SBA-15. Only 3 % loss of activity was observed after 4 times reuse.

Hamad et al. (2008) loaded tungstophosphoric acid on to the mesoporous silica. This catalyst was found highly acidic. It was tested in transesterification of rapeseed oil at 80 °C. Selectivity of ethylic ester obtained was 39 % at 15 % of conversion. On the other hand, leaching of active sites was reported.

### **3.3. Solvent Effects**

Solvent selection is also crucial point in fructose dehydration. Type of the solvents affects the reaction pathway, HMF yield and product distributions. Organic solvents (e.g. dimethylsulfoxide (DMSO), dimethylformamide (DMF), acetone), water, alcohols (e.g. butanol, propanol and ethanol) and ionic liquids are investigated in literature. Biphasic solvents have also been used.

Solvents can be considered in two groups such as high and low boiling point solvents. High selectivities are obtained by high boiling point solvents (DMSO, DMF). However separation them from reaction mixture is expensive. Thus, low boiling solvents are generally preferred. Satisfactory HMF yields couldn't be achieved by using these solvents yet. Solvents can have aprotic and protic properties. Protic solvents have a hydrogen atom bound to an oxygen where aprotic solvents don't have. The common polar protic solvents are water, ethanol, butanol, acetic acid and common polar aprotic solvents are DMSO, DMF and acetone. Polar aprotic solvents have an active role in reaction mechanism and increase the rate of fructose dehydration (Huang et al., 2009; Chedda et al., 2007).

#### **3.3.1. Single Phase Solvents**

Bicker et al. (2005) found that, organic solvents were very suitable in fructose dehydration. Some of these solvents play an important role in HMF formation and also no solid impurities are formed. HMF yield was achieved as 78 % in supercritical

acetone-water mixture at 180 °C. This yield value was much higher than that in water (53 % at 250 °C). Among the organic solvents, DMSO was found as the most effective one. It is a dipolar aprotic solvent and prevents the levulinic acid and humin formation during fructose dehydration (Tong et al., 2010). DMSO also has an active role in fructose dehydration as reported before, and can act as a catalyst and enhance the HMF yield (Amaresakara et al., 2008). Studies in ionic liquids are also performed for fructose dehydration (Shimizu et al., 2009; Qi et al., 2009). They have low vapor pressure, good thermal stability, hydrophobicity and they can reduce the activation energy of process. Moreover reactions were proceeded more rapidly than organic phase. These solvents also act as both solvent and catalyst in reactions.

Wang et al. (2013) used organic solvents (dimethyl amide (DMA) and DMSO) and water in fructose dehydration at 120 °C. Selectivity to HMF decreased significantly in DMA. In water, rehydration of HMF was observed and more side products; such as levulinic and formic acids were formed. It was observed that maximum yield of HMF was achieved in DMSO (88 %) in which all of the fructose was consumed. The high selectivity and conversion results were attributed to the presence of high content of furanoid forms in DMSO and prevention of rehydration products in DMSO medium. Similarly, Qi et al. (2009) reported, 71 % HMF selectivity could be achieved at complete fructose conversion in DMSO at 130 °C.

Leshkov et al. (2009) investigated the effect of different alcohols (propanol, butanol, hexanol, pentanol) on HMF yield. Fructose dehydration was carried out at 180 °C. Homogeneous HCl catalyst was used. The highest selectivity (~90 %) was achieved at a conversion of 77 % in 2-butanol solvent. It was stated that solvents containing four carbon atoms provided higher selectivity results than the other solvents, due to the higher affinity of HMF and low water miscibility. This prevented the side reactions.

Zhang et al. (2011) pursued fructose dehydration without using a catalyst in an ionic liquid [C<sub>4</sub>mim]Cl 180 °C. Water and water-acetone solvents were also studied for comparison purpose. The highest HMF yield was observed as 97 % at 97 % fructose conversion in [C<sub>4</sub>mim]Cl. This was attributed to the suppression of the side reactions (HMF rehydration and hydrolysis) by ionic liquid and acidic properties of the [C<sub>4</sub>mim]Cl. Similar discussions were also made by Guo et al. (2012). In their study non acidic SBA-15 catalyst exhibited 42 % of HMF yield. It was reported that SBA-15 had no acid sites; thus, yield was related to the acidic ionic liquid BmimCl.

In spite of the advantages of ionic liquids they have very high costs.

### 3.3.2. Multiphase Solvents

HMF reacts with water present in reaction medium and selectivity decreases by the formation of side products. Thus, most researchers prefer non-aqueous solvents to reduce the rehydration rate. Non-aqueous solvents have some disadvantages; such as difficult separation from reaction mixture. The first convenient route to increase the HMF selectivity in literature is removing the produced water from the reaction medium (using vacuum or molecular sieve) (Shimizu et al., 2009). Second one is using biphasic solvents (aqueous and organic phases). In biphasic systems, HMF was transferred to organic phase from aqueous phase. Then, possible rehydration is prevented or minimized. To enhance the mass transfer rate of HMF from aqueous phase, some people used salts (KCl, NaCl) which increase the partition coefficient of the HMF transfer (Leshkov et al., 2009).

Ordonsky et al. (2012) investigated the effect of MIBK addition as second phase on the selectivity to HMF. In the presence of water, adsorbed HMF molecules on acid sites were transformed into side products (by reacting with water or another products) unless it was transferred from the reaction medium. It was observed that addition of MIBK into water increased the selectivity to HMF from 40 % to 79 %. After addition of MIBK, HMF transferred to the MIBK phase so selectivity was enhanced. Selectivity to HMF increased as the ratio of MIBK/Water increased. The highest selectivity (79 %) was obtained at MIBK/water =3 ratio. Reduction in the catalytic activity (fructose conversion) was related to the occupation of acid sites by adsorbed MIBK molecules.

Leshkov et al. (2006) also investigated the effect of solvent composition on HMF yield. The reaction was carried out at 180 °C by using HCl catalyst. Biphasic system was formed between Water-DMSO-polyvinylpyrrolidone (PVP) and Butanol-MIBK. Different compositions of these solvents were tested. PVP was used to increase the partition coefficient of HMF. The addition of 2-butanol to MIBK improved HMF selectivity by accelerating HMF transfer. Maximum HMF yield (89 %) was achieved at

optimum solvent composition 7:3(8:2 Water: DMSO): PVP - 7:3 MIBK:2-butanol. Side products formation was minimized at this composition.

Qi et al. (2009) investigated the effect of Acetone-DMSO composition (0, 20, 50, 70 % acetone in DMSO) on fructose dehydration using ion exchange resins at 150 °C. It was aimed to reduce the DMSO composition for easy separation. The maximum selectivities (90 %) were obtained using 70 % acetone and 20 % acetone in acetone-DMSO mixture. Both solvent compositions exhibited the same activity and selectivity results. This was attributed to the analogy in the structure of acetone and DMSO as shown in Figure 3.3. Only central sulfur atom in DMSO is carbon in acetone. The high selectivities were also attributed to the higher amount of the furanoid forms of the fructose present in acetone-DMSO mixture.

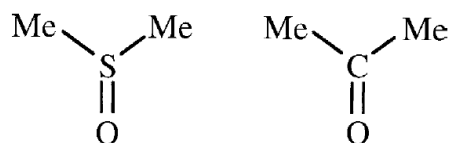


Figure 3.3. Structural analogies of DMSO and acetone  
(Source: Bicker et al., 2005).

Zhu et al. (2011) investigated the effect of tetrahydrofuran (THF) addition into methanol solvent on the HMF yield. Fructose dehydration was carried out at 120 °C. The highest HMF yield (~28 %) was achieved by ratio of methanol/THF 1/4. Lower selectivity results were due to the formation of 5-methoxymethylfurfural (MMF) in presence of methanol. Methanol solvent was found as promoter for side reactions.

### 3.4. Effect of Reaction Parameters

Reactant concentration, catalyst amount, mixing speed and reaction temperature are also important parameters for fructose dehydration as they affect the product distribution, activity, selectivity and type of the possible reactions in pathway. Fructose dehydration to HMF is generally carried out at high temperatures since the activation energy of HMF formation is higher than HMF consumption as mentioned in kinetic study part. Most fructose dehydration reactions are also carried out under inert nitrogen

atmosphere to obtain the oxygen-free atmosphere for side reaction minimization. (Schimizu et al., 2000).

Guo et al. (2012-A) stated that when the reaction temperature was below 110 °C, side product formation is favored due to the slower reaction rate of HMF formation, on the other hand when the temperature was above 150 °C, HMF selectivity decreased due to the secondary decomposition of HMF.

In the study of Guo et al. (2012-B), effect of fructose concentration (10-60 wt %) on fructose conversion and HMF yield was investigated. Reaction was carried out over sulfonated SBA-15 catalyst in BmimCl ionic liquid at 120 °C. It was found that fructose conversion and HMF yield decreased with the amount of the fructose and maximum HMF yield was achieved with 10 wt % fructose, as 82 % at 88 % conversion. This was due to the formation of polymeric products by the collision of fructose molecules at higher fructose concentrations. Polymeric condensation of fructose with HMF and formation of insoluble humins at high fructose concentrations were also found by Bicker et al. (2005) and Zhang et al. (2012).

Qi et al. (2009) performed fructose dehydration over DOWEX resin catalyst in DMSO solvent. The effect of catalyst loadings ( $R = \text{weight of fructose} / \text{weight of catalyst}$ ,  $R = 0.5, 1, 2$  and  $2.5$ ) on fructose conversion and HMF yield was investigated. Effect of reaction temperature (100, 120, 150 and 150 °C) was also studied. Decrease in  $R$  value improved the HMF yield and fructose conversion. The highest HMF yield and fructose conversions were 87 and 99 % respectively at  $R = 0.5$  which were 77 and 89 % when  $R = 2$ . Increasing the temperature from 100 to 150 °C, improved the selectivity to HMF from 84 to 92 % and fructose conversion from 33 to 100 %. This was attributed to the reduction in formation rate of side products.

In the study of Lourvanij et al. (1993), effect of mixing (300 and 1200 rpm) speed on glucose conversion was investigated. Reaction was carried out over Y-zeolite in water at 130 °C. Increasing the mixing speed from 300 to 1200 rpm did not affect the catalytic activity. Glucose conversion was obtained as 80 % for both mixing speeds. Thus, it was reported that 300 rpm is enough to minimize the mass transfer limitations.

Leshkov et al. (2009) carried out the fructose dehydration using HCl catalyst in 1-butanol solvent. In this study, effects of temperatures 150-180 °C were investigated. It was found that increase in reaction temperature from 150 to 180 °C improved the selectivity to HMF from 69 to 82 %.

Asghari et al. (2006) investigated the effect of fructose/catalyst ratio (1, 2, 4) on fructose conversion and HMF yield. Zirconium phosphate (ZrP) was used under subcritical-water (sub-CW) condition (240 °C). Best results were obtained with fructose/catalyst ratio 2 for 120 s of residence time. HMF selectivity and fructose conversion were 61 and 80 %, respectively at these conditions.

### 3.5. Literature Outcomes and Statement of Work

Reaction mechanism, catalysts, solvents and conditions studied were given in literature section (section 3.4). From these informations following findings were reached. The findings obtained are given below.

Homogeneous catalysts (especially mineral acids) are very active and selective. On the other hand, they cause many problems such as difficult separation, corrosion of reactors and impossible reusability. Among these catalysts satisfactory results are achieved by sulfuric acid, since sulfate groups are effective and responsible for HMF formation. Some homogeneous mineral acids (HCl, H<sub>3</sub>PO<sub>4</sub>, H<sub>2</sub>SO<sub>4</sub>) were also tested to investigate the role of sulfate and tested for comparison.

Fructose dehydration occurs on the acid sites of the catalyst. Lewis acids are responsible for the fructose conversion to the fructofuranose intermediates where Brønsted acids are responsible for the HMF formation from these intermediates. For that reasons, the catalyst should have both Brønsted and Lewis sites having high Brønsted/Lewis ratio. Sulfated catalysts are known as strong Brønsted acidic catalysts. When they are loaded on a metal, superacid sites may form including both Brønsted and Lewis centers.

There are many studies on sulfated zirconia. Pure zirconia have monoclinic and tetragonal phases. Tetragonal phases have acidic properties where monoclinic phases exhibit basic properties. Sulfur content and calcination temperature affect phases formed. Sulfated zirconia (SO<sub>4</sub>/ZrO<sub>2</sub>) is leached in the presence of alcohol and water. It was selected to investigate the effect of sulfate ions on catalytic activity and HMF yield in DMSO. Transformation of monoclinic phase to tetragonal phase occurs when sulfur content is between 2-4 wt % in sulfated zirconia. Thus, three different sulfur contents were determined as 2.5, 3 and 3.5 wt %. Chlorosulfonic acid has higher acidic strength

and concentration than other sulfating agents, so it was selected as sulfating agent. Calcination temperature was selected as 450 °C since sulfates decompose at ~500 °C.

In order to improve the stability, dispersion and surface area of the sulfated catalyst, also effect of carbon ions on reaction, activated carbon (AC) was determined as support. Sulfated AC was prepared. Zirconium sulfate loaded AC was also prepared to investigate the effect of Zr and SO<sub>4</sub> interaction with this support.

Pore size of the catalyst affect the fructose conversion and HMF yield. Molecular size of fructose and HMF molecules are very large (0.87 nm fructose and 0.6 nm HMF). Thus catalyst should has mesopores for rapid fructose adsorption. In micropores this adsorption was found very slow and pore blockages occur (Juan et al., 2008). Mesoporous silica was selected to investigate the effect of porosity. Sulfate and zirconium sulfate loaded silica were prepared.

It was reported that single metal oxides include solely Lewis acid sites and some basic sites. Sulfation of these oxides create Brønsted acid sites. On the other hand, leaching problems were also reported in literature in sulfated single metal oxides. In order to overcome this problem, mixed metal oxides, such as titania silicates were sulfated since strong bonds and superacid sites form during sulfation. The strongest interaction of sulfur with mixed oxides was found in sulfated titania silicates by chelating bidentate bonds (Yang et al., 2009). Thus mesoporous sulfated titania silica and sulfated titania incorporated SBA-15 catalysts were determined. Three different Ti contents (2-6 wt. %) were investigated. Calcination temperature of titania silicates were determined as 550 °C. Temperature higher than 550 °C, more basic sites form. After sulfation titania silicates were again calcined at 450 °C to prevent the decomposition of sulfates when temperature was 500 °C. Li et al. (2013) found La<sup>3+</sup> as a good stabilizer for TiO<sub>2</sub>-SiO<sub>2</sub> catalyst. In the presence of La, sulfur make strong bond with Ti, Si and La. La incorporated sulfated titania silicate and sulfated titania-SBA-15 were prepared and tested.

Solvents ranging from organic ones to the alcohols, ionic liquids to aqueous based ones are studied. Ionic liquids are very expensive inspite of its high effectivity. Organic solvents, especially high boiling point ones, provide satisfactory HMF selectivities. Nevertheless, they are very expensive due to their high boiling points. Most of them are also not environmentally benign. Environmental solvents are alcohols and water. But there is still need for a highly stable and active catalyst to work in water

and alcohols with high HMF yields. Water in the reaction medium cause rehydration of HMF and side products form seuch as levulinic and formic acids. Biphasic solvents, such as MIBK-water mixture reduce the rehydration and side products. In the presence of MIBK as an extracting phase, HMF formed transfer from water to the MIBK thus rehydration was minimized. Addition of butanol increase the mass transfer rate of HMF between organic-aqueous phases. For that reasons, water, water-MIBK and water-MIBK-butanol solvents were determined for the present study. DMSO was also studied for comparison purpose.

Fructose concentration has an important effect on product distribution. When fructose was lower side products form at short reaction times due to the rapid conversion. On the other hand, when fructose was higher collision of fructose molecules occur which cause humins and insoluble polymers formation. Thus, different fructose/catalyst weight ratios (0.5, 1 and 2) were also examined in the proposed study.

Reaction temperature affect the product distribution significantly. Reaction constant of HMF formation was found higher than side reactions. Thus, higher HMF yields were obtained at higher reaction temperatures. Three different reaction temperatures (110, 160 and 200 °C) were studied to investigate the reaction kinetics and temperature effects on product distributions.

In the light of the literature review given in this chapter, it was aimed to prepare  $\text{SO}_4/\text{ZrO}_2$ ,  $\text{SO}_4/\text{AC}$ ,  $\text{SO}_4/\text{SiO}_2$ ,  $\text{Zr-SO}_4/\text{AC}$ ,  $\text{Zr-SO}_4/\text{SiO}_2$ ,  $\text{SO}_4/\text{TiO}_2\text{-SiO}_2$  and  $\text{SO}_4/\text{Ti-SBA-15}$  catalysts. Different Ti contents and La addition  $\text{SO}_4/\text{TiO}_2\text{-SiO}_2$  were studied. Single (Water and DMSO) and biphasic solvents (water-MIBK and water-MIBK-butanol) were also investigated. Different reaction temperatures (110, 160 and 200 °C) and fructose/catalyst weight ratios (0.5, 1 and 2) were studied for determining the reaction kinetics.

## CHAPTER 4

### EXPERIMENTAL STUDY

#### 4.1. Materials

List of the chemicals used in this study are given in Table 4.1.

Table 4.1. List of the chemicals used.

Chemicals	
2-butanol	Sigma Aldrich, 99.5 %
Activated charcoal	Sigma-Aldrich
Ammonium hydroxide solution	Riedel de Haen, 26 %
Ammonium sulfate	Sigma Aldrich, $\geq 99$ %
Chlorosulfonic Acid	Sigma-Aldrich, $\geq 99$ %
Dichloromethane	Sigma-Aldrich, $\geq 99.5$ %
Dimethyl sulfoxide	Sigma-Aldrich, $\geq 99.7$ %
Ethanol	Sigma Aldrich, $\geq 99.8$ %
Hydrochloric Acid	Sigma-Aldrich, 37 %
Methyl isobutyl ketone	Sigma Aldrich, $\geq 98.5$ %
Phosphoric acid	Sigma-Aldrich, $\geq 85$ %
Pluronic P123	Aldrich average $M_n \sim 5,800$
Silica gel	Sigma-Aldrich, DAVISIL grade, 99 %
Sulfuric Acid	Sigma Aldrich, 98 %
Tetraethyl orthosilicate	Sigma-Aldrich, 98 %
Titanium(IV) isopropoxide	Sigma-Aldrich, $\geq 97$ %
Zirconium(IV) oxychloride octahydrate	Sigma-Aldrich, $\geq 99.5$ %
Zirconium(IV) sulfate hydrate	Sigma-Aldrich, 99.99 %

## 4.2. Catalyst Preparation

### 4.2.1. Sulfated Zirconia, Silica and AC Preparation

Sulfated zirconia, silica and AC were prepared as follows. Zirconium oxychloride solution (0.5 M) was precipitated with 0.5 M  $\text{NH}_4\text{OH}$  at pH 9-10 to obtain  $\text{ZrO}(\text{OH})_2$ . The precipitate was washed with deionized water until the pH of the solution reached to 7. Then, it was dried for 24 h at 100 °C. Different concentrations (0.375, 0.425 and 0.525 M) of chlorosulfonic acid agents in dichloromethane were prepared to obtain 2.5, 3.0 and 3.5 wt. % S loaded catalysts, respectively.  $\text{ZrO}(\text{OH})_2$  (1 g) prepared was immersed into 15 ml of chlorosulfonic acid solution and the mixture was mixed for 5 min. After the obtained products were washed with hot water (80 °C), it was dried at 120 °C for 24 h. Obtained materials were calcined at 450 °C for 6 h to obtain  $\text{SO}_4/\text{ZrO}_2$  catalysts.

For sulfated  $\text{SiO}_2$  preparation, 0.5 M chlorosulfonic acid in dichloromethane was prepared.  $\text{SiO}_2$  (1 g) was immersed into 15 ml of the dichloromethane solution and this mixture was stirred for 5 min. Obtained slurry was dried at 120 °C for 24 h. Dried powder was calcined at 450 °C for 6 h to obtain  $\text{SO}_4/\text{SiO}_2$ .

Sulfated activated carbon catalysts ( $\text{SO}_4/\text{AC}$ ) were prepared via hydrothermal treatment. AC (0.1 g) sample of was added into 50 ml of 1 M  $\text{H}_2\text{SO}_4$  solution. This mixture was placed into an autoclave and kept in an oven at 85 °C for 4 h. Then, the sample was cooled in ice bath. After washing with hot distilled water (80 °C), it was dried overnight at 100 °C to obtain  $\text{SO}_4/\text{AC}$ .

Labeling of prepared sulfated zirconia catalysts containing 2.5, 3.0 and 3.5 wt. % of sulfur and prepared sulfated silica and AC are given in Table 4.2.

Table 4.2. The labels of the sulfated zirconia catalysts.

<b>Catalysts</b>	<b>Labels</b>
Sulfated zirconia, 2.5 % sulfated loading	SO <sub>4</sub> /ZrO <sub>2</sub> -2.5
Sulfated zirconia, 3.0 % sulfated loading	SO <sub>4</sub> /ZrO <sub>2</sub> -3.0
Sulfated zirconia, 3.5 % sulfated loading	SO <sub>4</sub> /ZrO <sub>2</sub> -3.5
Sulfated silica	SO <sub>4</sub> /SiO <sub>2</sub>
Sulfated activated carbon	SO <sub>4</sub> /AC

#### 4.2.2. Silica and AC Supported Zirconium Sulfate Preparation

Silica and activated carbon supported zirconium sulfate were prepared as follows. Zirconium sulfate (0.1 g) was dissolved in water (25 ml) at room temperature and silica (1 g) was added into this solution. The mixture was stirred for 2 h. Then it was evaporated at 50 °C under 180 mbar vacuum in rotary evaporator. The powder obtained was dried at 120 °C for 24 h and then calcined at 450 °C for 6 h to obtain zirconium sulfate loaded silica (ZS/SiO<sub>2</sub>).

The same procedure was applied for the preparation of sulfated activated carbon (ZS/AC). In this preparation obtained powder was calcined at 160 °C for 8 h to obtain ZS/AC.

Prepared silica and activated carbon supported zirconium sulfates and their labels are given in Table 4.3.

Table 4.3. The labels of the zirconium sulfate loaded catalysts.

<b>Catalysts</b>	<b>Labels</b>
Zirconium sulfate loaded silica (ZrSO <sub>4</sub> /SiO <sub>2</sub> )	ZS/SiO <sub>2</sub>
Zirconium sulfate loaded activated carbon (ZrSO <sub>4</sub> /AC)	ZS/AC

### 4.2.3. Titania-Silicate and Sulfated Titania-Silicate Preparation

Titania silica and sulfated titania silica were prepared as follows. A solution of tetraethylorthosilicate (TEOS (7 ml)), H<sub>2</sub>O (40 ml) and ethanol (35 ml) was prepared. Hydrochloric acid (1 M) was added dropwise until the solution pH reached to 3. After stirring this solution for 2 h, different amounts of titanium isopropoxide (TISOP) (0.5 and 1.5 ml for 2 and 6 wt. % Ti loadings, respectively) dissolved in ethanol (TISOP/ethanol=1:10) was added. The solution temperature was kept around 20 °C during TISOP addition in order to prevent the precipitation of Ti particles. For La loaded catalyst, 0.1 g lanthanum (III) nitrate hexahydrate was also added. After that, solution temperature was increased to 80 °C to complete the gelation. Formed gel was dried at 80 °C for 24 h. The dried samples were grinded and calcined at 550 °C for 6h. TiO<sub>2</sub>-SiO<sub>2</sub> formed was then sulfated using 5 ml of a 1 M (NH<sub>4</sub>)<sub>2</sub>SO<sub>4</sub> solution per gram of catalyst. Sulfated TiO<sub>2</sub>-SiO<sub>2</sub> was calcined at 450 °C for 6 h to obtain SO<sub>4</sub>/TiO<sub>2</sub>-SiO<sub>2</sub> and SO<sub>4</sub>/La-TiO<sub>2</sub>-SiO<sub>2</sub>.

Prepared titania silica, sulfated titania silica and La containing sulfated titania silica catalysts with 2 and 6 wt. % of Ti and their labels are given in Table 4.4.

Table 4.4. The labels of different titania silicate catalysts prepared.

	<b>Catalysts</b>	<b>Labels</b>
<b>1)</b>	TiO <sub>2</sub> -SiO <sub>2</sub> -2 wt. % Ti	TS-2
<b>2)</b>	TiO <sub>2</sub> -SiO <sub>2</sub> -6 wt. % Ti	TS-6
<b>3)</b>	SO <sub>4</sub> /TiO <sub>2</sub> -SiO <sub>2</sub> -2 wt. % Ti	SO <sub>4</sub> /TS-2
<b>4)</b>	SO <sub>4</sub> /TiO <sub>2</sub> -SiO <sub>2</sub> -6 wt. % Ti	SO <sub>4</sub> /TS-6
<b>5)</b>	SO <sub>4</sub> /La~TiO <sub>2</sub> -SiO <sub>2</sub> - (1 wt. % La and 6 wt % Ti)	SO <sub>4</sub> /La-TS-6

#### 4.2.4. Ti-SBA-15 and Sulfated Ti-SBA-15 Preparation

Mixture of 9 g Pluronic P-123 and 220 ml water was stirred for 2 h at 40 °C. After adding 4.54 g of HCl (1 M) to this solution, different amounts of TISOP (0.8 and 2.4 ml for 2 and 6 wt. % Ti loadings, respectively) and 20 g TEOS were added. For La loaded catalyst, 0.16 g Lanthanum (III) nitrate hexahydrate was also added. The solution obtained was stirred for 24 h at 40 °C. The resulting gel was transferred to the autoclave and kept at 100 °C for 24 h for hydrothermal synthesis. Final product was washed, centrifuged, dried at 100 °C for 24 h and calcined at 550 °C for 6 h. Obtained Ti-SBA-15 was sulfated using 5 ml of 1 M (NH<sub>4</sub>)<sub>2</sub>SO<sub>4</sub> solution per gram of catalyst. Sulfated catalysts were calcined at 450 °C for 6 h to obtain SO<sub>4</sub>/TiSBA-15 and SO<sub>4</sub>/La-TiSBA-15.

Prepared sulfated titania SBA-15 catalysts with 2 and 6 wt. % of Ti and La containing titania SBA-15 catalysts and their labels are given in Table 4.5.

Table 4.5. Different sulfated Ti-SBA-15 catalysts prepared.

Catalysts	Catalyst Labels
SO <sub>4</sub> /Ti-SBA-15 -2 wt. % Ti	SO <sub>4</sub> /TiSBA-2
SO <sub>4</sub> /Ti-SBA-15-6 wt. % Ti	SO <sub>4</sub> /TiSBA-6
SO <sub>4</sub> /La-Ti-SBA-15 – (1 wt. % La and 6 wt. % Ti)	SO <sub>4</sub> /La-TiSBA-6

#### 4.2.5. Homogeneous Catalysts Studied

HCl, H<sub>3</sub>PO<sub>4</sub> and H<sub>2</sub>SO<sub>4</sub> were tested as homogeneous catalysts in fructose dehydration. Initial amounts of mineral acids was given in reaction tests section.

### **4.3. Characterization of the Catalysts Prepared**

#### **4.3.1. X-Ray Diffraction (XRD)**

The crystalline structures of the samples were determined by Philips X'Pert diffractometer with CuK $\alpha$  radiation. The scattering angle  $2\theta$  was varied from 5° to 70°, with a step length of 0.02.

#### **4.3.2. N<sub>2</sub> Adsorption/Desorption Tests (BET)**

Nitrogen physisorption studies were performed using Micromeritics ASAP 2010 model static volumetric adsorption instrument. The samples were dried in oven at 100°C over night prior to degassing. Then catalysts were outgassed at 300 °C for 24 hours under 5  $\mu$ mHg vacuum.

#### **4.3.3. Temperature Programmed Desorption (TPD)**

The acidity of the samples was determined by Temperature-Programmed Desorption of Ammonia (NH<sub>3</sub>-TPD) method using Micromeritics AutoChem II Chemisorption Analyzer instrument. The sample was heated up to 500 °C by increasing the temperature at a rate of 5 °C/min and kept at this temperature for 1 h under He gas flow of 70 ml/min. Then the sample was cooled under He flow of 30 ml/min to 90 °C at a rate of 5 °C/min. This was followed by switching the flow to NH<sub>3</sub>-He gas mixture (10 %) at the rate of 30 ml/min for 30 min. Physically adsorbed NH<sub>3</sub> was removed by degassing the sample at 90 °C under He flow of 70 ml/min for 120 min and then at the rate of 30 ml/min for 150 min. NH<sub>3</sub> desorption of the sample was analyzed by heating the sample at the rate of 10 °C/min from 90 °C to 600 °C. TCD signal was recorded during the NH<sub>3</sub>-TPD.

#### **4.3.4. Fourier Transform Infrared Spectroscopy (FT-IR)**

Nature of the acid sites of the catalysts was measured by IR spectroscopy with pyridine adsorption method. The samples were degassed at 400 °C under vacuum ( $2 \times 10^{-2}$  mmHg) for 2 h. Adsorption of pyridine was carried out at 150 °C for 30 min. Before FT-IR analysis the samples were kept at 150 °C under vacuum ( $2 \times 10^{-2}$  mmHg) for 30 min to desorb the physisorbed pyridine.

IR characterizations were carried out between 400 and 4000  $\text{cm}^{-1}$  wavenumbers with Shimadzu FT-IR-8201 model Fourier Transformed Infrared Spectrometer using KBr pellet technique. KBr pellets were prepared by pressing a mixture of 4.5 mg catalyst sample and 150 mg KBr.

#### **4.3.5. X-Ray Fluorescence Spectroscopy (XRF)**

Elemental composition of the catalyst was analyzed with XRF before and after the reaction. The analysis was performed with powder method by using Spectro IQ II instrument and  $\text{CuK}\alpha$  radiation.

### **4.4. Fructose Dehydration Tests**

Activity tests at 110 °C were performed in a 200 ml stirred multiple batch reactor under  $\text{N}_2$  atmosphere as follows. Initially, 0.5 g catalyst was added into 40 ml DMSO solvent. This mixture was stirred in the reactor until desired reaction temperature was reached. Then, 6 wt. % of fructose dissolved in 10 ml solvent was added to the reactor. Samples were taken at every 30 min during 180 min of reaction time. After removing solid particles by centrifugation, each sample was diluted 25 times with 5 mM  $\text{H}_2\text{SO}_4$  solution for analysis.

Activity tests at higher temperatures (160 and 200 °C) were performed in a 2 L stirred high pressure batch reactor under  $\text{N}_2$  atmosphere. Initially, 5 g catalyst was added to 400 ml solvent. This mixture was stirred until the reaction temperature was reached. Then, 6 wt. % of fructose dissolved in 100 ml solvent was added to the reactor.

Samples were taken every 30 min during 180 min of reaction time. Each sample was centrifuged and diluted 25 times with 5 mM H<sub>2</sub>SO<sub>4</sub> solution for analysis.

Activity tests of the catalysts were also carried out in different solvents which were DMSO, water, water-MIBK (30/70 %) and water-MIBK-butanol (30/60/10 %).

For reusability tests, used catalysts were regenerated by washing them with water and MIBK, and calcination at 550 °C for 6 h. After this treatment, they were tested up to 4 times.

Reaction products were analyzed by using High Pressure Liquid Chromatography (HPLC) equipped with UV-Vis and Refractive Index Detector (RID) with a Bio-Rad Aminex HPX-87H column.

The fructose conversion, HMF selectivity and yield were calculated as follows:

Fructose conversion (mol %):

$$X = \frac{\text{Moles of fructose reacted}}{\text{Initial moles of fructose}} \times 100\%$$

HMF selectivity (mol %):

$$S = \frac{\text{Moles of HMF produced}}{\text{Moles of fructose reacted}} \times 100\%$$

HMF yield (mol %):

$$Y = \frac{\text{Moles of HMF produced}}{\text{Initial moles of fructose}} \times 100\%$$

## CHAPTER 5

### RESULTS AND DISCUSSIONS

List of the different catalysts prepared and their labels are given in Table 5.1.

Table 5.1. Different sulfated catalysts prepared.

Catalysts	Labels
SO <sub>4</sub> /ZrO <sub>2</sub> - 2.5 % S	SO <sub>4</sub> /ZrO <sub>2</sub> -2.5
SO <sub>4</sub> /ZrO <sub>2</sub> - 3.0 % S	SO <sub>4</sub> /ZrO <sub>2</sub> -3.0
SO <sub>4</sub> /ZrO <sub>2</sub> - 3.5 % S	SO <sub>4</sub> /ZrO <sub>2</sub> -3.5
SO <sub>4</sub> /SiO <sub>2</sub>	SO <sub>4</sub> /SiO <sub>2</sub>
SO <sub>4</sub> /AC	SO <sub>4</sub> /AC
ZrSO <sub>4</sub> /SiO <sub>2</sub>	ZS/SiO <sub>2</sub>
ZrSO <sub>4</sub> /AC	ZS/AC
TiO <sub>2</sub> -SiO <sub>2</sub> -2 wt. % Ti	TS-2
TiO <sub>2</sub> -SiO <sub>2</sub> -6 wt. % Ti	TS-6
SO <sub>4</sub> /TiO <sub>2</sub> -SiO <sub>2</sub> -2 wt. % Ti	SO <sub>4</sub> /TS-2
SO <sub>4</sub> /TiO <sub>2</sub> -SiO <sub>2</sub> -6 wt. % Ti	SO <sub>4</sub> /TS-6
SO <sub>4</sub> /La~TiO <sub>2</sub> -SiO <sub>2</sub> - (1 wt. % La and 6 wt % Ti)	SO <sub>4</sub> /La-TS-6
SO <sub>4</sub> /Ti-SBA-15 -2 wt. % Ti	SO <sub>4</sub> /TiSBA-2
SO <sub>4</sub> /Ti-SBA-15-6 wt. % Ti	SO <sub>4</sub> /TiSBA-6
SO <sub>4</sub> /La-Ti-SBA-15 - (1 wt. % La and 6 wt. % Ti)	SO <sub>4</sub> /La-TiSBA-6

#### 5.1. Homogeneous Catalysts

Fructose dehydration tests were also carried out over homogeneous catalysts (HCl, H<sub>3</sub>PO<sub>4</sub> and H<sub>2</sub>SO<sub>4</sub>) and without using a catalyst in DMSO at 110 °C. Product distributions, activity and selectivity results are given in the following section.

### 5.1.1. Activities of Homogeneous Catalysts in DMSO

Product distributions obtained in blank reaction (test without using a catalyst) and over homogeneous mineral acid catalysts (HCl, H<sub>3</sub>PO<sub>4</sub> and H<sub>2</sub>SO<sub>4</sub>) are given in Figures 5.1, 5.2, 5.3 and 5.4. As fructose reacted, HMF was formed. The main by-products observed were levulinic acid, formic acid and glucose. In blank reaction, formic acid concentration increased rapidly due to the rehydration. Less HMF and more by-products were formed without catalyst. In mineral acids, most of the fructose was sharply consumed in 1 min. The highest amount of HMF (306 mmol/L at 150 min) was formed with H<sub>2</sub>SO<sub>4</sub>. Rehydration of HMF was also observed in H<sub>3</sub>PO<sub>4</sub> and H<sub>2</sub>SO<sub>4</sub>, since formic and levulinic acids formation raised as HMF concentration was reduced. Much amount of formic acid was also produced over HCl.

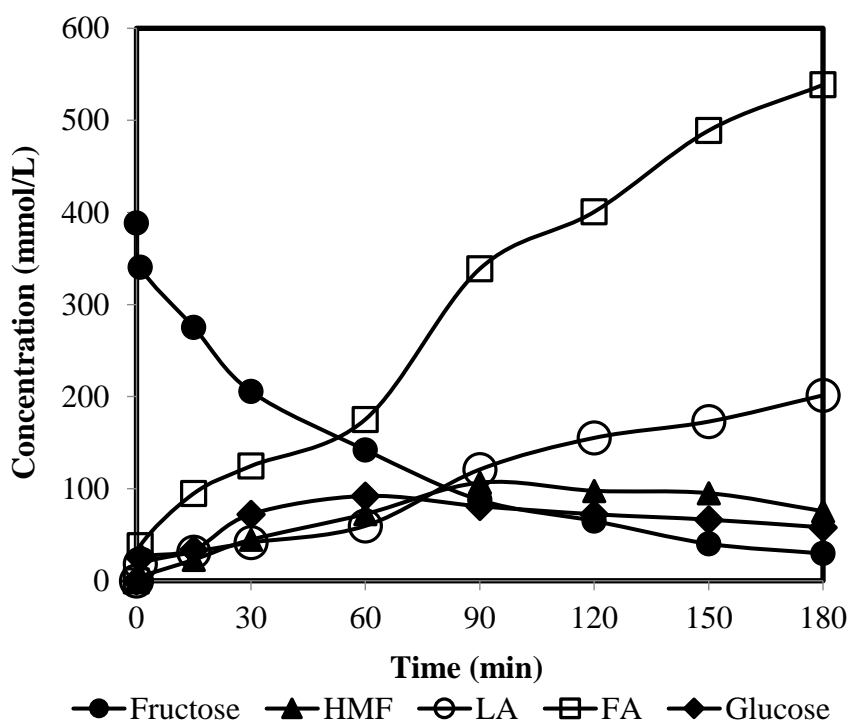


Figure 5.1. Product distribution without using a catalyst at 110 °C in DMSO.

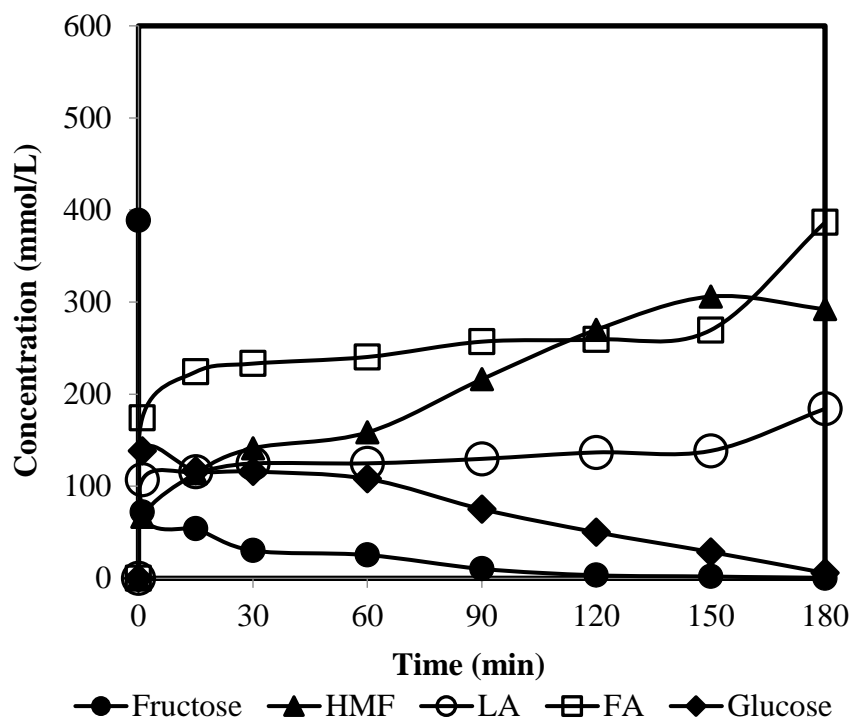


Figure 5.2. Product distribution over homogeneous H<sub>2</sub>SO<sub>4</sub> at 110 °C in DMSO.

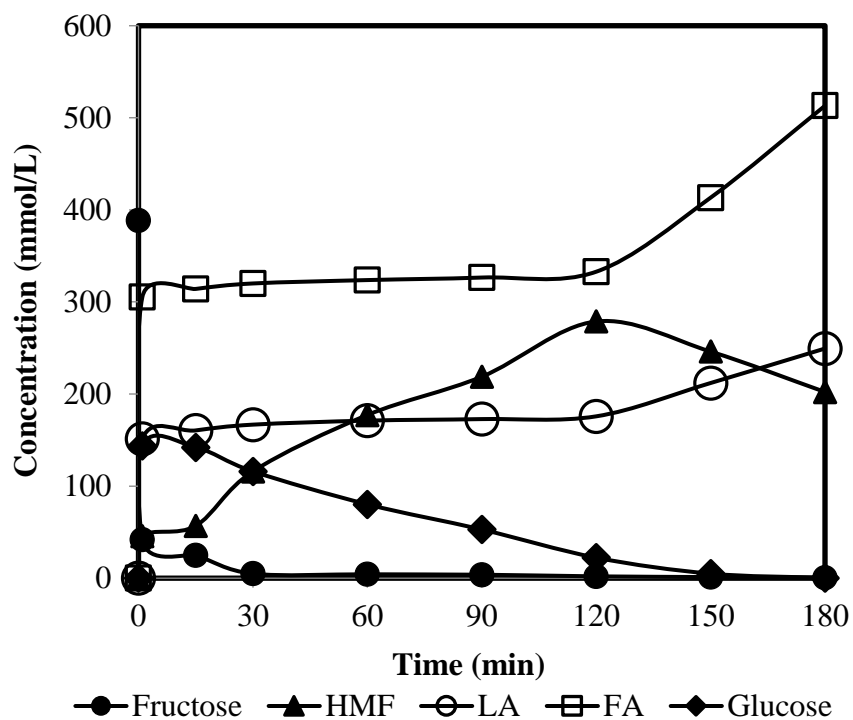


Figure 5.3. Product distribution over homogeneous H<sub>3</sub>PO<sub>4</sub> at 110 °C in DMSO.

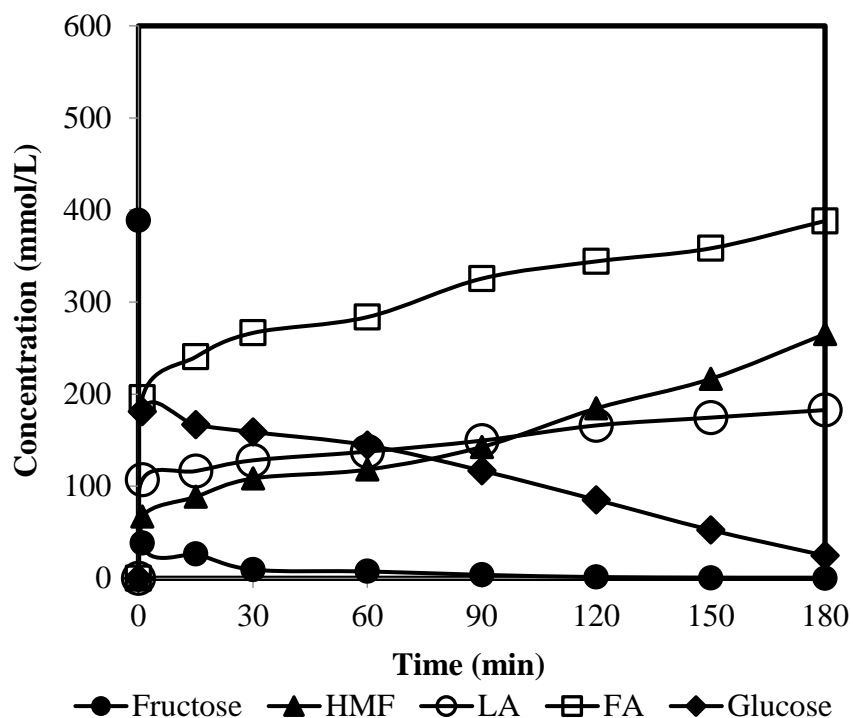


Figure 5.4. Product distribution over homogeneous HCl at 110 °C in DMSO.

Fructose conversions obtained without using a catalyst and with homogeneous mineral acids are given in Figure 5.5. Conversions increased with reaction time. Without a catalyst, fructose conversion was lower at the beginning of the reaction but 93 % of the fructose was consumed in 180 min. DMSO also acted as catalyst as discussed in chapter 3 which was the reason of the high fructose conversion in blank test. Over homogeneous catalysts fructose was rapidly consumed with time. All of the catalysts were very active. Conversion reached 80-90 % in less than 1 min and complete conversion of fructose was achieved in 90 min with these catalysts.

Selectivities to HMF achieved in blank reaction and over homogeneous are given in Figure 5.6. Selectivities changed with the homogeneous catalyst used and without a catalyst. In blank reaction, selectivity increased with reaction time up to 90 min, reached 35 %. After 90 min, it was reduced slowly up to 21 % in 3 h. Obtained selectivity in blank reaction was attributed to the dual role of DMSO as solvent and reaction mediator. Besides, higher amounts of furanoid forms of fructose provided higher HMF selectivities. Bicker et al. (2005) stated that furanoid forms were much favored in DMSO. Selectivity also improved with reaction time over homogeneous acid catalysts. After 120-150 min, HMF was rehydrated thus selectivity was reduced over  $H_2SO_4$  and  $H_3PO_4$ ; this reduction was rapid over  $H_3PO_4$ . Selectivity was lower with HCl catalyst at the beginning, and then reached to 69 % at 180 min. The highest selectivity

(80 %) was obtained with  $\text{H}_2\text{SO}_4$  at 150 min. This result was attributed to the highest acid strength of  $\text{H}_2\text{SO}_4$  among the homogeneous catalysts and also effects of sulfate ions in fructose dehydration.

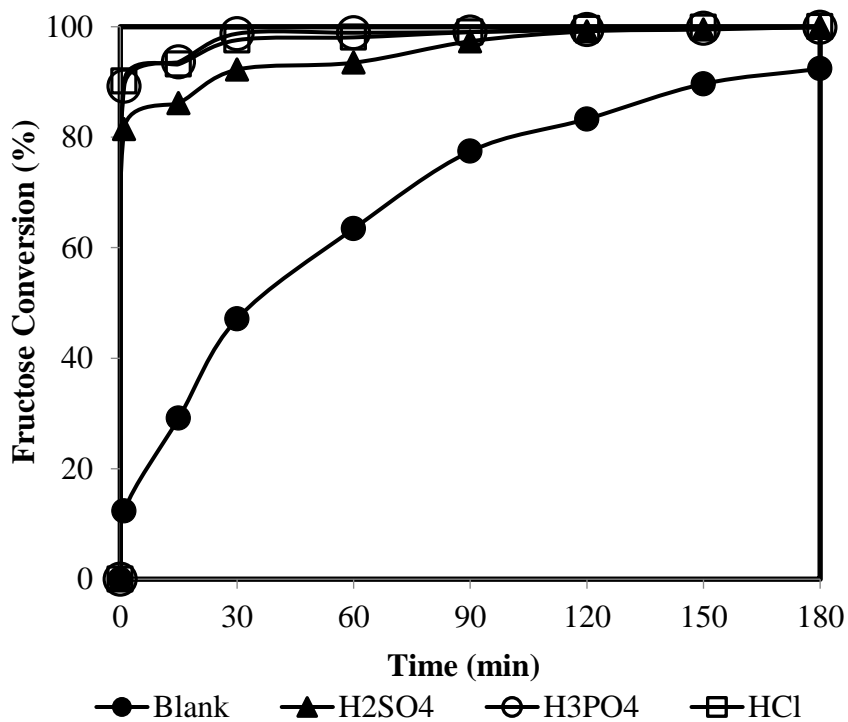


Figure 5.5. Fructose conversions over homogeneous catalysts and without a catalyst at 110 °C in DMSO.

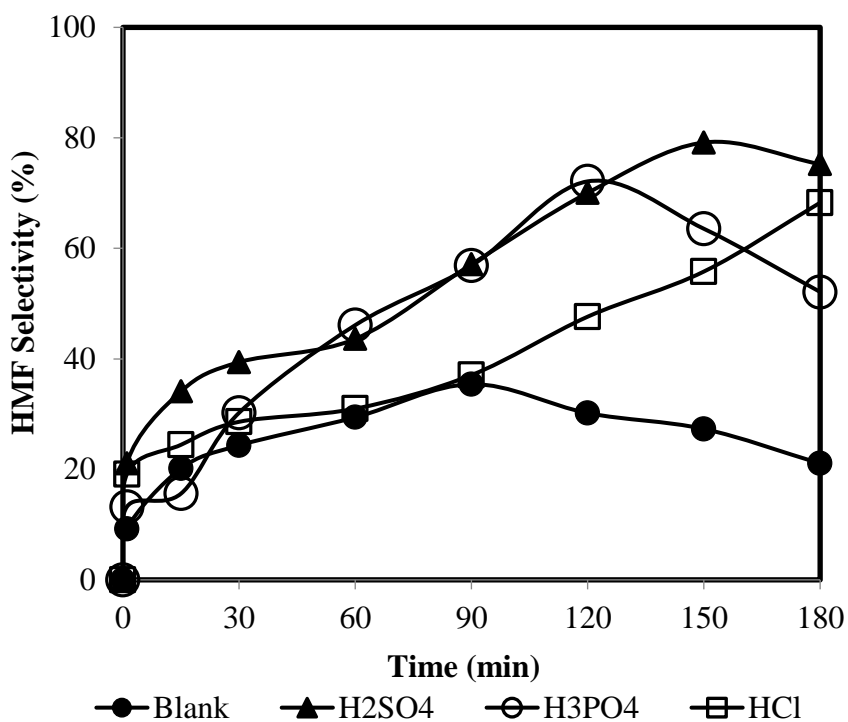


Figure 5.6. HMF selectivities over homogeneous catalysts and without a catalyst at 110 °C in DMSO.

## 5.2. Sulfated Zirconia Catalysts

### 5.2.1. Characterization of the Sulfated Zirconia Catalysts

XRD patterns of the  $\text{SO}_4/\text{ZrO}_2$ -2.5,  $\text{SO}_4/\text{ZrO}_2$ -3 and  $\text{SO}_4/\text{ZrO}_2$ -3.5 are given in Figure 5.7. All the patterns were found to be compatible with the literature.  $\text{SO}_4/\text{ZrO}_2$ -2.5 and  $\text{SO}_4/\text{ZrO}_2$ -3.5 contained a mixture of monoclinic and tetragonal phases whereas  $\text{SO}_4/\text{ZrO}_2$ -3 had almost mainly tetragonal phase. This was also discussed in previous chapter and same findings were observed by Qi et al. (2009) and Farcasiu et al. (1997). They reported that although pure zirconia has monoclinic phases, tetragonal phases are formed from monoclinic ones during calcination between 450 and 450°C. The amount of monoclinic crystals was minimized at 3 % S loading and most of them were transformed into tetragonal phase above 400 °C during calcination (450 °C).

The sulfur content, acidities and textural properties of the prepared sulfated zirconia catalysts are given in Table 5.2.  $\text{SO}_4/\text{ZrO}_2$ -3.5 had the highest amount of sulfur. Sulfated zirconia catalysts had mesopores and low surface area. Slight reduction in surface area was observed when amount of sulfur loading increased. Pore size also decreased as sulfur loaded. This was due to the pore narrowing by adsorption of sulfur ions on to pore mouths. Sulfur content of the sulfated zirconia catalysts also measured and the results are given in Table 5.2.

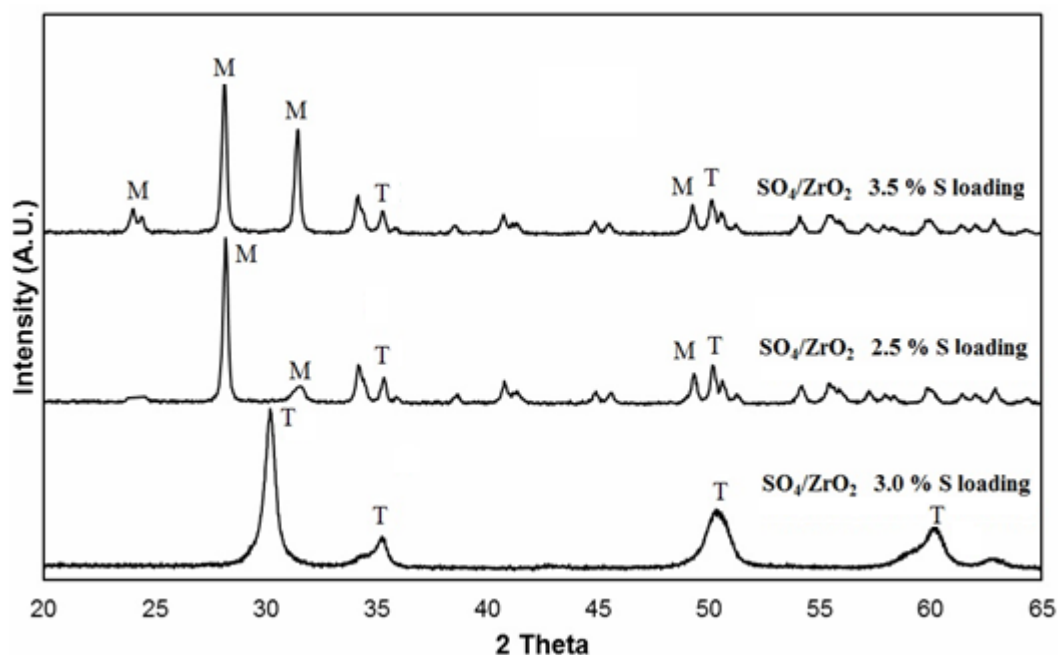


Figure 5.7. XRD patterns of different sulfated zirconia catalysts (T: tetragonal, M: monoclinic).

Table 5.2. Textural properties of sulfated zirconia catalysts.

	* Surface Area (m <sup>2</sup> /g)	** Pore Diameter (Å)	Total Acidity (μmol NH <sub>3</sub> / gcat)	Brønsted Area	Lewis Area	Sulfur Content (wt. %)
SO <sub>4</sub> /ZrO <sub>2</sub> -2.5	132.1	56.3	429.4	0.185	0.175	2.68
SO <sub>4</sub> /ZrO <sub>2</sub> -3.0	120.4	52.4	474.2	0.395	0.284	3.09
SO <sub>4</sub> /ZrO <sub>2</sub> -3.5	109.0	43.5	493.1	0.388	0.423	3.55

\* Surface area calculated by using BET model.

\*\* Pore diameter calculated by using Barrett-Joyner-Halenda (BJH) method.

The amount of acid sites and acid strength of SO<sub>4</sub>/ZrO<sub>2</sub> catalysts measured by NH<sub>3</sub>-TPD are given in Figure 5.8. The desorption peaks centered at low temperature (200°C) and high temperature (450 °C) regions are referred to as weak and strong acid sites, respectively. All of the SO<sub>4</sub>/ZrO<sub>2</sub> catalysts had both weak and strong acid sites. SO<sub>4</sub>/ZrO<sub>2</sub>-3 exhibited the highest amount of strong acid sites. This was attributed to the presence of more amounts of tetragonal phases in this catalyst, since these phases are known as strong acidic sites (Qi et al., 2009). Temperature-programmed desorption of ammonia also allows quantitative determination of the total amount of the acid sites. Results are given in Table 5.2. The amount of acid sites increased with sulfur loading.

Although total acid sites of  $\text{SO}_4/\text{ZrO}_2\text{-3.5}$  were slightly higher than  $\text{SO}_4/\text{ZrO}_2\text{-3.0}$ ,  $\text{SO}_4/\text{ZrO}_2\text{-3.5}$  had significantly lower amount of strong sites.

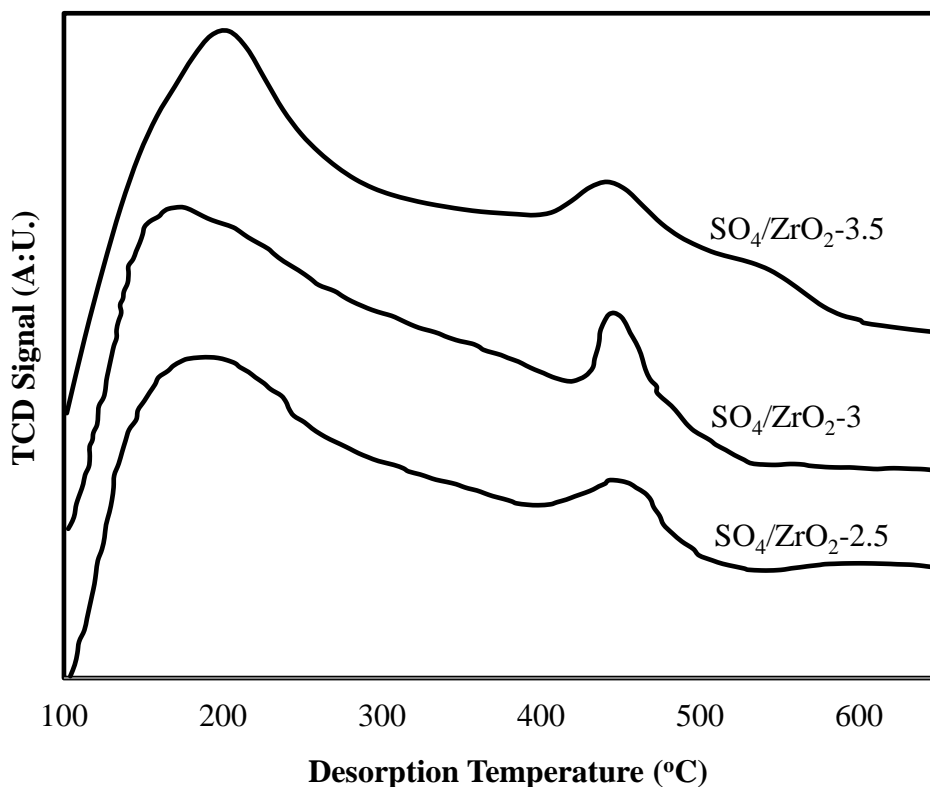


Figure 5.8.  $\text{NH}_3$ -TPD profiles of the sulfated zirconia catalysts.

The nature of the acid sites of the  $\text{SO}_4/\text{ZrO}_2$  catalysts determined by FT-IR spectroscopy by pyridine adsorption is given in Figure 5.9. There is a broad band at  $1548\text{ cm}^{-1}$  which is assigned to Brønsted acid sites. The intense band at  $1490\text{ cm}^{-1}$  is assigned to Brønsted and Lewis acid sites. The band at  $1455\text{ cm}^{-1}$  is related to Lewis acidity. Peak areas increased with acidity of the catalysts. It was observed from each spectrum that all the catalysts had Brønsted and Lewis acid sites. Total acid sites increased with the amount of S loading as obtained by  $\text{NH}_3$ -TPD. On the other hand, Brønsted sites in  $\text{SO}_4/\text{ZrO}_2\text{-3.5}$  were slightly lower than in  $\text{SO}_4/\text{ZrO}_2\text{-3}$  catalyst, since  $\text{SO}_4/\text{ZrO}_2\text{-3.5}$  had fewer amounts of acidic tetragonal phases.

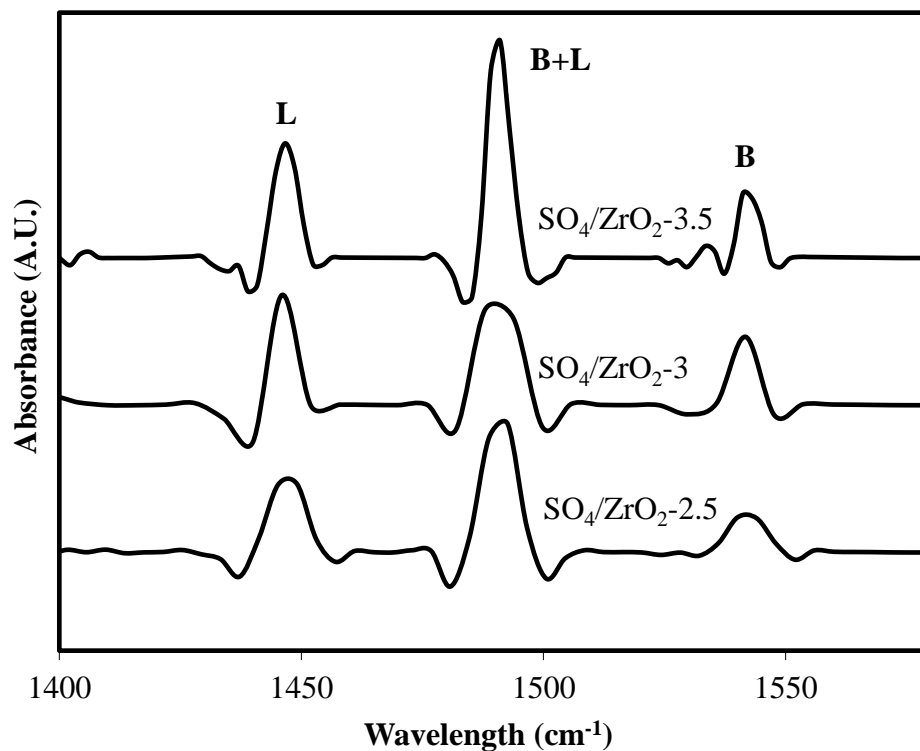


Figure 5.9. FT-IR spectra of the sulfated zirconia catalysts after pyridine adsorption (B: Brønsted acid sites, L: Lewis acid sites).

### 5.2.2. Activities of the Sulfated Zirconia Catalysts in DMSO

Product distributions obtained over sulfated zirconia catalysts with different sulfur loadings are given in Figures 5.10, 5.11 and 5.12. HMF was formed as fructose consumed. The main by-products were glucose, levulinic and formic acids. Over  $\text{SO}_4/\text{ZrO}_2\text{-3.0}$ , LA and FA concentrations increased sharply in 15 min due to the rapid fructose conversion; then changed slowly. On the other hand, over  $\text{SO}_4/\text{ZrO}_2\text{-3.5}$ , amounts of LA and FA formed raised steadily. The least amount of HMF and also rehydration products were observed with  $\text{SO}_4/\text{ZrO}_2\text{-2.5}$ . This was attributed to the lowest amounts of Brønsted sites of  $\text{SO}_4/\text{ZrO}_2\text{-2.5}$  which are responsible from HMF formation. The highest amount of HMF (309 mmol/L) was obtained with  $\text{SO}_4/\text{ZrO}_2\text{-3.0}$  catalyst. Rehydration of HMF occurred over all catalysts after 90-120 min.

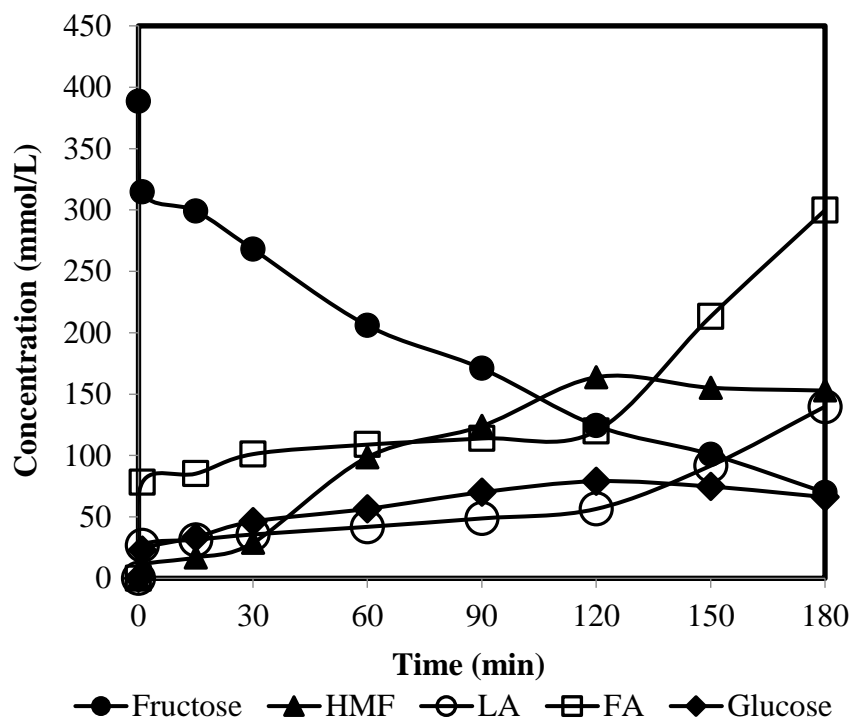


Figure 5.10. Product distribution obtained over SO<sub>4</sub>/ZrO<sub>2</sub>-2.5 at 110 °C in DMSO.

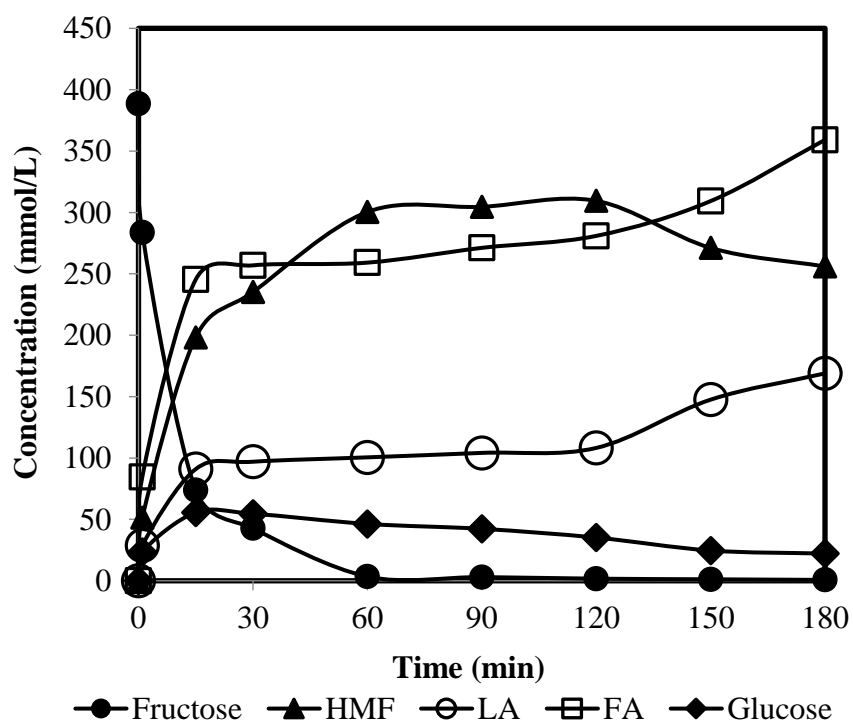


Figure 5.11. Product distribution obtained over SO<sub>4</sub>/ZrO<sub>2</sub>-3.0 at 110 °C in DMSO.

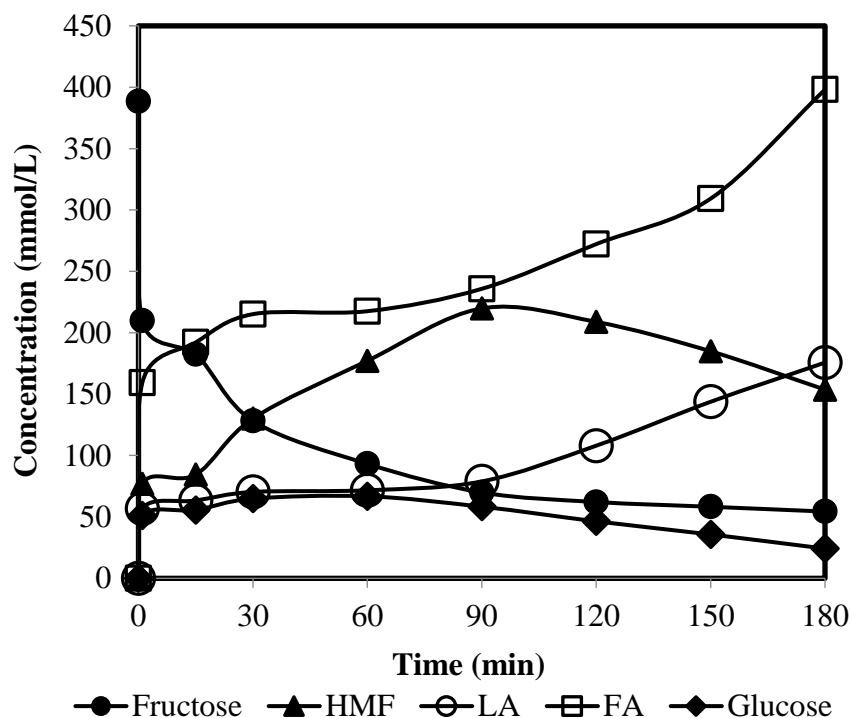


Figure 5.12. Product distribution obtained over  $\text{SO}_4/\text{ZrO}_2\text{-3.5}$  at  $110\text{ }^\circ\text{C}$  in DMSO.

Fructose conversions over  $\text{SO}_4/\text{ZrO}_2$  catalysts are given in Figure 5.13.  $\text{SO}_4/\text{ZrO}_2\text{-3}$  catalyst was found the as the most active catalyst. Complete fructose conversion was obtained in 60 min with this catalyst. However, fructose consumptions were 80 % at 180 min over  $\text{SO}_4/\text{ZrO}_2\text{-2.5}$  and  $\text{SO}_4/\text{ZrO}_2\text{-3.5}$ . More rapid reaction over  $\text{SO}_4/\text{ZrO}_2\text{-3}$  was attributed to its higher acidity.

Selectivity to HMF was affected by sulfur loadings significantly as shown given in Figure 5.14. The highest HMF selectivity (81 %) at complete fructose conversion was obtained with  $\text{SO}_4/\text{ZrO}_2\text{-3}$  catalyst. More amount of tetragonal phases, highest amount of acid sites and Brønsted sites in this catalyst promoted HMF formation which accordingly improved the selectivity to HMF. Levulinic acid and formic acid formations due to rehydration were also observed in  $\text{SO}_4/\text{ZrO}_2$  catalysts, consequently HMF selectivity reduced significantly with  $\text{SO}_4/\text{ZrO}_2\text{-2.5}$  (14 %) and  $\text{SO}_4/\text{ZrO}_2\text{-3.5}$  (23 %); this reduction was slight in  $\text{SO}_4/\text{ZrO}_2\text{-3}$  (9 %).

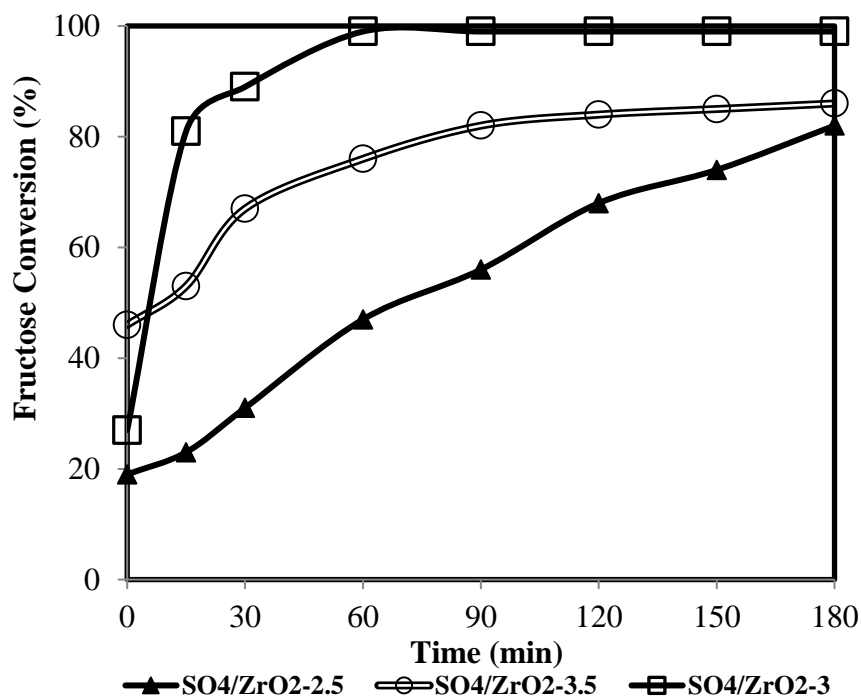


Figure 5.13. Fructose conversions over sulfated zirconia catalysts in DMSO at 110 °C.

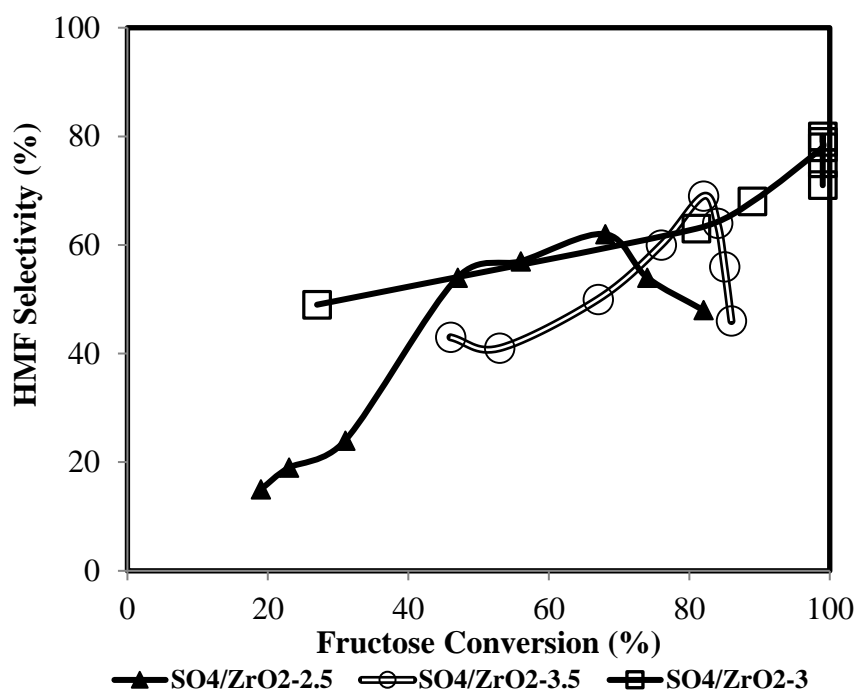


Figure 5.14. HMF selectivities over sulfated zirconia catalysts in DMSO at 110 °C.

Sulfur content of the catalyst was also measured before and after the reaction to investigate the stability of the catalysts. The results are given in Table 5.3. SO<sub>4</sub>/ZrO<sub>2</sub>-2.5 and SO<sub>4</sub>/ZrO<sub>2</sub>-3.5 exhibited low stability, significant sulfur leaching (25-27 %) was also observed over these catalysts. Slight sulfur leaching (3.2 %) was observed over SO<sub>4</sub>/ZrO<sub>2</sub>-3.0.

Reusability tests were also performed in DMSO at 110 °C over sulfated zirconia catalysts. These catalysts were reused up to 4 times. Results are given in Figure 5.15. SO<sub>4</sub>/ZrO<sub>2</sub>-3.0 exhibited high stability, only 6 % of activity loss was observed after 4<sup>th</sup> reuse. Significant activity loss was observed with SO<sub>4</sub>/ZrO<sub>2</sub>-2.5 and SO<sub>4</sub>/ZrO<sub>2</sub>-3.5 due to the sulfur leaching as given in Table 5.3. Higher stability of SO<sub>4</sub>/ZrO<sub>2</sub>-3.0 was attributed to the tetragonal phases in this catalyst. However, sulfated zirconia catalysts were leached and exhibited low stabilities; hence they were not used in the further studies.

Table 5.3. Sulfur leaching from sulfated zirconia catalysts.

	Sulfur Content before reaction (wt. %)	Sulfur Content after reaction (wt. %)
SO <sub>4</sub> /ZrO <sub>2</sub> -2.5	2.68	1.93
SO <sub>4</sub> /ZrO <sub>2</sub> -3.0	3.09	2.99
SO <sub>4</sub> /ZrO <sub>2</sub> -3.5	3.55	2.51

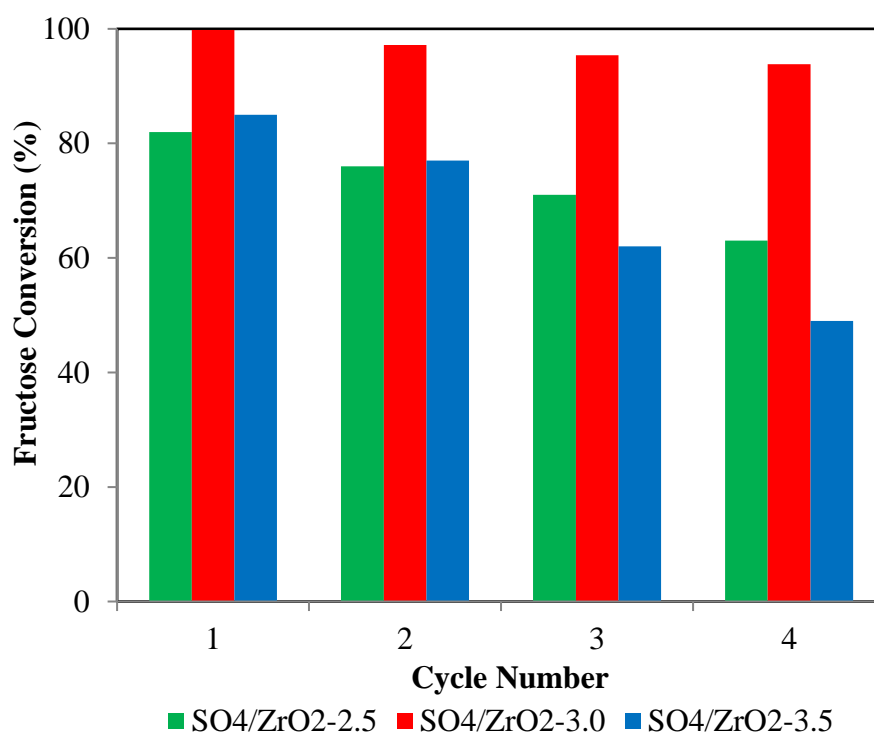
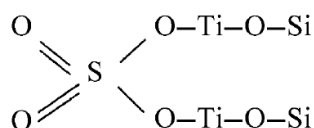


Figure 5.15. Reusability of sulfated zirconia catalysts.

## 5.3. Sulfated and Zirconium Sulfate Loaded Catalysts

### 5.3.1. Characterization of Sulfated and Zirconium Sulfate Loaded Catalysts

Textural properties of the sulfated activated carbon (SO<sub>4</sub>/AC), sulfated silica (SO<sub>4</sub>/SiO<sub>2</sub>), sulfated titania silicate (SO<sub>4</sub>/TS-6) and sulfated Ti-SBA15 (SO<sub>4</sub>/TiSBA-6) are given in Table 5.4. It was found that all of the catalysts had very high surface area. SO<sub>4</sub>/AC had the highest surface area. However, AC supported catalysts had the smallest pores among the sulfated catalysts. The largest mesopores were obtained with SO<sub>4</sub>/TS-6 and SO<sub>4</sub>/TiSBA-6 catalysts. SO<sub>4</sub>/TS-6 had the highest amount of sulfur (~4 wt. %). Most of the sulfur decomposes from the support during calcination regardless of the loading amount. On the other hand, strong chelating bonds formed in titania silicates prevent the sulfur loss in calcination step. Due to these bonds, more sulfur retained on the titania silicates.



Chelating bitentate bonds in sulfated titania-silicates (Yang et al., 2003).

Table 5.4. Textural properties of sulfated catalysts.

	BET Surface Area (m <sup>2</sup> /g)	BJH Pore Diameter (Å)	Total Acidity (μmol NH <sub>3</sub> /gcat)	Brønsted Area	Lewis Area	Sulfur Content (wt. %)
SO <sub>4</sub> /AC	683.2	19.1	-	-	-	2.75
SO <sub>4</sub> /SiO <sub>2</sub>	518.4	35.3	659.0	0.165	0.522	3.23
ZS/SiO <sub>2</sub>	416.0	25.2	806.3	0.133	1.461	2.74
ZS/AC	543.1	13.1	-	-	-	2.58
SO <sub>4</sub> /TS-6	321.1	51.4	967.4	0.583	0.613	3.92
SO <sub>4</sub> /TiSBA-6	519.1	48.4	1565.3	0.812	1.617	3.26

The acidities of the catalysts determined by NH<sub>3</sub>-TPD are given in Figure 5.16. Peaks at 130–250 °C were classified as weak acid sites, peaks at 260–400 °C were

medium acid sites, and those at 400–600 °C were classified as strong acid sites (Carniti et al., 2011). Acidity of the activated carbon supported catalysts couldn't be measured by NH<sub>3</sub>-TPD. The strengths of the acid sites of the catalysts were different. All the catalysts had weak acid sites. SO<sub>4</sub>/TS-6 and SO<sub>4</sub>/SiO<sub>2</sub> catalyst had medium and strong acid sites centered at 300 and 520 °C, respectively. They had the highest amount of strong acid sites. This might be attributed to the good dispersion of the sulfur ions on the SiO<sub>2</sub> support for SO<sub>4</sub>/SiO<sub>2</sub> catalyst and formation of strong chelating bonds in titania silicates. SO<sub>4</sub>/Ti-SBA-6 had medium and strong acid sites (peak at 440 °C), the majority of which were the medium acid sites. SO<sub>4</sub>/SiO<sub>2</sub> had the lowest amount of strong acid sites. From NH<sub>3</sub>-TPD measurement of the catalysts, total acidities of the catalysts were calculated and given in Table 5.4. Titanium containing catalysts had much higher acidities than other catalysts. Although the highest acidity was found in SO<sub>4</sub>/TiSBA-15 catalyst, SO<sub>4</sub>/TS-6 had the largest acid site density (amounts of acid sites per unit surface area of the catalyst, this was 3.01 μmol NH<sub>3</sub>/ m<sup>2</sup>cat in SO<sub>4</sub>/TS-6).

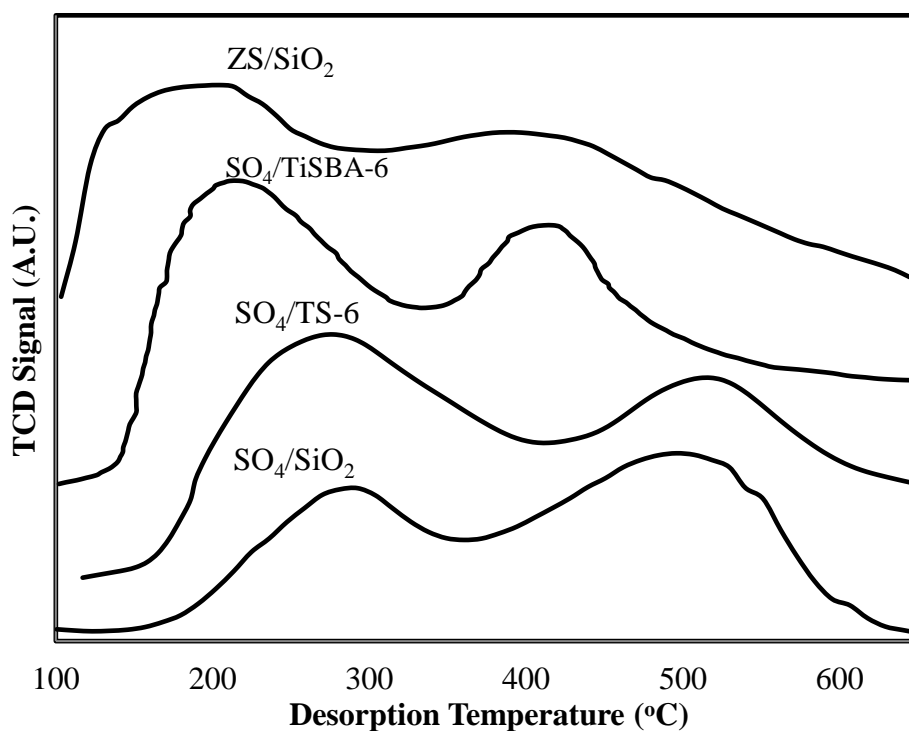


Figure 5.16. NH<sub>3</sub>-TPD profiles of sulfated catalysts.

The pyridine adsorption spectra of the heterogeneous catalysts obtained by FT-IR spectroscopy is given in Figure 5.17 except for that of SO<sub>4</sub>/AC. Pyridine adsorption on SO<sub>4</sub>/AC did not give any acidity peaks. It was observed from each spectrum that all

of the catalysts had Brønsted and Lewis acid sites. ZS/SiO<sub>2</sub> had the high amount of Lewis sites but it possessed low Brønsted acid sites compared to other catalysts. Sulfated titania silicates (SO<sub>4</sub>/Ti-SBA-15 and SO<sub>4</sub>/TiO<sub>2</sub>-SiO<sub>2</sub>) had higher amount of Brønsted and Lewis acid sites than other catalysts. Among the titania silicates SO<sub>4</sub>/TS-6 had the largest amount of Brønsted sites.

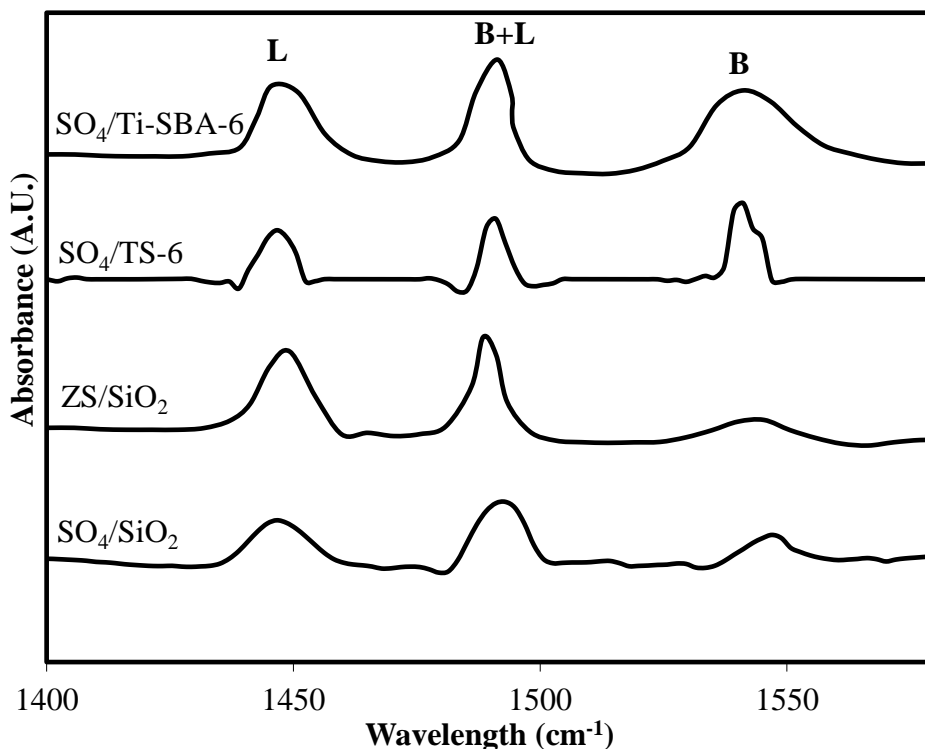


Figure 5.17. FT-IR spectra of sulfated catalysts after pyridine adsorption (B: Brønsted acid sites, L: Lewis acid sites).

### 5.3.2. Activities of the Zirconium Sulfate Loaded Catalysts in DMSO

Product distributions obtained over zirconium sulfate loaded activated carbon and silica catalysts (ZS/SiO<sub>2</sub> and ZS/AC) are given in Figures 5.18 and 5.19. Concentration of HMF increased as fructose consumed linearly. The main by-products were observed as glucose, levulinic and formic acids. Over ZS/AC, FA formation suddenly raised after 120 min since formed HMF converted to FA and LA. More rehydration products (LA and FA) and less HMF were formed over ZS/SiO<sub>2</sub> than ZS/AC. The highest amount of HMF formed was observed with ZS/AC as 267 mmol/L at 120 min.

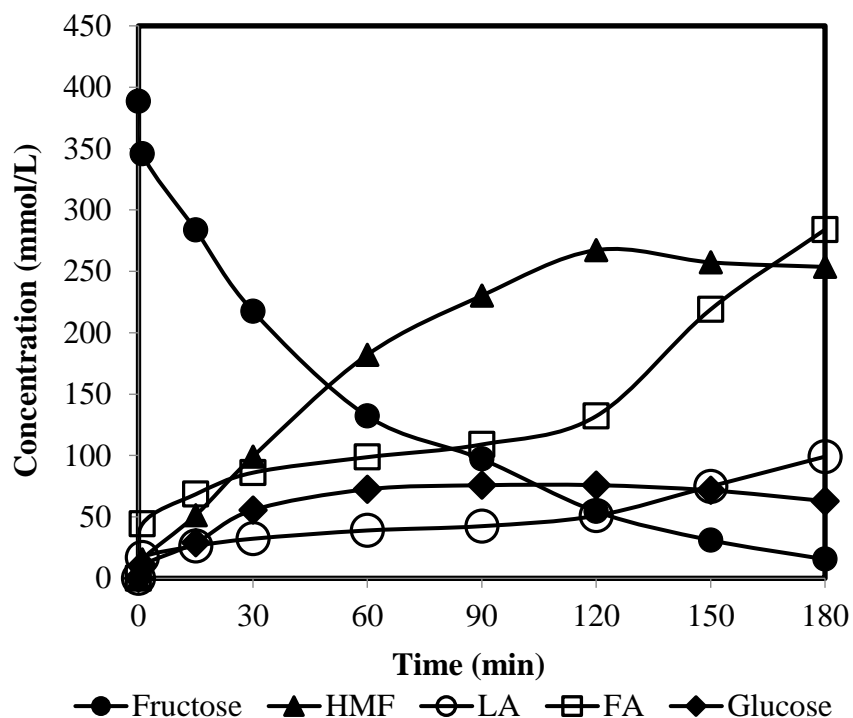


Figure 5.18. Product distribution obtained over ZS/AC at 110 °C in DMSO.

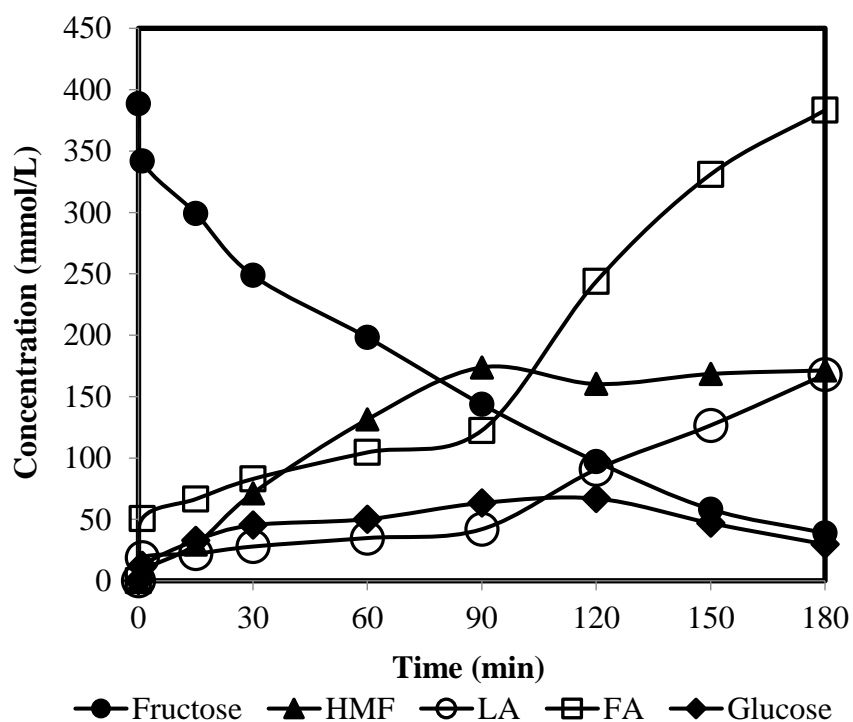


Figure 5.19. Product distribution obtained over ZS/SiO<sub>2</sub> at 110 °C in DMSO.

Zirconium sulfate loaded (ZS/SiO<sub>2</sub> and ZS/AC) catalysts' activities in fructose dehydration are given in Figure 5.20. Conversion increased with the reaction time. ZS/AC gave higher conversions than ZS/SiO<sub>2</sub>. This might be attributed to the role of activated carbon in fructose consumption.

The selectivities to HMF obtained over ZS/SiO<sub>2</sub> and ZS/AC are given in Figure 5.21. Over ZS/SiO<sub>2</sub>, selectivity increased up to 60 % fructose conversion, and then reduced sharply due to transformation of HMF to the LA and FA. ZS/AC exhibited higher selectivities at higher conversions. Rehydration of HMF as well as reduction in selectivity over ZS/AC occurred at conversion higher than 86 %.

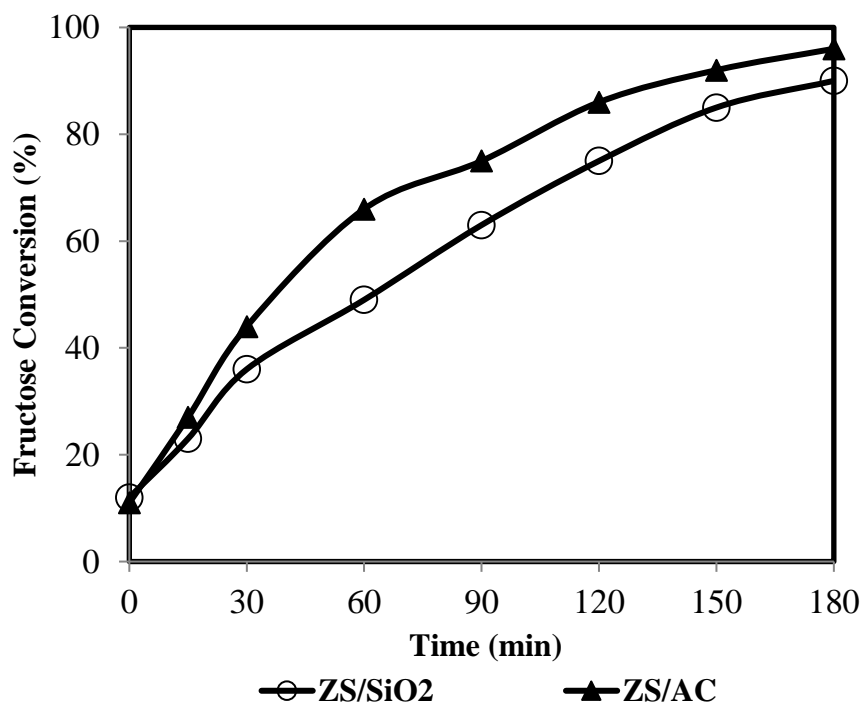


Figure 5.20. Fructose conversions over ZS/SiO<sub>2</sub> and ZS/AC at 110 °C in DMSO.

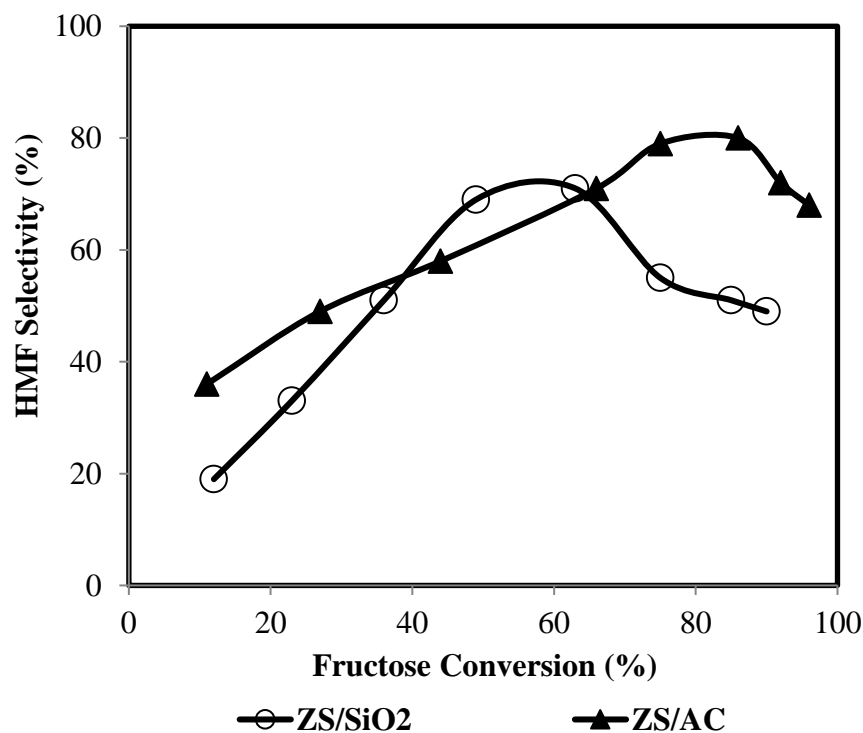


Figure 5.21. HMF selectivities over ZS/SiO<sub>2</sub> and ZS/AC at 110 °C in DMSO.

Sulfur contents of the catalyst measured before and after the reaction to investigate the stability of the catalysts are given in Table 5.5. Leaching was found as 7.5 % for ZS/AC and 11 % for ZS/SiO<sub>2</sub>. This indicated that ZS/AC and ZS/SiO<sub>2</sub> exhibited low stability.

Reusability tests performed in DMSO at 110 °C over ZS/AC and ZS/SiO<sub>2</sub> up to 4 times reuse are shown in Figure 5.22. Both ZS/AC and ZS/SiO<sub>2</sub> catalysts lost their activities in every cycle. Reduction in activity was higher in ZS/SiO<sub>2</sub> since more sulfur leached from ZS/SiO<sub>2</sub>. This could be attributed to the weak interaction of Si, Zr and S. These catalysts exhibited low stability and reusability; hence they were not used in the further studies.

Table 5.5. Sulfur leaching from zirconium sulfate loaded catalysts.

	Sulfur Content before reaction (wt. %)	Sulfur Content after reaction (wt. %)
ZS/AC	2.58	2.41
ZS/SiO <sub>2</sub>	2.74	2.48

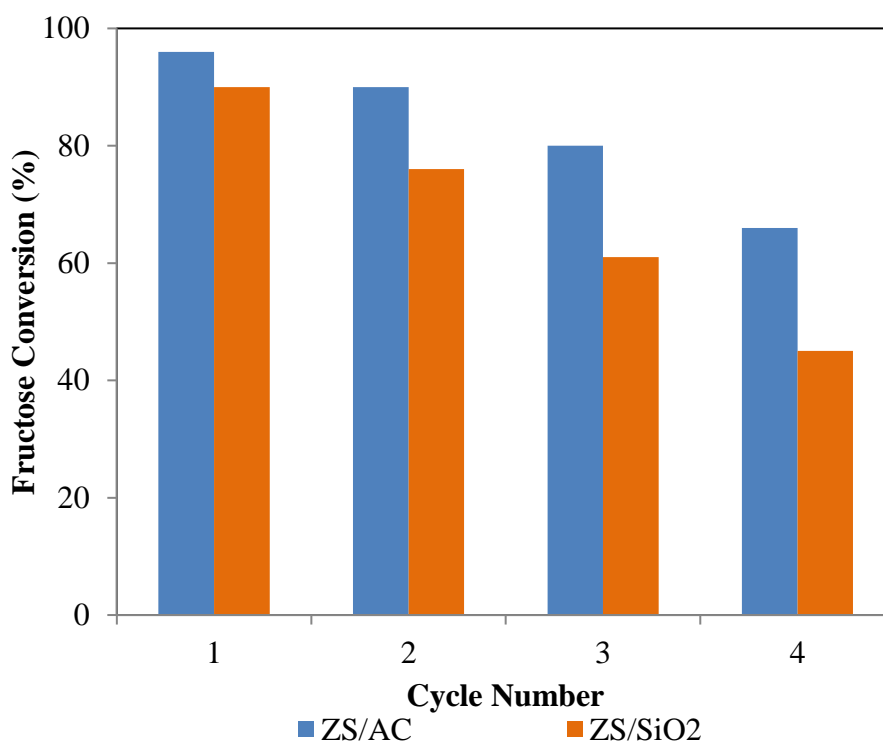


Figure 5.22. Reusability of zirconium sulfate loaded catalysts.

### 5.3.3. Activities of the Different Sulfated Catalysts in DMSO

Product distributions obtained over different sulfated catalysts ( $\text{SO}_4/\text{AC}$ ,  $\text{SO}_4/\text{SiO}_2$ ,  $\text{SO}_4/\text{TS-6}$  and  $\text{SO}_4/\text{Ti-SBA-6}$ ) are given in Figures 5.23, 5.24, 5.25 and 5.26. Concentration of HMF increased with time. The main by-products were found as glucose, levulinic and formic acids. Most HMF was formed  $\text{SO}_4/\text{TS-6}$  over as 299 mmol/L at 180 min. Rapid rehydration and formation of FA was observed over  $\text{SO}_4/\text{AC}$  and  $\text{SO}_4/\text{SiO}_2$ . The highest amounts of rehydration products (LA and FA) were formed over  $\text{SO}_4/\text{SiO}_2$ . Lower amounts of by-product formation over titania-silicate based catalysts ( $\text{SO}_4/\text{TS-6}$  and  $\text{SO}_4/\text{Ti-SBA-6}$ ) were due to the higher amount of Brønsted acid sites of these catalysts. Since Brønsted acid sites favor the HMF formation and minimize the side reactions.

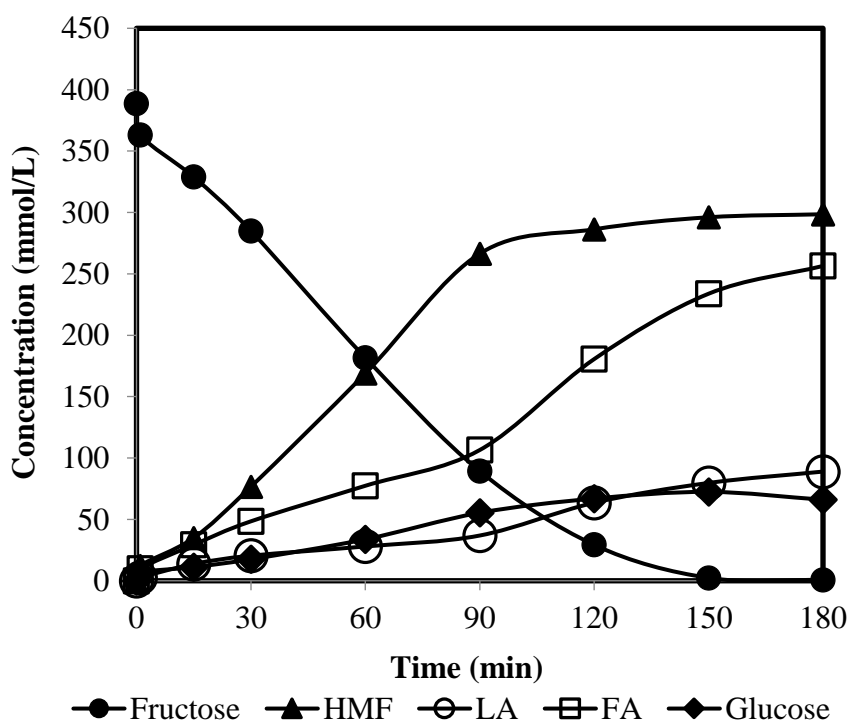


Figure 5.23. Product distribution obtained over  $\text{SO}_4/\text{TS-6}$  at 110 °C in DMSO.

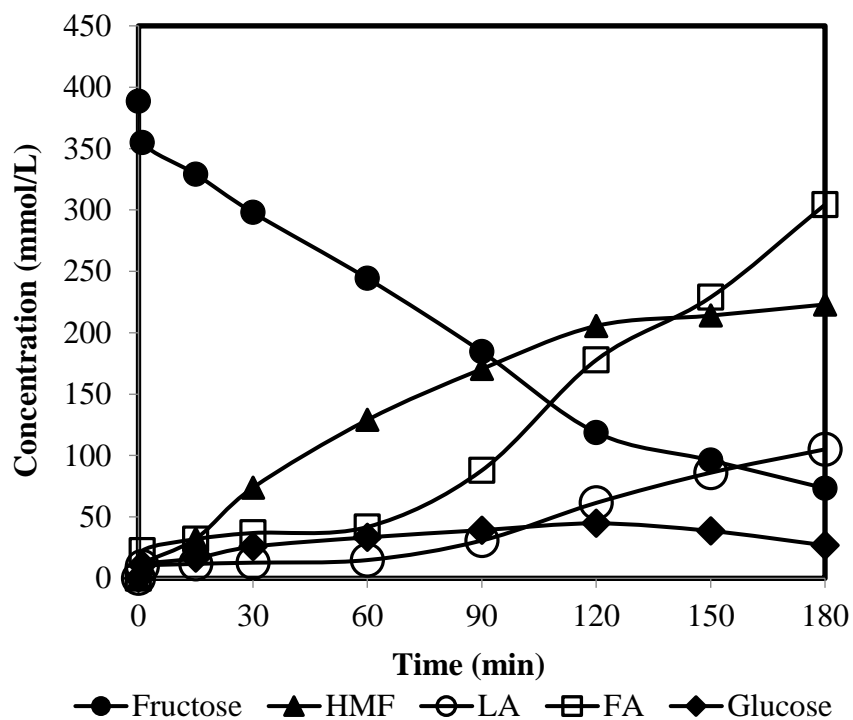


Figure 5.24. Product distribution obtained over SO<sub>4</sub>/Ti-SBA-6 at 110 °C in DMSO.

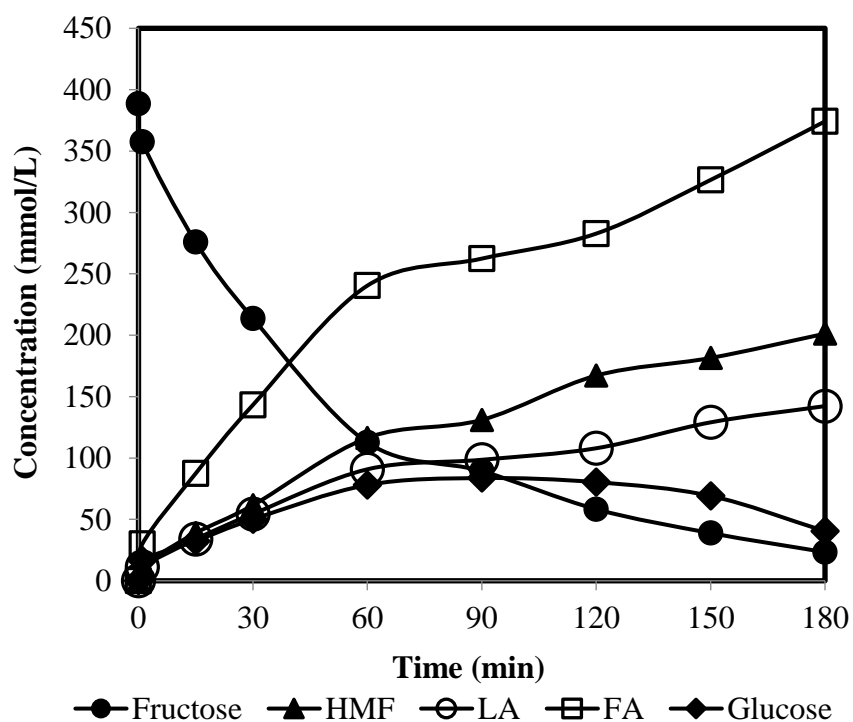


Figure 5.25. Product distribution obtained over SO<sub>4</sub>/SiO<sub>2</sub> at 110 °C in DMSO.

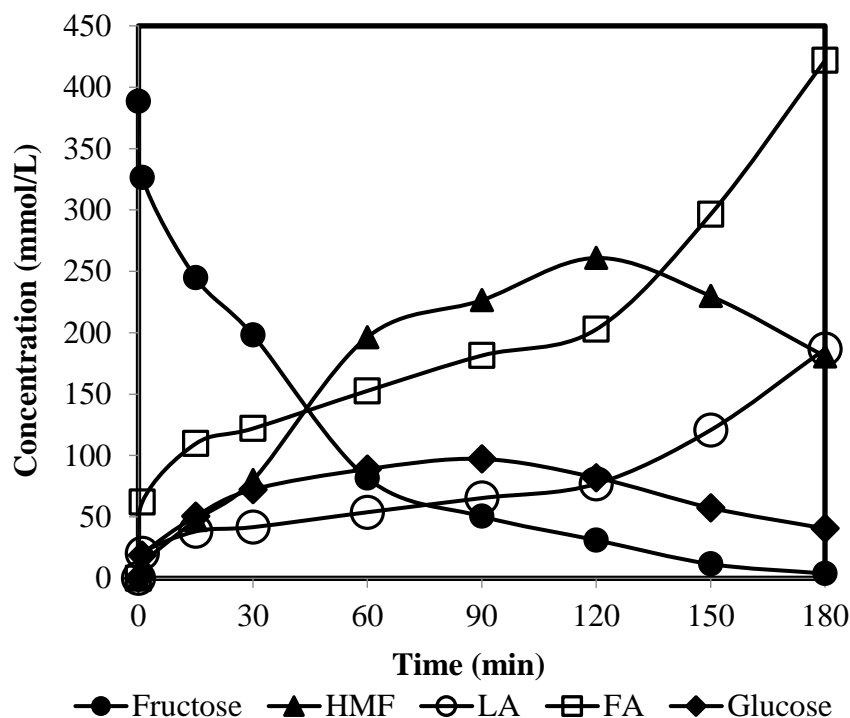


Figure 5.26. Product distribution obtained over  $\text{SO}_4/\text{AC}$  at  $110\text{ }^\circ\text{C}$  in DMSO.

Fructose conversions over sulfated catalysts ( $\text{SO}_4/\text{AC}$ ,  $\text{SO}_4/\text{SiO}_2$ ,  $\text{SO}_4/\text{TS-6}$  and  $\text{SO}_4/\text{Ti-SBA-6}$ ) are given in Figure 5.27. Conversion increased with the reaction time and differed depending on the catalyst applied. All of the catalysts were active. But only  $\text{SO}_4/\text{TS-6}$  and  $\text{SO}_4/\text{AC}$  converted fructose almost completely in 3 h. This could be attributed to the presence of more Lewis acid sites in  $\text{SO}_4/\text{TS-6}$  which were responsible for fructose conversion as discussed in chapter 3. The lowest conversion (77 % fructose conversion) was obtained with  $\text{SO}_4/\text{Ti-SBA-6}$  catalyst.

The selectivity to HMF obtained over  $\text{SO}_4/\text{AC}$ ,  $\text{SO}_4/\text{SiO}_2$ ,  $\text{SO}_4/\text{TS-6}$  and  $\text{SO}_4/\text{Ti-SBA-6}$  are given in Figure 5.28. The most selective catalysts were  $\text{SO}_4/\text{TS-6}$  (82 % at 77 % of fructose conversion),  $\text{SO}_4/\text{Ti-SBA-6}$  (74 % at 75 % of fructose conversion) and  $\text{SO}_4/\text{AC}$  (73 % at 92 % fructose conversion). The high selectivities of Ti based catalysts were due to the presence of chelating bonds in these catalysts which were known as strong Brønsted sites.  $\text{NH}_3\text{-TPD}$  and FT-IR results indicated that these two catalysts also had the highest amount of strong acid sites and Brønsted sites among all of the catalysts. These sites were responsible for HMF formation from intermediates. Selectivity achieved by  $\text{SO}_4/\text{TS-6}$  was comparable with the selectivity observed in homogeneous  $\text{H}_2\text{SO}_4$  catalyst (82 %). Significant reduction in selectivity was observed over  $\text{SO}_4/\text{Ti-SBA-6}$  when fructose conversion exceeded 37 %. HMF rehydrated rapidly to LA and FA after 37 % conversion as obtained in product distributions. High

selectivities (73 %) were obtained with SO<sub>4</sub>/AC at high conversions (90 %). However rapid decrease in selectivity was obtained since by product formation was promoted after 92 % conversion. The lowest selectivity result (50 % at 90 % fructose conversion) was obtained with SO<sub>4</sub>/SiO<sub>2</sub> catalyst.

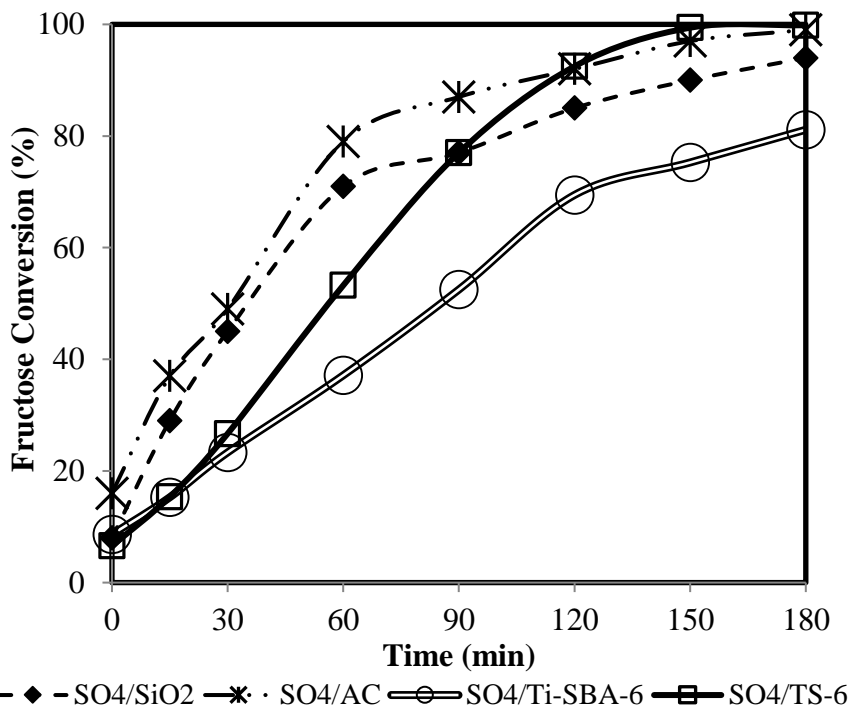


Figure 5.27. Fructose conversions over different sulfated catalysts at 110 °C in DMSO.

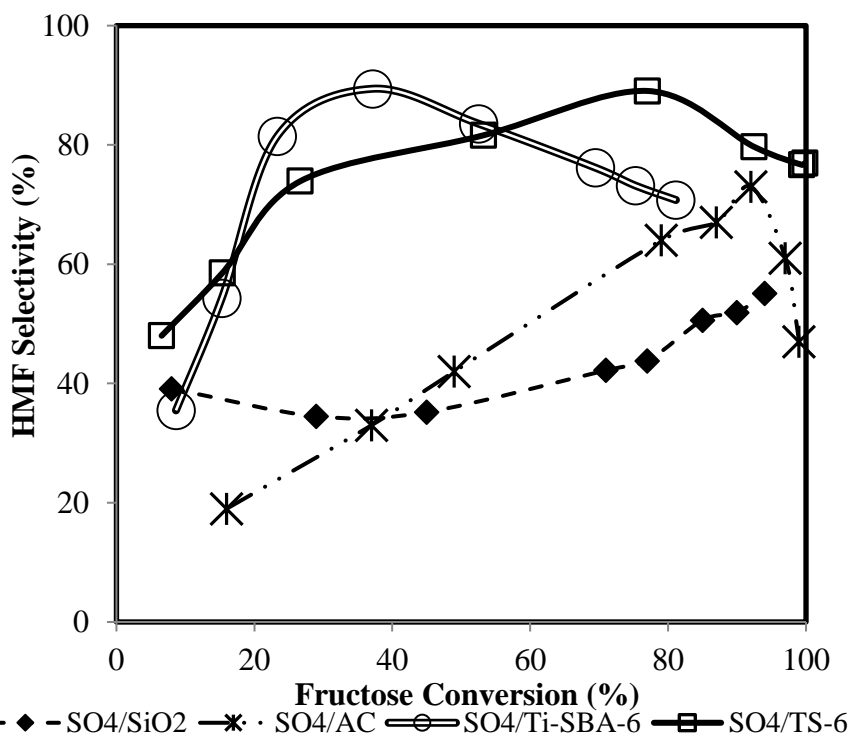


Figure 5.28. HMF selectivities over different sulfated catalysts at 110 °C in DMSO.

Sulfur contents of the sulfated catalysts measured before and after the reaction to investigate the stability are given in Table 5.6. Sulfated titania silicates (SO<sub>4</sub>/TS-6 and SO<sub>4</sub>/TiSBA-6) exhibited high stabilities. Sulfur content in these catalysts remained almost constant after the reaction. This was due to the strong support-metal-sulfur interaction as well as chelating bitentate bonds as discussed in chapter 3. Significant amounts of sulfur leaching were observed over SO<sub>4</sub>/AC and SO<sub>4</sub>/SiO<sub>2</sub> which was 17 % in SO<sub>4</sub>/AC and 35 % in SO<sub>4</sub>/SiO<sub>2</sub>.

Reusability tests of the sulfated catalysts were also performed in DMSO at 110 °C. Results are given in Figure 5.29. SO<sub>4</sub>/TS-6 and SO<sub>4</sub>/TiSBA-6 preserved their activities up to 4 times. This is in agreement with the leaching test. SO<sub>4</sub>/AC and SO<sub>4</sub>/SiO<sub>2</sub> lose their activities significantly at every reuse. After 4 reuse, drop in activity was 51 % in SO<sub>4</sub>/SiO<sub>2</sub> and 29 % in SO<sub>4</sub>/AC. Thus, SO<sub>4</sub>/SiO<sub>2</sub> and SO<sub>4</sub>/AC catalysts were not used in the further studies.

Table 5.6. Sulfur leaching from different sulfated catalysts.

	Sulfur Content before reaction (wt. %)	Sulfur Content after reaction (wt. %)
SO <sub>4</sub> /AC	2.75	2.27
SO <sub>4</sub> /SiO <sub>2</sub>	3.23	2.09
SO <sub>4</sub> /TS-6	3.92	3.97
SO <sub>4</sub> /TiSBA-6	5.13	5.08

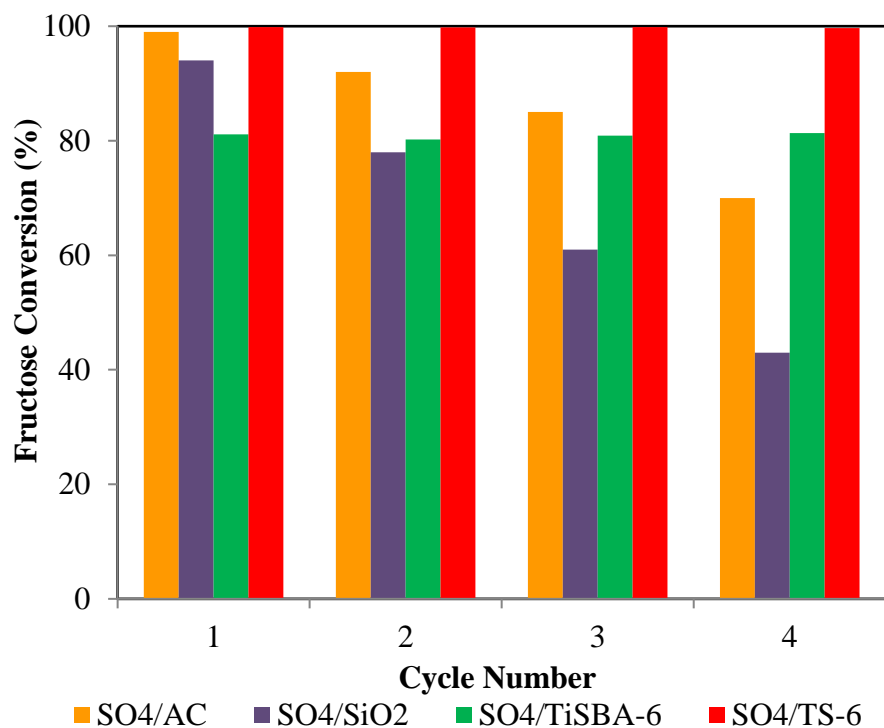


Figure 5.29. Reusability results of sulfated catalysts.

## 5.4. Titania-Silicate Based Catalysts

### 5.4.1. Characterization of Titania-Silicate Based Catalysts

Textural properties and sulfur content of the TS-2, TS-6, SO<sub>4</sub>/TS-2, SO<sub>4</sub>/TS-6 and SO<sub>4</sub>/La-TS-6 catalysts are given in Table 5.7. All of the catalysts were found to be mesoporous with high surface area. Their surface area and pore size decreased to some extent by Ti content, sulfation and La addition. The sulfur content of the catalysts increased with the Ti amount loaded which was attributed to more chelating bond formation between sulfur, titanium and silicon. La containing catalyst had the highest amount of sulfur which could be due to prevention of sulfur decomposition by La during calcination (Li et al., 2013). This might be due to more bond formation and strong interaction between sulfur and the catalyst surface.

Table 5.7. Textural properties of titania silica catalysts.

Catalyst Name	BET Surface Area (m <sup>2</sup> /g)	BJH Pore Diameter (Å)	Total Acidity (μmol NH <sub>3</sub> / g.cat)	Brønsted Area	Lewis Area	Sulfur Content (wt. %)
TS-2	577.4	85.4	104.4	0.022	1.050	-
TS-6	571.2	66.3	226.1	0.051	1.972	-
SO <sub>4</sub> /TS-2	348.3	53.2	434.3	0.214	0.412	1.71
SO <sub>4</sub> /TS-6	321.1	51.4	967.4	0.583	0.613	3.92
SO <sub>4</sub> /La-TS-6	293.1	47.1	1723.2	1.163	0.816	5.46

Amount and strength of the acidity of the catalysts determined by NH<sub>3</sub>-TPD is given in Figure 5.30. The desorption peaks centered at low temperature (200 °C) and high temperature (550 °C) regions are referred to as weak and strong acid sites, respectively (Carniti et al., 2011). Strong acid sites were just found over sulfated catalysts. An increase in the Ti and S content enhanced the strong and total amount of acid sites due to a higher amount of sulfur capture. La addition also significantly improved the acid strength, acid concentration and amount of strong acid sites. This catalyst had the highest amount of strong acid sites. The total amount of the acid sites of the catalysts determined from NH<sub>3</sub>-TPD data is given in Table 5.7. Amount of acid sites was also improved with sulfur content and it doubled when the Ti content increased from 2 to 6 wt. %. Similarly, La addition doubled the amount of the acid sites. These acid sites were related to the formation of chelating bonds when sulfate was loaded on titania silicates (Yang et al., 2011; Li et al., 2013).

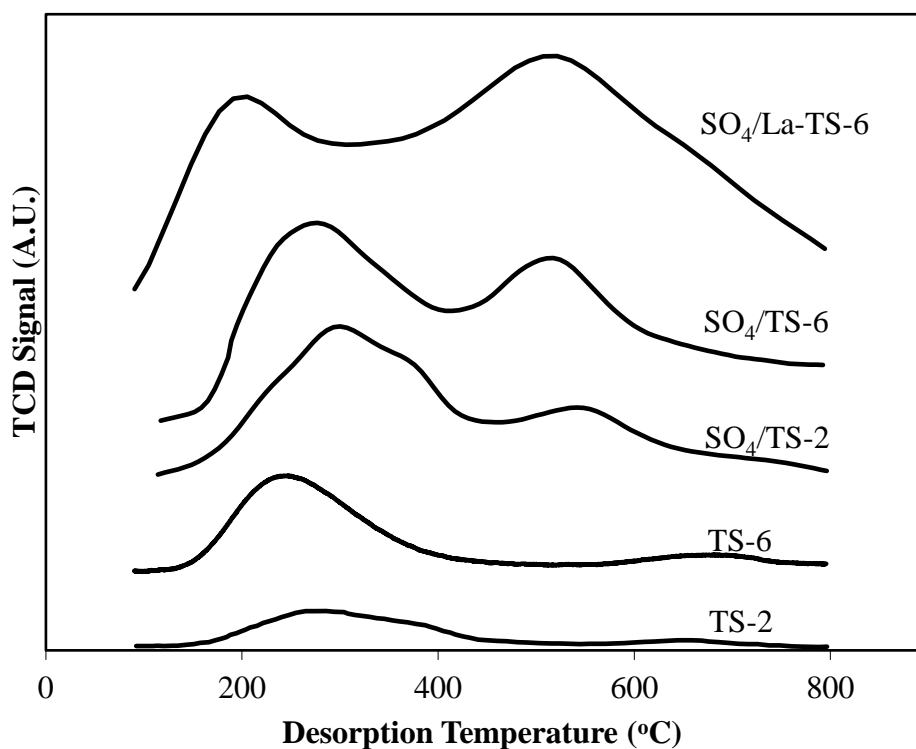


Figure 5.30.  $\text{NH}_3$ -TPD profiles of the titania-silicate based catalysts.

FT-IR spectra of the catalysts after pyridine adsorption are given in Figure 5.31. Titania-silicates had solely Lewis acid sites. However, all of the sulfated titania silicate catalysts had both Brønsted and Lewis acid sites. The amount of Brønsted sites in sulfated catalysts increased with the Ti content since more sulfates were loaded when the Ti content was higher. La addition also improved the amount of Brønsted acid sites further. The area under the peaks increased with the amount of Ti and S loading which indicated an increase in total amount of acid sites as obtained by  $\text{NH}_3$ -TPD.

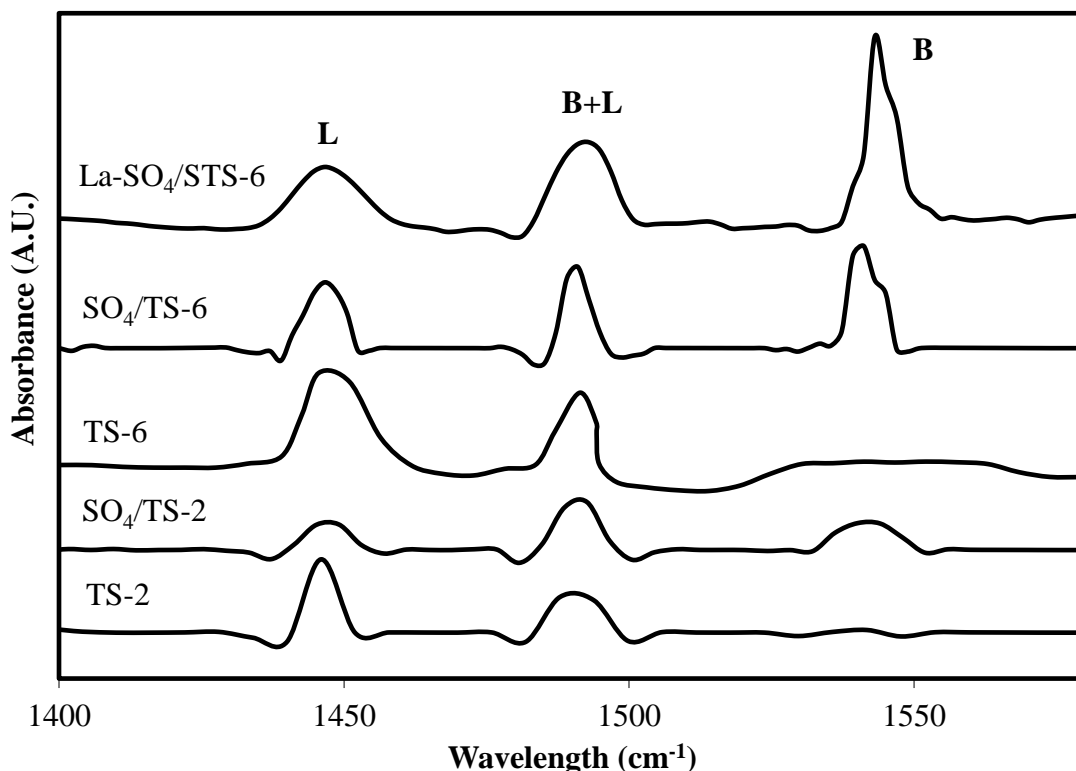


Figure 5.31. FT-IR spectra of titania silica catalysts after pyridine adsorption (B: Brønsted acid sites, L: Lewis acid sites).

#### 5.4.2. Activities of Titania-Silicate Based Catalysts in DMSO

Product distributions obtained over titania-silicate based catalysts: TS-2, TS-6, SO<sub>4</sub>/TS-2, SO<sub>4</sub>/TS-6 and SO<sub>4</sub>/La-TS-6 are given in Figures 5.32, 5.33, 5.34, 5.35 and 5.36, respectively. HMF, levulinic acid, formic acid and glucose formation were observed over these catalysts. As fructose was consumed, HMF was formed. Its amount first increased with reaction time and close to fructose depletion its concentration reduced over 2 wt. % Ti containing catalysts; and remained constant over 6 wt. % Ti containing catalysts. Increase in HMF concentration, enhanced the LA and FA concentration due to rehydration of HMF with water in reaction medium. Glucose formation was due to the isomerization of fructose molecules. Higher amounts of HMF were produced over sulfated catalysts and significant amounts of by-products such as LA, FA and glucose were formed over non-sulfated titania silicates. SO<sub>4</sub>/La-TS-6 exhibited different catalytic activity; fructose concentration decreased and HMF concentration increased linearly up to 150 min.

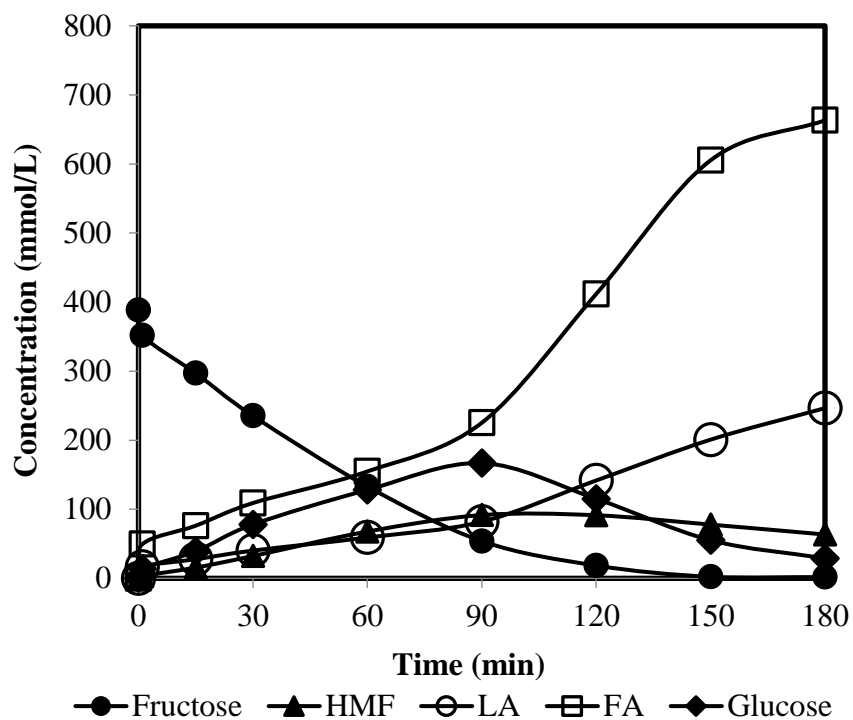


Figure 5.32. Product distribution of over TS-2 at 110 °C in DMSO.

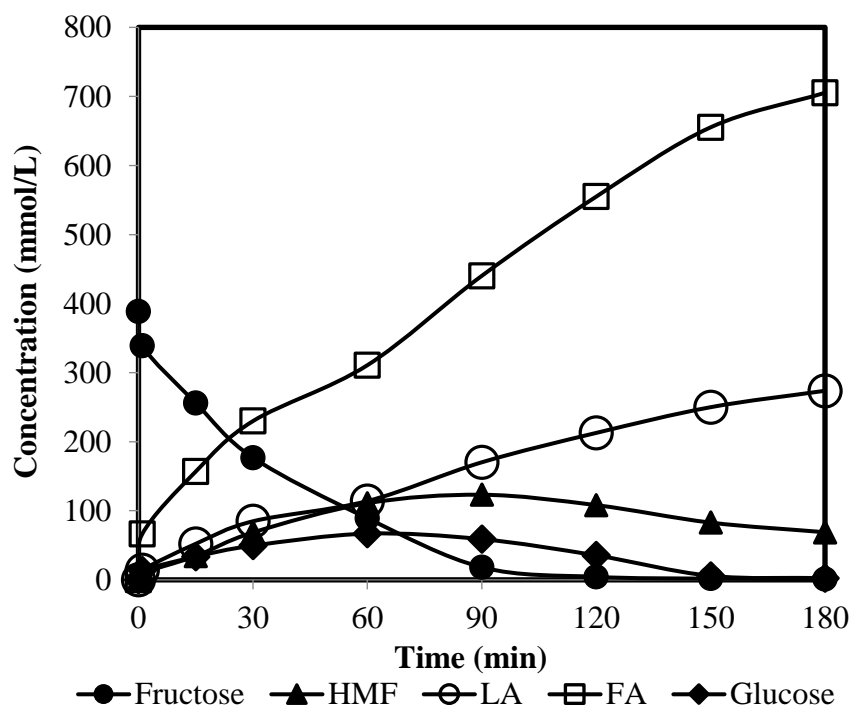


Figure 5.33. Product distribution of over TS-6 at 110 °C in DMSO.

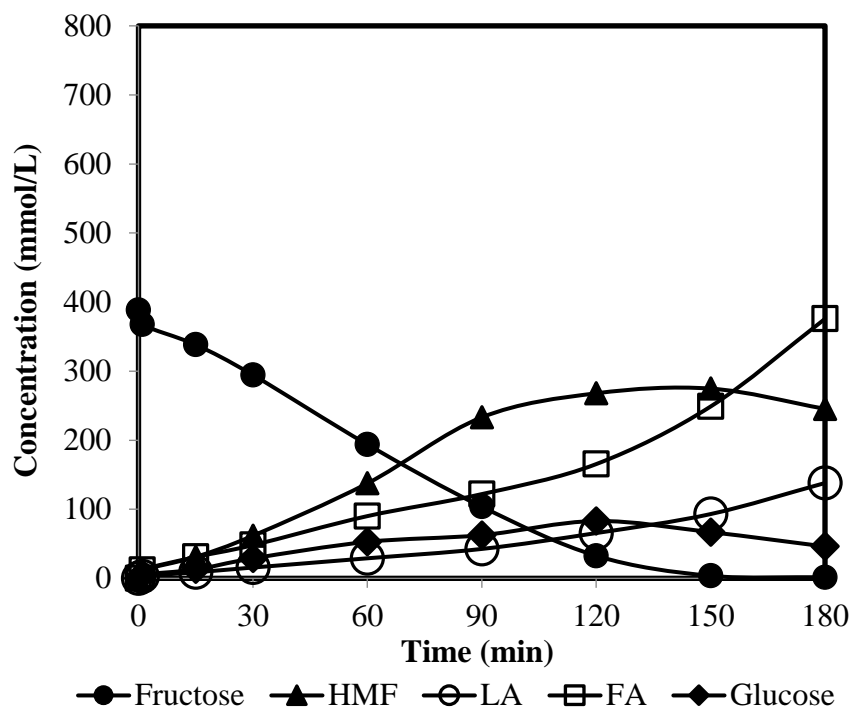


Figure 5.34. Product distribution of over SO<sub>4</sub>/TS-2 at 110 °C in DMSO.

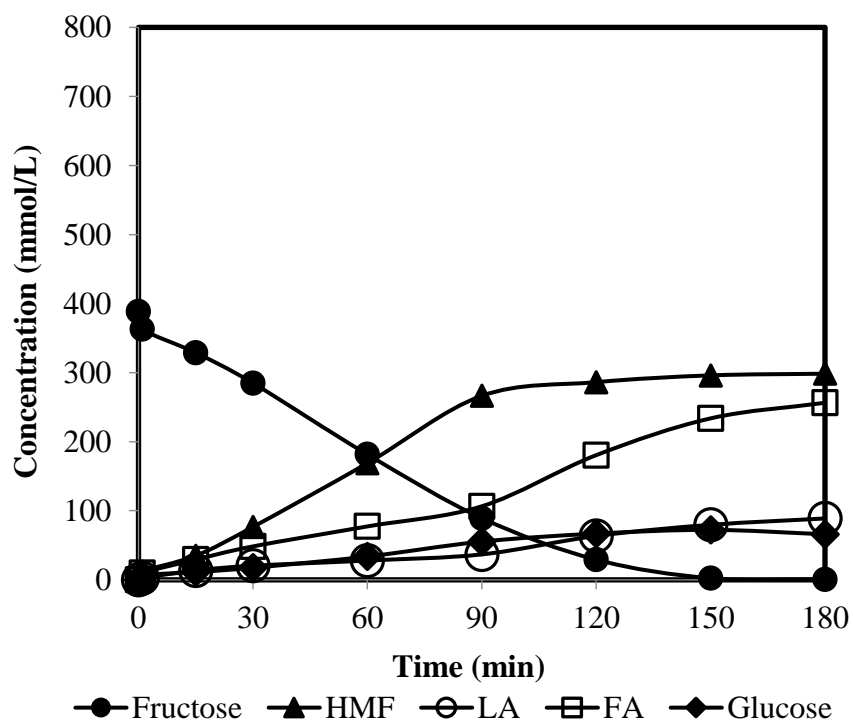


Figure 5.35. Product distribution of over SO<sub>4</sub>/TS-6 at 110 °C in DMSO.

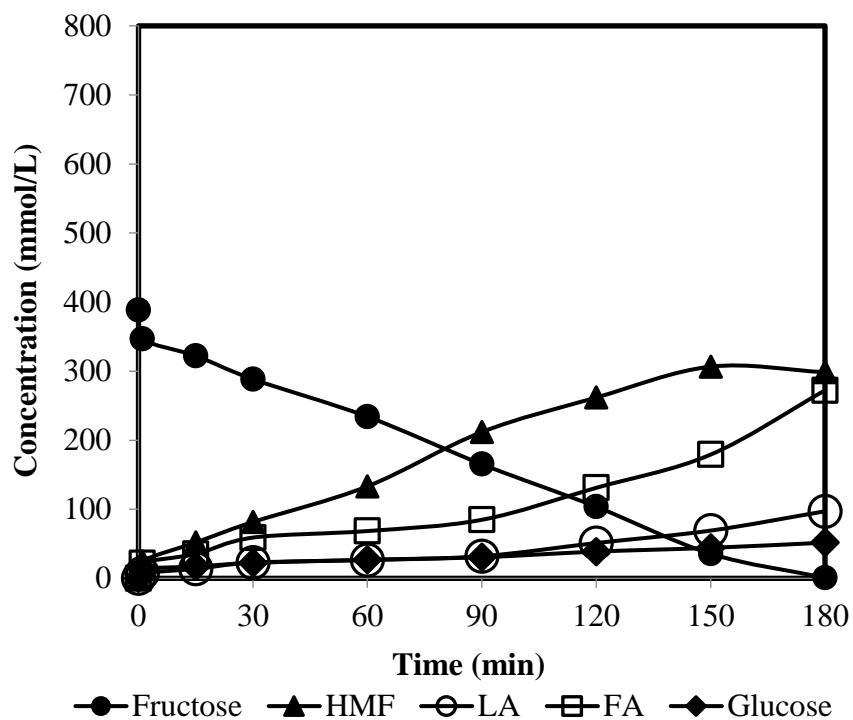


Figure 5.36. Product distribution of over  $\text{SO}_4/\text{La-TS-6}$  at  $110^\circ\text{C}$  in DMSO.

Fructose conversions obtained over the titania silica based catalysts are given in Figure 5.37. All of the catalysts were active; conversion increased rapidly with reaction time and fructose was consumed in 3h. Non-sulfated catalysts exhibited higher conversions than sulfated catalysts. This was attributed to their Lewis centers, since sugar conversion was directly related to Lewis acid sites (Weingarten et al., 2009). As discussed in the characterization part, these catalysts had higher amount of Lewis acid sites than sulfated ones. Reaction was slower over La containing catalyst during 2h, and then it reached complete conversion at the end of the reaction.

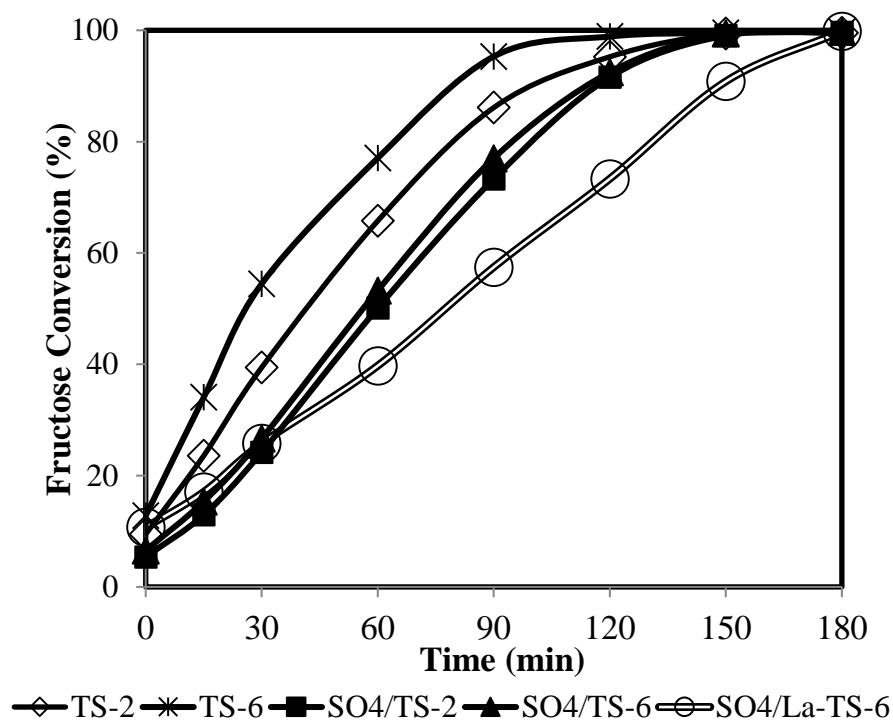


Figure 5.37. Fructose conversions over titania silicates at 110 °C in DMSO.

The selectivities to HMF obtained over titania silica based catalysts are given in Figure 5.38. Selectivity to HMF increased with Ti content of the catalyst. This was attributed to the octahedral coordination sites of Ti in titania silicates. These sites are selective acidic sites and increased with the amount of Ti. Increase in Ti content also increased the total number of the acid sites, sulfur loaded as well as Brønsted acidities. Accordingly, HMF selectivity was improved. However, upon sulfation of the titania silicates, this improvement was significant. This indicated that Brønsted acid sites formed after sulfation resulted in a higher HMF formation as found in product distributions. The most selective catalyst was found to be SO<sub>4</sub>/La-TS-6 (95 % HMF selectivity at 58 % fructose conversion). This was due to the highest amount of strong and Brønsted acid sites of on this catalyst. These acid sites were formed by the formation of chelating bonds when sulfates were loaded on titania silicates as discussed in characterization part. At higher conversions, selectivity decreased slightly. This was due to the reaction of HMF giving LA and FA. Consequently, HMF selectivity was reduced significantly after 80 % fructose conversion.

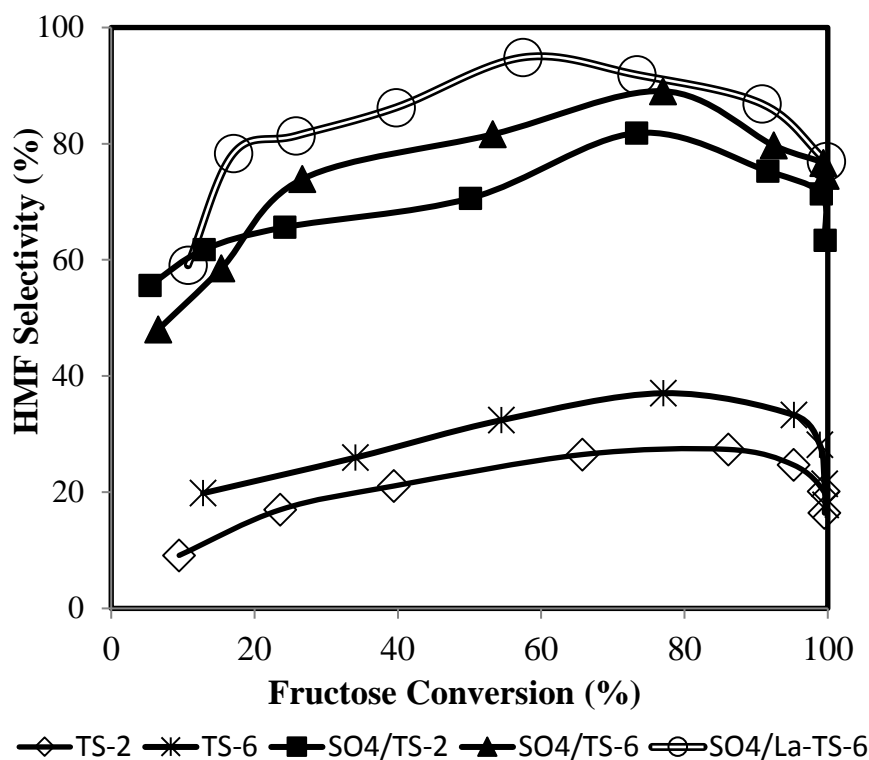


Figure 5.38. HMF selectivities over titania silicates in DMSO at 110 °C.

The optimum (maximum) HMF yields over different catalysts prepared are given in Table 5.8. HMF yield increased with the amount of the Brønsted acid sites. High yields were obtained over the sulfated catalysts. La incorporated catalyst (SO<sub>4</sub>/La-TS-6) provided the highest yield, 78.90 %.

Table 5.8. Optimum HMF yields over the catalysts prepared.

Catalyst	Reaction Time (min)	HMF Yield (mol %)
TS-2	120	23.50
TS-6	90	31.72
SO <sub>4</sub> /TS-2	180	63.16
SO <sub>4</sub> /TS-6	150	76.20
SO <sub>4</sub> /La-TS-6	150	78.90

Sulfur contents of the sulfated titania silica catalysts measured before and after the reaction to investigate the stability, are given in Table 5.9. All sulfated titania silicates (SO<sub>4</sub>/TS-2, SO<sub>4</sub>/TS-6 and SO<sub>4</sub>/La-TS-6) exhibited high stabilities. Sulfur

content in these catalysts remained constant after reaction. This was due to the chelating bitentate bonds formation as discussed in chapter 3.

Reusability tests performed in DMSO at 110 °C are given in Figure 5.39. All the titania silicates also non-sulfated ones were reused up to 4 times without losing their activities. These results also confirmed no sulfur leaching from sulfated titania-silicates.

Table 5.9. Sulfur leaching from titania-silicates.

Catalyst Name	Sulfur Content before reaction (wt. %)	Sulfur Content after reaction (wt. %)
TS-2	-	-
TS-6	-	-
SO <sub>4</sub> /TS-2	0.71	0.69
SO <sub>4</sub> /TS-6	2.92	2.97
SO <sub>4</sub> /La-TS-6	5.46	5.47

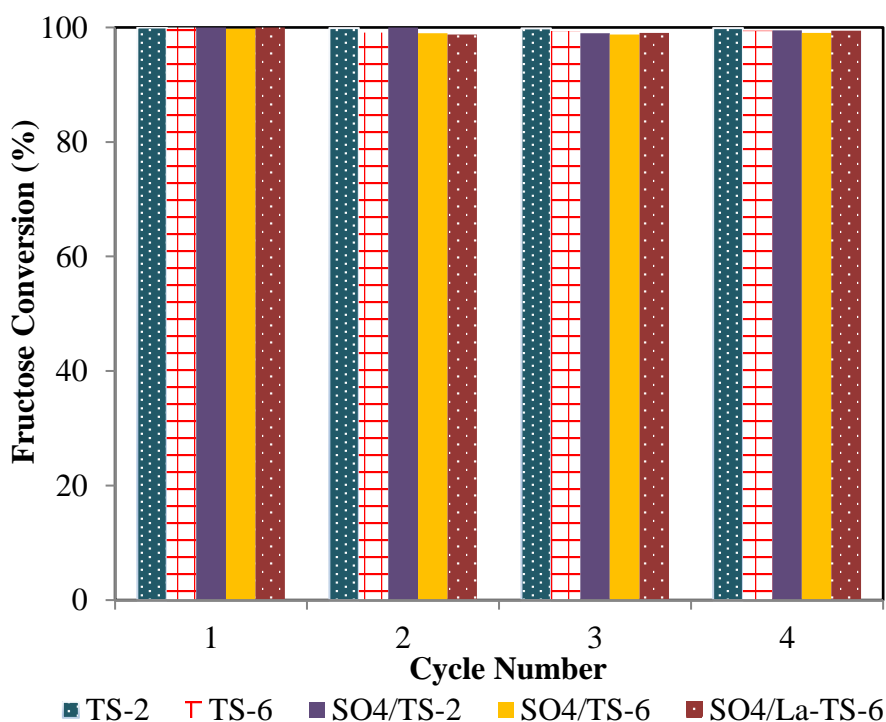


Figure 5.39. Reusability tests of titania silicates.

## 5.5. Sulfated Ti-SBA-15 Based Catalysts

### 5.5.1. Characterization of Sulfated Ti-SBA-15 Based Catalysts

Textural properties of the sulfated Ti-SBA-15 based catalysts are given in Table 5.10. It was found that all of the catalysts had high surface area and mesopore structure. Surface area of the catalysts reduced with titanium, sulfur and lanthanum as TiO<sub>2</sub>-SiO<sub>2</sub> catalysts. Pore sizes were also affected by Ti content and La. However, this change was not significant after La addition. More sulfur was captured with increase in Ti content. The amount captured was improved with the incorporation of La ion. La incorporated catalyst had the highest amount of sulfur due to its role in calcination as discussed in chapter 3.

Table 5.10. Textural properties of sulfated catalysts.

Catalyst Name	BET Surface Area (m <sup>2</sup> /g)	BJH Pore Diameter (Å)	Total Acidity (μmol NH <sub>3</sub> /gcat)	Brønsted Area	Lewis Area	Sulfur Content (wt. %)
SO <sub>4</sub> /TiSBA-2	586.3	56.2	1129.2	0.326	0.207	1.19
SO <sub>4</sub> /TiSBA-6	519.1	48.4	1565.3	0.812	1.617	3.26
SO <sub>4</sub> /La-TiSBA-6	467.4	45.1	1725.1	1.567	1.114	6.13

Amount, type and strength of the acid sites of Ti-SBA-15 catalysts was measured by NH<sub>3</sub>-TPD is given in Figure 5.40. The desorption peaks centered at low temperature (250 °C) and high temperature (450 °C) regions are referred to as weak and strong acid sites, respectively (Carniti et al., 2011). All of the catalysts had both weak and strong acid sites. Increase in Ti content enhanced the weak, strong and so total amount of acid sites. La addition slightly affected the strong acidity and acid strength. Total amount of the acid sites of the catalysts determined from NH<sub>3</sub>-TPD data is given in Table 5.10. Total amounts of acid sites were also improved significantly with the sulfur loadings.

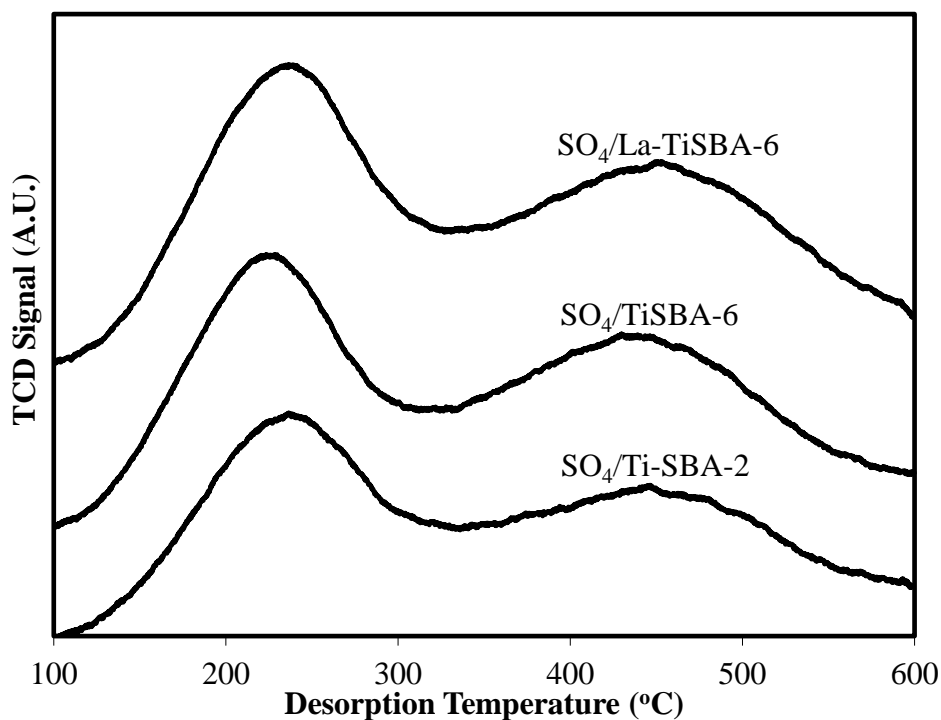


Figure 5.40. NH<sub>3</sub>-TPD profiles of the sulfated Ti-SBA-15 catalysts.

Nature of the acid sites of the Ti-SBA-15 based catalysts determined from pyridine FT-IR spectroscopy are given in Figure 5.41. All the catalysts had Brønsted and Lewis acid sites. Peaks area increased with sulfur loading and Ti content which indicated enhancement of the acidity of the catalysts as determined by NH<sub>3</sub>-TPD measurements. Amount of Brønsted sites was improved with Ti content since sulfate loaded also increased with Ti content. Thus the highest amount of Brønsted sites was observed for SO<sub>4</sub>/La-Ti-SBA-6. Chelating bitentate bonds were probably formed when sulfates were loaded (Yang et al., 2011). The amount of Brønsted sites could be related to the number of chelating bitentate bonds and sulfur content. Lewis acid sites of the catalysts increased also with Ti and La. The highest amount of Lewis acid sites was observed for SO<sub>4</sub>/La-Ti-SBA-6 catalyst.

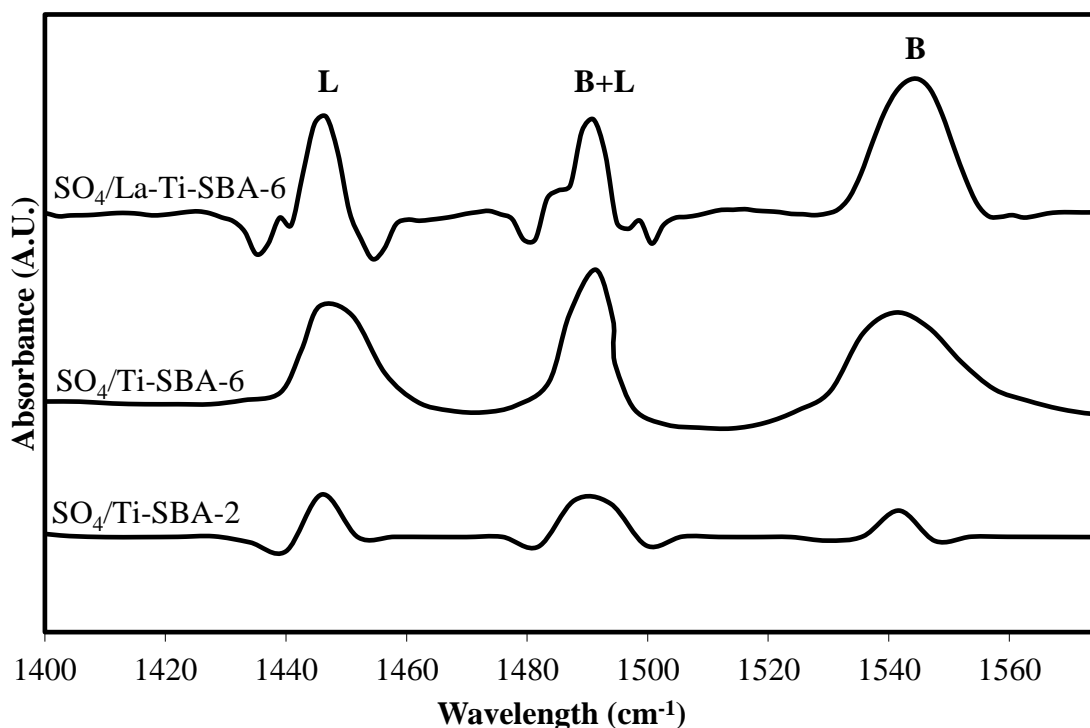


Figure 5.41. FT-IR spectra of sulfated Ti-SBA-15 catalysts after pyridine adsorption (B: Brønsted acid sites, L: Lewis acid sites).

### 5.5.2. Activities of Sulfated Ti- SBA-15 Based Catalysts in DMSO

Product distributions obtained over sulfated Ti-SBA-15 catalysts:  $\text{SO}_4/\text{TiSBA-2}$ ,  $\text{SO}_4/\text{TiSBA-6}$  and  $\text{SO}_4/\text{La-TiSBA-6}$  are given in Figures 5.42 to 5.44. HMF, levulinic acid, formic acid and glucose were the main products. HMF was formed as fructose concentration reduced steadily. Increase in HMF concentration, LA and FA concentration also increased due to rehydration of HMF. The highest amount of HMF was formed over  $\text{SO}_4/\text{TiSBA-6}$ , which was 223 mmol/L.

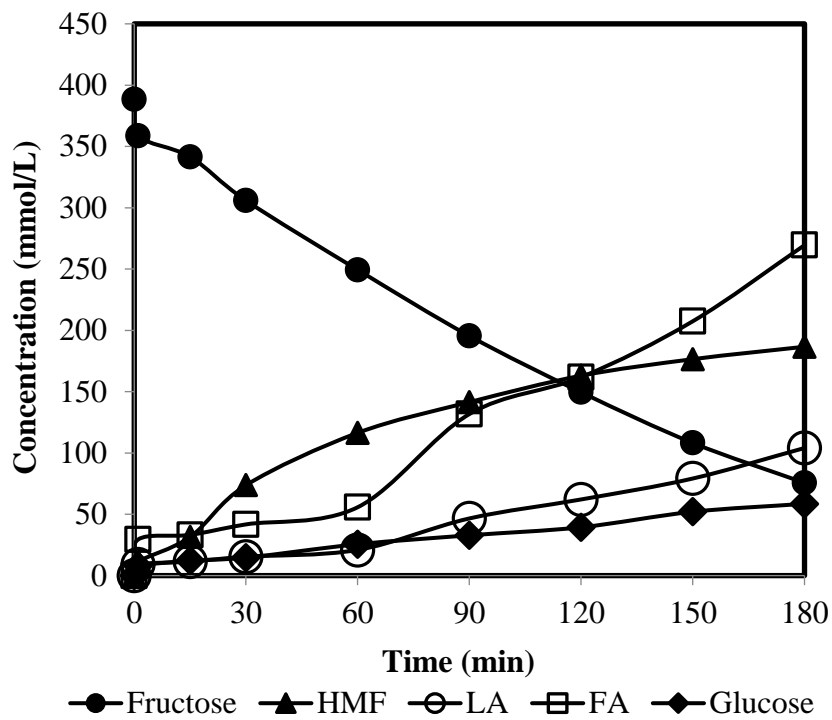


Figure 5.42. Product distribution over SO<sub>4</sub>/Ti-SBA-2.

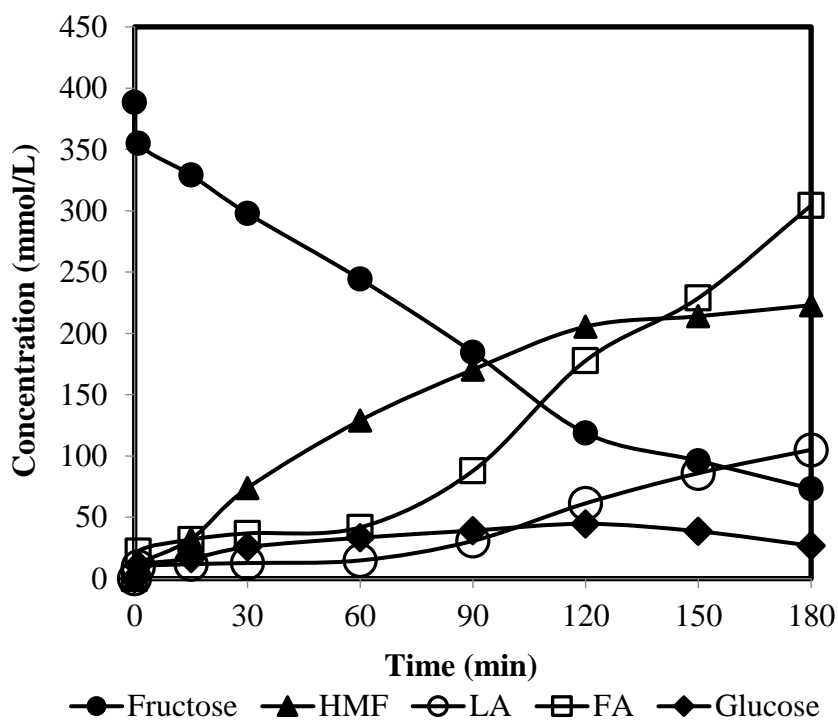


Figure 5.43. Product distribution over SO<sub>4</sub>/Ti-SBA-6.

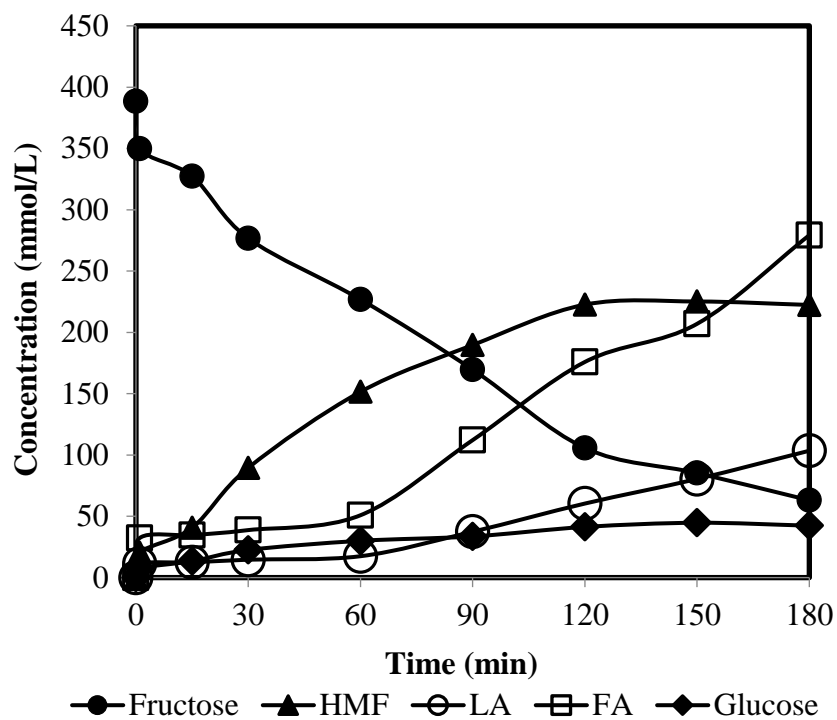


Figure 5.44. Product distribution over SO<sub>4</sub>/La-Ti-SBA-6.

Fructose conversions obtained over SO<sub>4</sub>/TiSBA-15 based catalysts are given in Figure 5.45. All the catalysts were active. Fructose conversion increased with reaction time and 80 % of conversion was obtained in 3h. This activity was attributed to presence of Lewis acid sites as discussed in literature review. Sulfated Ti-SBA-15 had also high amount of Lewis sites as given in characterization part. Although amount of Lewis acid sites increased with Ti content, this did not affect the fructose conversions significantly.

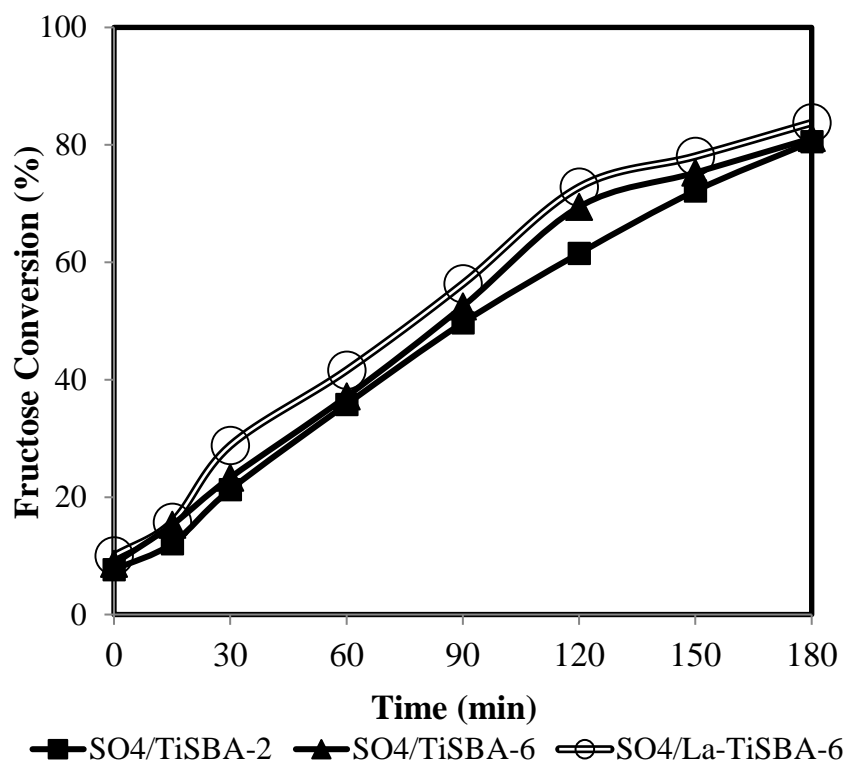


Figure 5.45. Fructose conversions over sulfated Ti-SBA-15 catalysts at 110 °C in DMSO.

The selectivities to HMF obtained over sulfated Ti-SBA-15 catalysts are given in Figure 5.46. High selectivities were obtained at lower conversions. Selectivity to HMF increased with Ti content of the catalyst and also with La addition, at conversions greater than 40 %. Higher selectivities were achieved at high fructose conversions with 6 wt. % Ti containing catalysts. This was also attributed to the octahedral coordination sites of Ti in titania silicates. Amount of these sites increased with Ti content. Increase in Ti content also increased the total number of the acid sites and Brønsted sites, accordingly HMF selectivity was improved. The most selective catalyst was found to be SO<sub>4</sub>/La-TiSBA-6 (94 % HMF selectivity at 42 % fructose conversion). This was attributed to the highest amount of strong and Brønsted acid sites of this catalyst. HMF was rehydrated with the water in the medium and formed LA and FA. Thus, selectivity to HMF was reduced significantly at high fructose conversions.

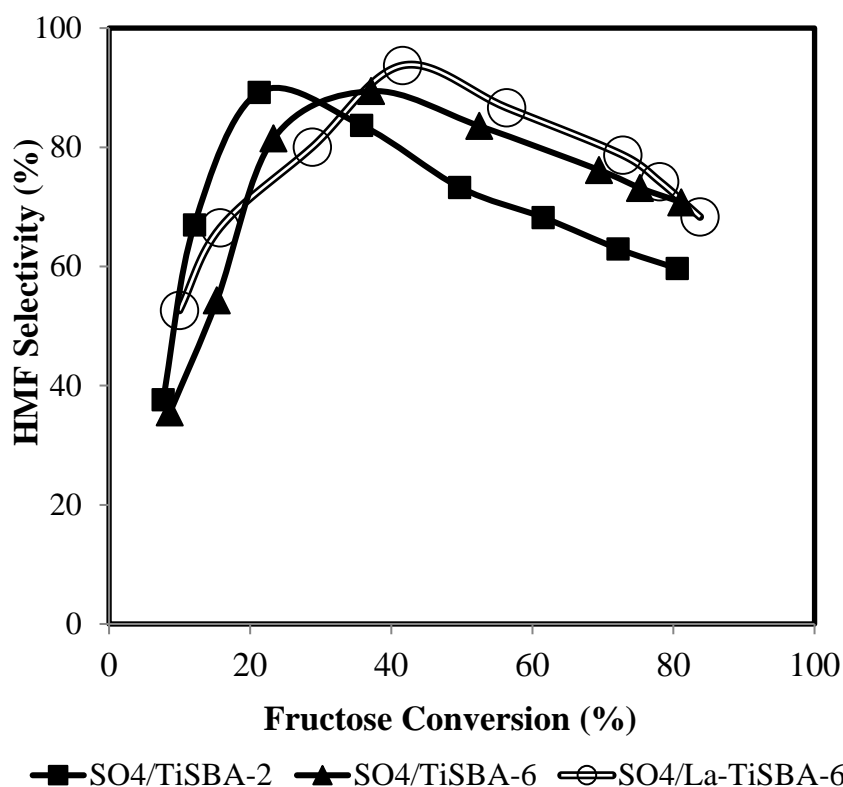


Figure 5.46. Selectivities to HMF over sulfated Ti-SBA catalysts at 110 °C in DMSO.

Sulfur contents of the sulfated Ti-SBA-15 catalysts were measured before and after the reaction to investigate the stability. They are given in Table 5.11. Slight leaching was observed without La addition. This leaching was 14 % in SO<sub>4</sub>/TiSBA-2 and 7 % in SO<sub>4</sub>/TiSBA-6. La containing catalyst exhibited high stability and sulfur amount remained constant after the reaction. This stability was due to the role of La to make strong bonds between Ti, Si and S.

Reusability tests results obtained in DMSO at 110 °C are given in Figure 5.47. Activity dropped to some extent; almost 9 % after 4 re-use, over SO<sub>4</sub>/TiSBA-2 and SO<sub>4</sub>/TiSBA-6. This was due to the leaching of sulfur from these catalysts. La containing catalyst was reused up to 4 times without losing its activity. This is in agreement with the leaching tests.

Table 5.11. Sulfur leaching from sulfated Ti-SBA-15 catalysts.

Catalyst Name	Sulfur Content Before Reaction (wt. %)	Sulfur Content after Reaction (wt. %)
SO <sub>4</sub> /TiSBA-2	1.19	1.02
SO <sub>4</sub> /TiSBA-6	3.26	3.04
SO <sub>4</sub> /La-TiSBA-6	6.13	6.15

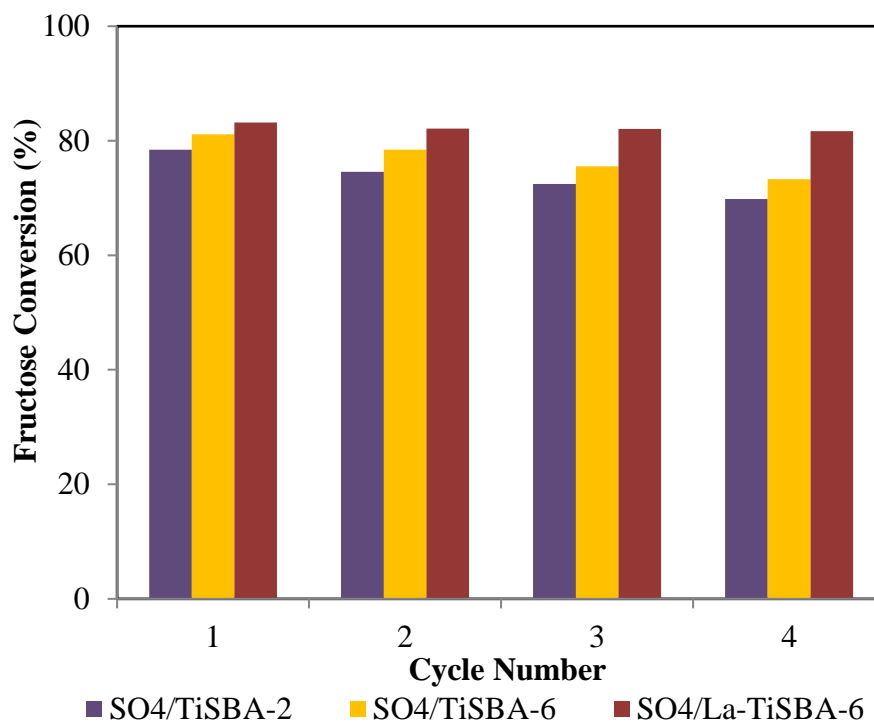


Figure 5.47. Reusability tests of sulfated Ti-SBA-15 catalysts.

Fructose dehydration tests in DMSO indicated that, the most active, stable and selective catalyst was SO<sub>4</sub>/La-TS-6. It provided 79 % selectivity at complete fructose conversion. For that reason, SO<sub>4</sub>/La-TS-6 was selected to be tested in water and in water-MIBK biphasic solvent.

## 5.6. Activities of SO<sub>4</sub>/La-TS-6 in Water and Water-MIBK

SO<sub>4</sub>/La-TS-6 determined in the previous part was tested in water, water-MIBK (biphasic) and water-butanol-MIBK (biphasic) at 110 °C. Product distributions obtained in these solvents are given in Figures 5.48 to 5.50. The main by-products were levulinic acid (LA), formic acid (FA) and glucose as obtained in DMSO. However, more FA and LA were formed in water compared to in DMSO (Figure 5.48). This was due to rehydration of HMF with water to LA and FA. Formic acid formation was reduced in the presence of MIBK (Figure 5.49). This was because of HMF transferred from reacting phase to the organic phase (MIBK) which prevented its rehydration. Addition of butanol to water-MIBK mixture increased the partition coefficient of HMF between water and MIBK (Liu et al., 2012); thus rehydration and FA and LA formation was

reduced slightly (Figure 5.50). Fructose consumption decreased in water-MIBK–butanol solvent, compared that in water-MIBK.

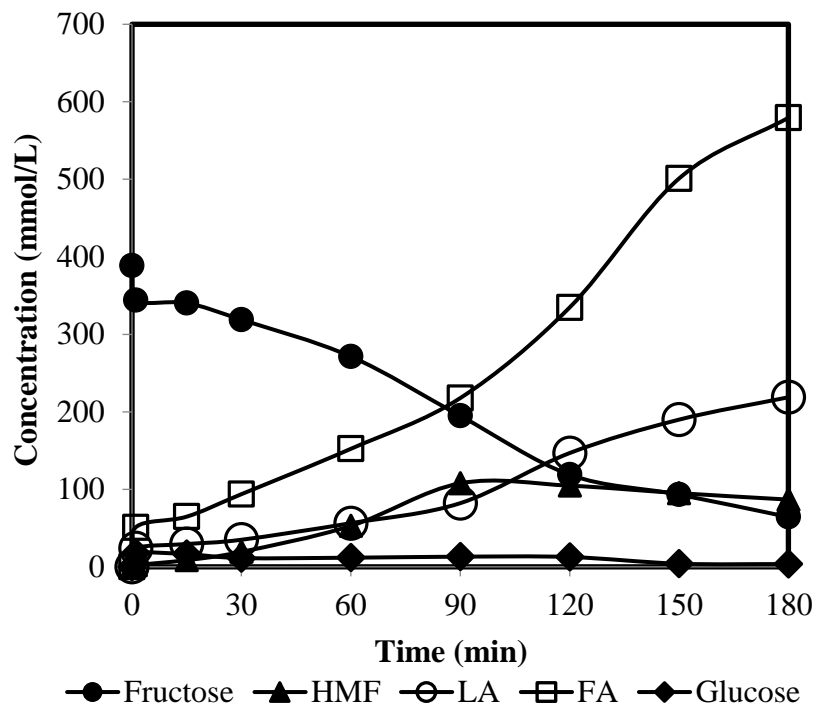


Figure 5.48. Product distribution over SO<sub>4</sub>/La-TS-6 at 110 °C in water.

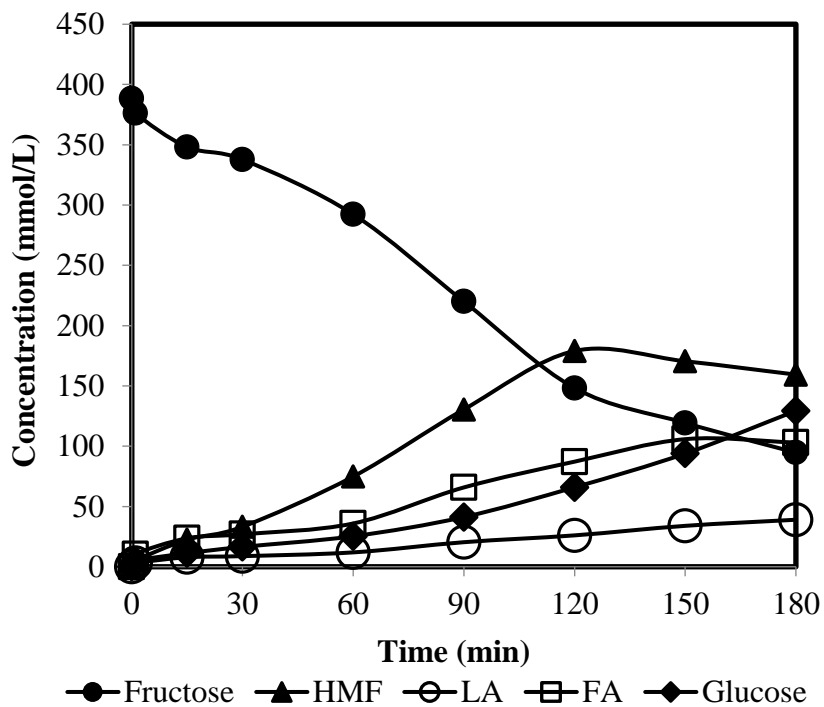


Figure 5.49. Product distribution over SO<sub>4</sub>/La-TS-6 at 110 °C in water-MIBK.

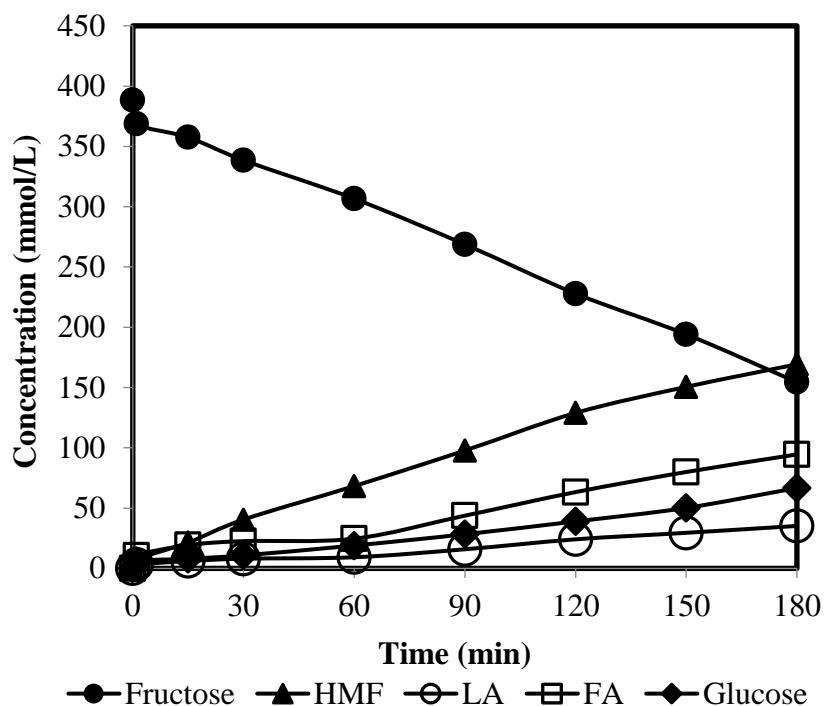


Figure 5.50. Product distribution over SO<sub>4</sub>/La-TS-6 at 110 °C in water-MIBK-butanol.

Fructose conversions obtained in DMSO, water, water-MIBK and water-MIBK-butanol are given in Figure 5.51. Fructose conversion increased with reaction time and changed with the solvent used. Complete conversion was obtained in DMSO. This could be partly due to DMSO activity toward fructose. The lower conversion observed in water could be due to blocking of the active acid sites (Ordonsky et al., 2012). Addition of the second phase (MIBK) to water reduced the conversion. Butanol addition decreased the conversion obtained further. This could be due to the adsorption of organic solvent on to the Lewis sites of the catalyst (Ordonsky et al., 2012).

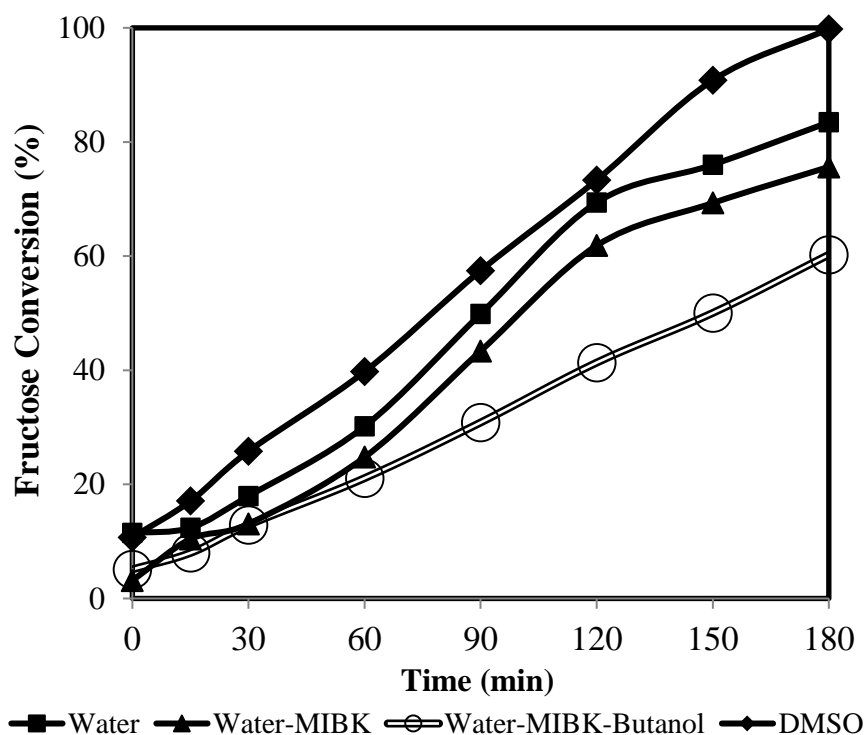


Figure 5.51. Fructose conversions in different solvents over SO<sub>4</sub>/La-TS-6 at 110 °C.

The selectivities to HMF over SO<sub>4</sub>/La-TS-6 in DMSO, water, water-MIBK and water-MIBK-butanol are given in Figure 5.52. HMF selectivity was the highest in DMSO which was 95 % at 58 % conversion. The next best selectivities were obtained in water-MIBK and water-MIBK-butanol, which were 77 % HMF selectivity at 43 % conversion in water-MIBK and 81 % HMF selectivity at 42 % conversion in water-MIBK-butanol. At higher conversions, the selectivity dropped significantly in aqueous solvents. Addition of MIBK into water as extracting phase enhanced the HMF selectivity by up to 20 %. This was due to transfer of HMF from water into MIBK which prevented its rehydration and also due to polar nature of MIBK (Lucas et al., 2013). MIBK molecules are reported to interact with Brønsted sites of the catalyst displace HMF from acid sites into reaction medium; thereby side reactions were prevented (Carniti et al., 2011). Butanol addition slightly improved the selectivity (6 %) at low conversions. However, at conversions higher than 50 %, its effect on selectivity was diminished. This was in agreement with literature (Leshkov et al., 2006). The lowest selectivity was observed in water. This was attributed to the formation of side products from the rehydration of HMF.

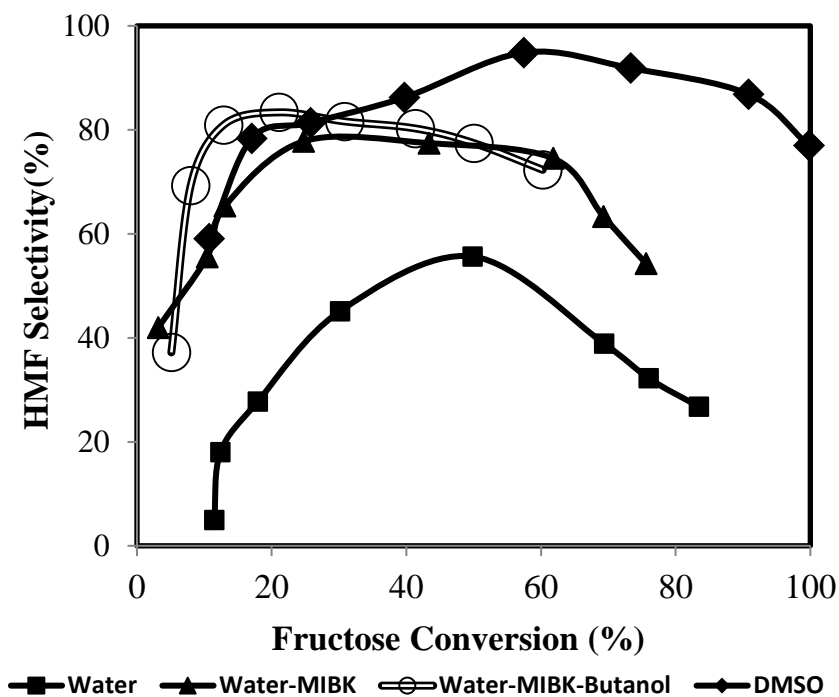


Figure 5.52. Selectivities to HMF in different solvents over La-SO<sub>4</sub>/TS-6 at 110 °C.

## 5.7. Fructose Dehydration Kinetics over SO<sub>4</sub>/La-TS-6 in Water-Butanol-MIBK

### 5.7.1. Effect of Reaction Temperature

The most active and selective catalyst (SO<sub>4</sub>/La-TS-6) was tested in water-MIBK-butanol being the most selective solvent studied at three different temperatures (110, 160 and 200 °C). Product distributions obtained at these temperatures are given in Figures 5.53 to 5.55. The main products were HMF, LA and FA. Increasing temperature from 110 to 160 °C, improved the HMF formed significantly (from 154 to 326 mmol/L at 180 min). On the other hand, increasing the temperature from 160 to 200 °C reduced the HMF significantly (from 326 to 197 mmol/L at 180 min). However, glucose concentration rapidly increased. The highest amount of HMF and the lowest amount of by-products were obtained at 160 °C.

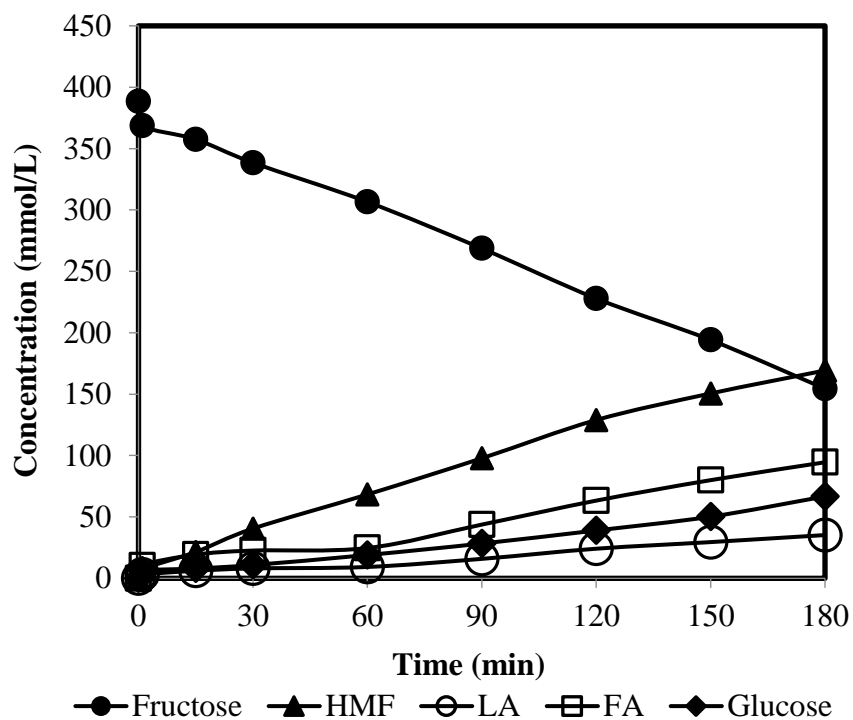


Figure 5.53. Product distribution at 110 °C over SO<sub>4</sub>/La-TS-6 in water-MIBK-butanol.

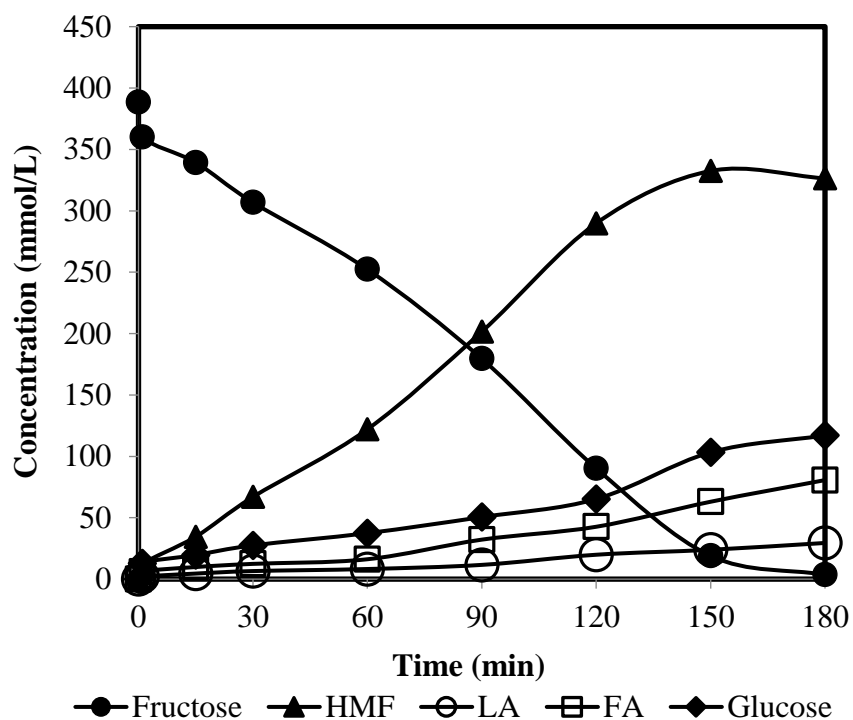


Figure 5.54. Product distribution at 160 °C over SO<sub>4</sub>/La-TS-6 in water-MIBK-butanol.

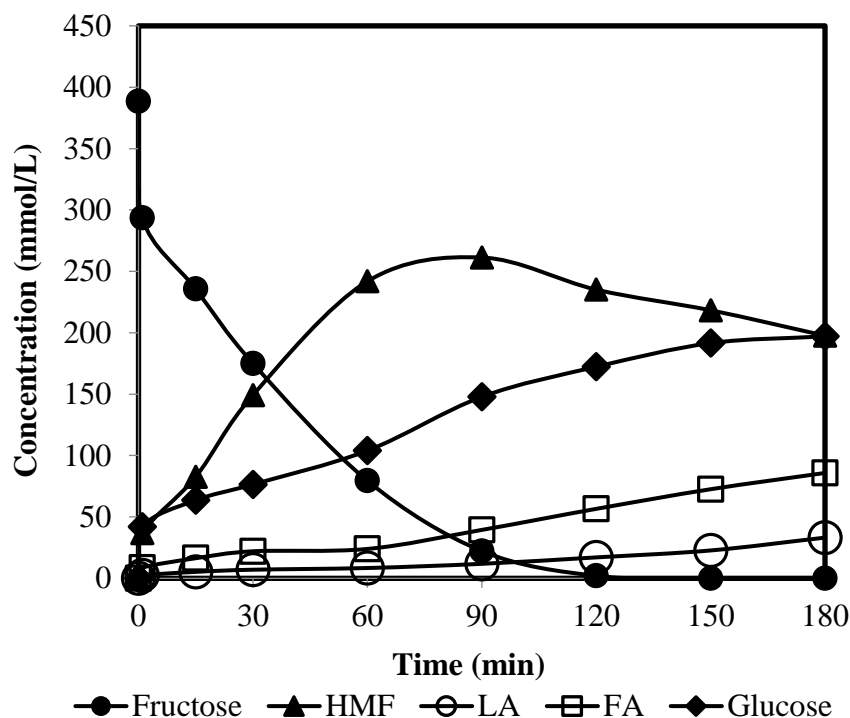


Figure 5.55. Product distribution at 200 °C over SO<sub>4</sub>/La-TS-6 in water-MIBK-butanol.

Fructose conversions over SO<sub>4</sub>/La-TS-6 in at three different reaction temperatures (110, 160 and 200 °C) are given in Figure 5.56. Fructose conversion increased with reaction temperature and complete conversion was observed at 160 and 200 °C. This was due to increase in the reaction rate constant with temperature. Rapid change with temperature showed that reaction was kinetically controlled. The influence of diffusion resistance was also determined by examining reactions at different temperatures. Initial reaction rates were determined as  $8.8 \times 10^{-5}$  mol/gcat.min at 110 °C,  $16.6 \times 10^{-5}$  mol/gcat.min at 160 °C and  $22.6 \times 10^{-5}$  mol/gcat.min at 200 °C. The initial rate doubled with temperature increase. This significant change with reaction temperature showed that the reaction was not mass transfer controlled under the conditions investigated.

Selectivities to HMF at three different reaction temperatures are given in Figure 5.57. Temperature affected the HMF selectivity significantly. Increase in reaction temperature from 110 to 160 °C enhanced the HMF selectivity. The highest selectivity to HMF (97 %) and 77 % conversion was achieved at 160 °C. Side product formation was minimized at that temperature. On the other hand, by rising the temperature to 200 °C reduced the selectivity by 19 % due to the rise in side product formation (especially glucose) as obtained in product distributions. HMF selectivity reduced almost 20 % at conversions higher than 80 %.

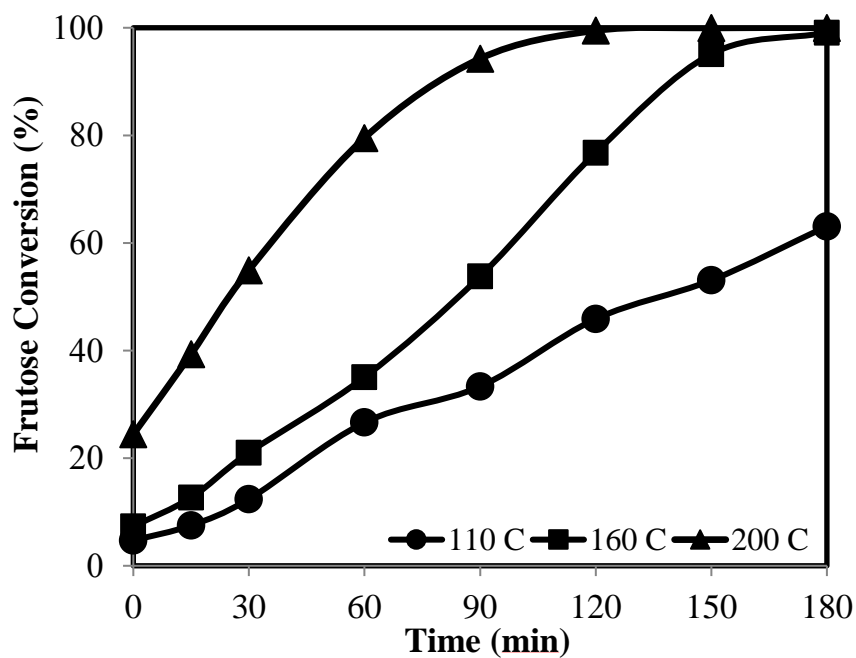


Figure 5.56. Fructose conversions at 110, 160 and 200 °C over SO<sub>4</sub>/La-TS-6 in water-butanol-MIBK.

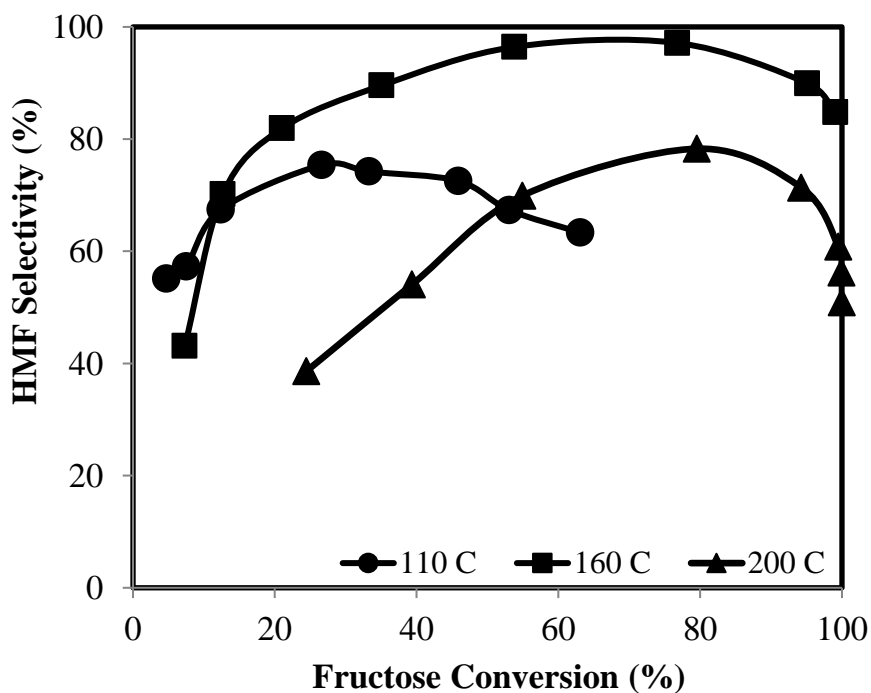


Figure 5.57. Selectivities to HMF at 110, 160 and 200 °C over SO<sub>4</sub>/La-TS-6 in water-butanol-MIBK.

Reusability tests results of the SO<sub>4</sub>/La-TS-6 in water-butanol-MIBK at 160 °C with fructose/catalyst ratio 1 are given in Figure 5.58. SO<sub>4</sub>/La-TS-6 exhibited high stability. Similar activities and selectivities were observed after 4<sup>th</sup> use. This may be due

to the strong sulfur-metal oxide interaction of these catalysts (Chelating bitentate bonds) which prevented the sulfur leaching during the reaction.

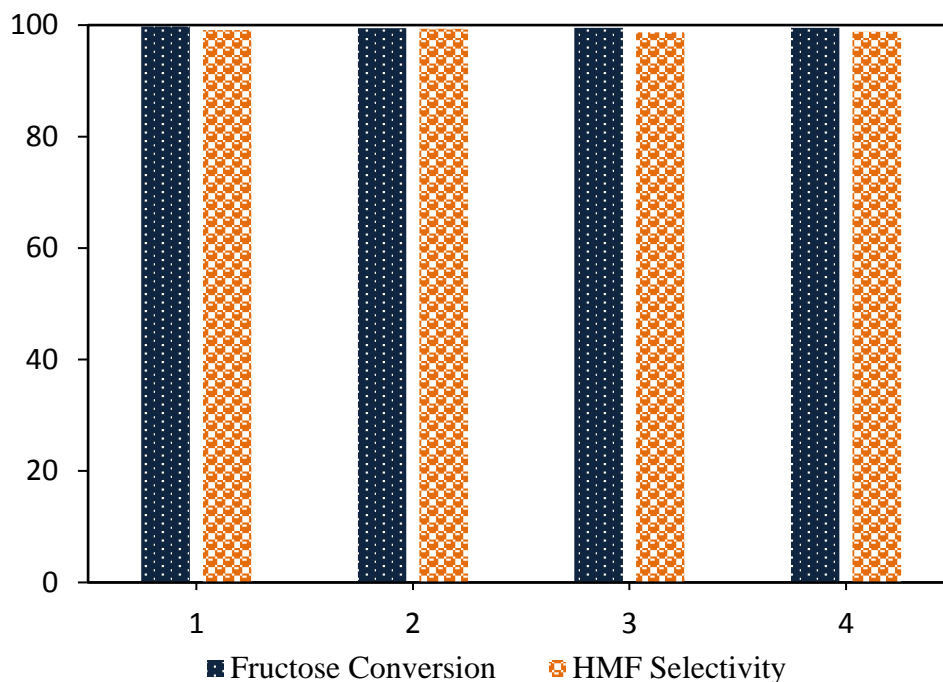


Figure 5.58. Reusability of the SO<sub>4</sub>/La-TS-6 in water-butanol-MIBK at 160 °C with fructose/catalyst ratio: 1.

### 5.7.2. Effect of Fructose/Catalyst Ratio

Product distributions obtained over SO<sub>4</sub>/La-TS-6 for fructose/catalyst weight ratios ( $W_{Fr}/W_{cat}$ ): 0.5, 1.0 and 2.0 at 160 °C are given in Figures 5.59, 5.60 and 5.61, respectively. The main products were fructose, HMF, LA, FA and glucose. As fructose was consumed, HMF concentration increased. Increasing HMF concentration increased the LA and FA concentration due to rehydration. Glucose formation was due to the isomerization of fructose molecules (Guo et al., 2012; Fan et al., 2011). At  $W_{Fr}/W_{cat}=2.0$  the highest amounts of LA were formed. More HMF was formed at  $W_{Fr}/W_{cat}=0.5$  and 1.

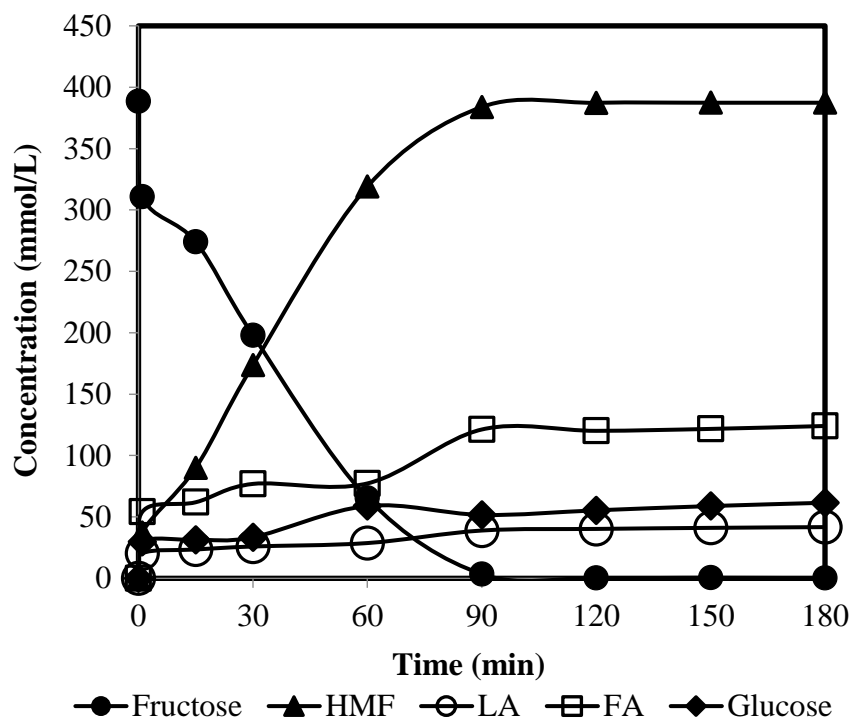


Figure 5.59. Product distribution of  $SO_4/La-TS-6$  in water-butanol-MIBK at  $160\text{ }^\circ C$  for  $W_{Fr}/W_{cat}:0.5$ .

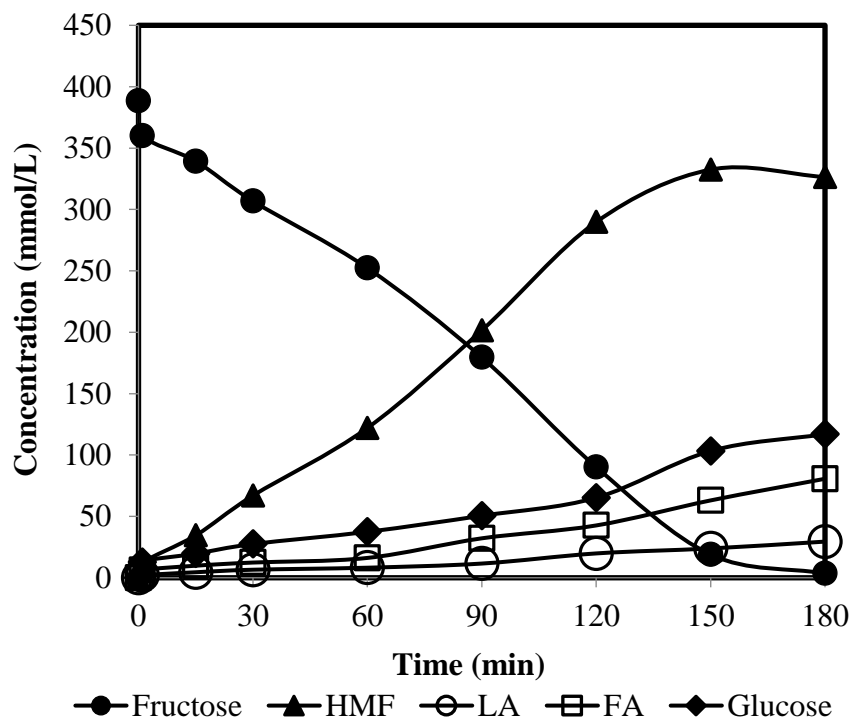


Figure 5.60. Product distribution of  $SO_4/La-TS-6$  in water-butanol-MIBK at  $160\text{ }^\circ C$  for  $W_{Fr}/W_{cat}: 1$ .

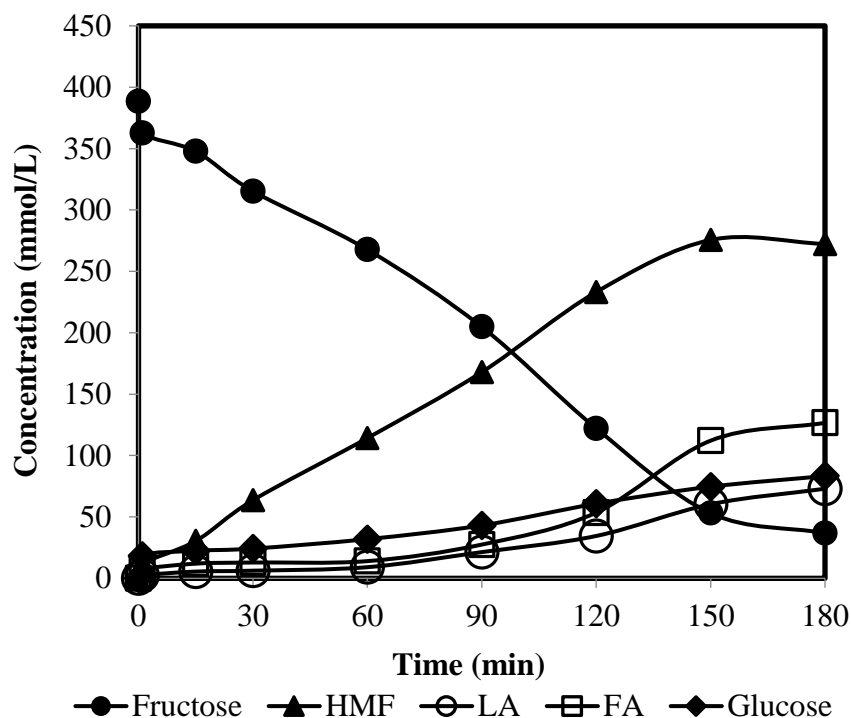


Figure 5.61. Product distribution of  $\text{SO}_4/\text{La-TS-6}$  in water-butanol-MIBK at  $160\text{ }^\circ\text{C}$  for  $W_{\text{Fr}}/W_{\text{cat}}$ : 2.

Fructose conversions over  $\text{SO}_4/\text{La-TS-6}$  in water-butanol-MIBK at  $160\text{ }^\circ\text{C}$  for three different  $W_{\text{Fr}}/W_{\text{cat}}$  ratios are given in Figure 5.62. Increasing  $W_{\text{Fr}}/W_{\text{cat}}$  from 1 to 2, slightly affected the catalytic activity. On the other hand, decreasing this ratio to 0.5, activity increased rapidly. This could be due to the occupation of acid sites by fructose molecules. When more amounts of acid sites were occupied by fructose molecules; fewer amounts of acid sites was accessible for fructose adsorption. Complete conversion was observed at  $W_{\text{Fr}}/W_{\text{cat}}$  0.5 and 1 after 180 min.

Selectivities to HMF over  $\text{SO}_4/\text{La-TS-6}$  for different  $W_{\text{Fr}}/W_{\text{cat}}$  are given in Figure 5.63. HMF selectivity of 99 % was achieved at complete conversion for  $W_{\text{Fr}}/W_{\text{cat}}=0.5$ . Increasing the  $W_{\text{Fr}}/W_{\text{cat}}$  from 0.5 to 2 reduced the selectivity to HMF from 98 to 82 % at high fructose conversions ( $\sim 90\%$ ). On the other hand, selectivity to HMF was higher for  $W_{\text{Fr}}/W_{\text{cat}}=1$  and 2 at lower fructose conversions.

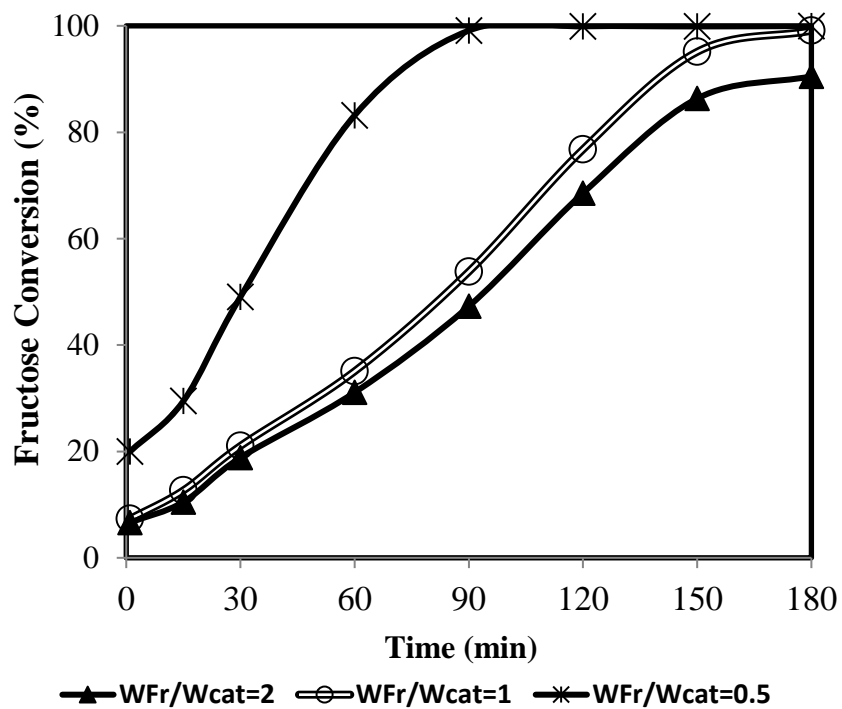


Figure 5.62. Fructose conversions for  $W_{Fr}/W_{cat}$ : 0.5, 1 and 2 over  $SO_4/La-TS-6$  in water-butanol-MIBK at 160 °C.

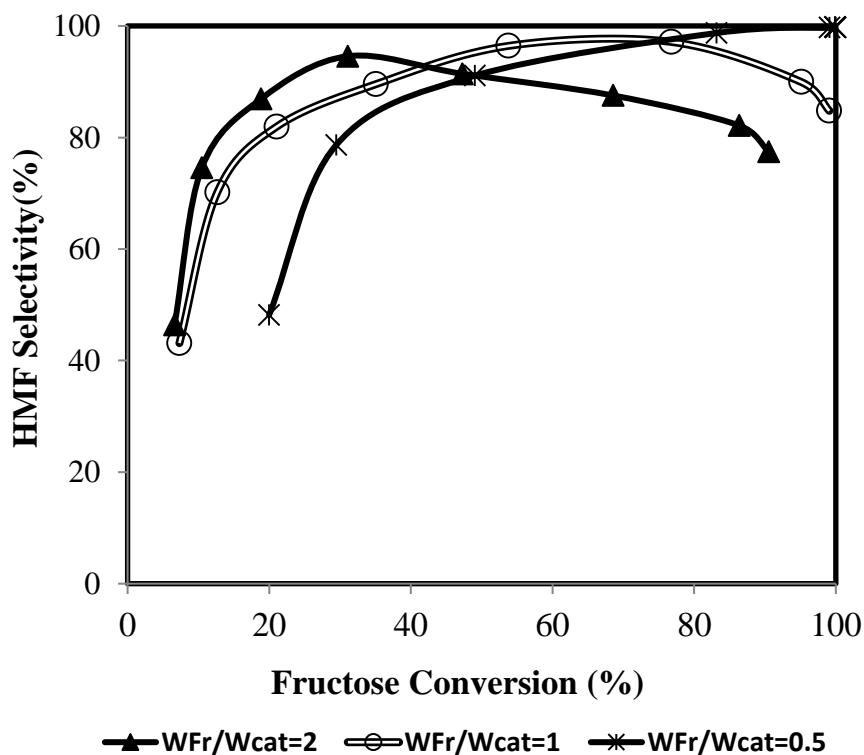


Figure 5.63. Selectivities to HMF for  $W_{Fr}/W_{cat}$ : 0.5, 1 and 2 over  $SO_4/La-TS-6$  in water-butanol-MIBK at 160 °C.

HMF yield over SO<sub>4</sub>/La-TS-6 for different W<sub>Fr</sub>/W<sub>cat</sub> ratios are given in Figure 5.64. As the W<sub>Fr</sub>/W<sub>cat</sub> increased, yield of HMF was reduced. The highest yield was observed as 100 % for W<sub>Fr</sub>/W<sub>cat</sub>= 0.5.

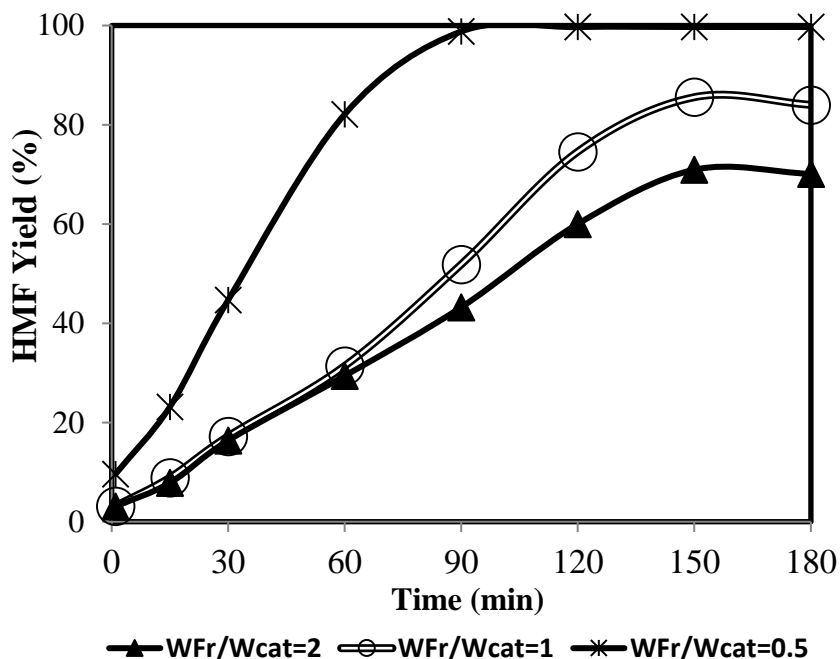


Figure 5.64. HMF yield over SO<sub>4</sub>/La-TS-6 in water-butanol-MIBK at 160 °C with fructose/catalyst for W<sub>Fr</sub>/W<sub>cat</sub>: 0.5, 1, 2.

In order to determine the order of the reaction, differential method of analysis was applied. Logarithmic plot of ln (dC<sub>A</sub>/dt) versus ln(C<sub>A</sub>) was plotted (Figure 5.65) at 160 and 200 °C. From the slopes of these lines reaction was found as first order. Reaction rate constants (k) for both 160 and 200 °C and activation energy were calculated and given in Table 5.12.

Table 5.12. Kinetic parameters of fructose dehydration.

T (°C)	k (L/gcat.min)
Rate constant (L/gcat.min)	0.006 (at 160 °C)
Activation Energy (kJ/mol)	52.069
Reaction Order	1

The rate equation of fructose dehydration over SO<sub>4</sub>/La-TS-6 in water-butanol-MIBK at 160 °C was obtained as:

$$r_{Fr} = 0.006 \cdot C_{Fr}$$

where r<sub>Fr</sub>: rate of fructose consumption in mmol/gcat.min.  
C<sub>Fr</sub>: Fructose concentration in mmol/L.

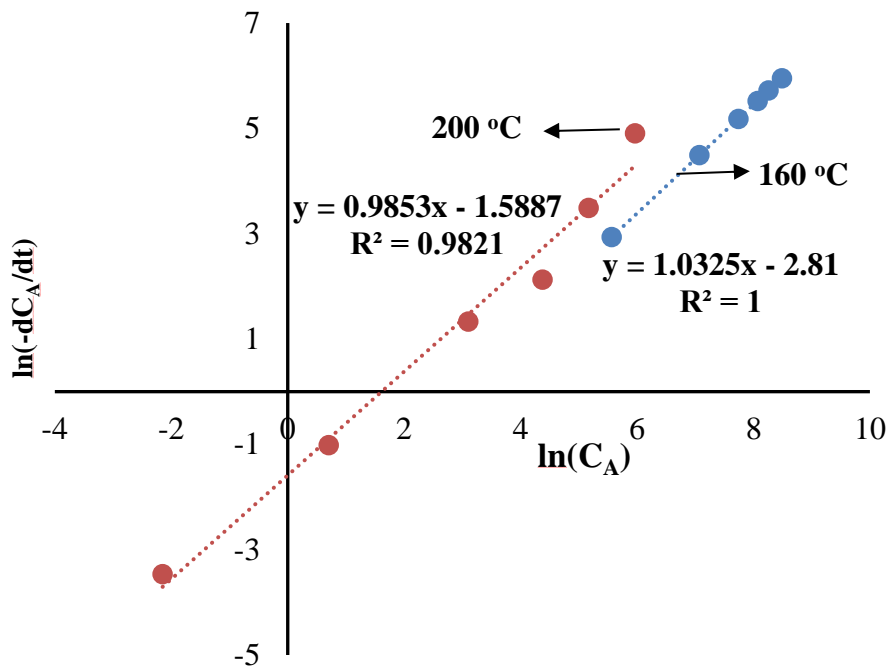


Figure 5.65. Logarithmic change of fructose concentrations with reaction time at 110 and 200 °C over  $\text{SO}_4/\text{La-TS-6}$  in water-butanol-MIBK at  $W_{\text{Fr}}/W_{\text{cat}}$ : 1.

## CHAPTER 6

### CONCLUSIONS

Homogeneous catalysts (HCl, H<sub>3</sub>PO<sub>4</sub> and H<sub>2</sub>SO<sub>4</sub>) were tested in DMSO for fructose dehydration for comparison with heterogeneous catalysts activities. All of them exhibited high activities and selectivities in DMSO. The highest selectivity (82 %) was obtained over H<sub>2</sub>SO<sub>4</sub>. This was attributed to its high acid strength.

Initially conclusions regarding the activities of the heterogeneous catalysts in DMSO will be given. Sulfated zirconia catalysts phases, monoclinic and tetragonal phases were affected by sulfur loading (2.5, 3.0 and 3.5 wt. %). The highest amount of tetragonal phases was observed with 3 % loading (SO<sub>4</sub>/ZrO<sub>2</sub>-3). SO<sub>4</sub>/ZrO<sub>2</sub>-3 also exhibited the highest amount of strong and Brønsted acid sites. Much amount of tetragonal phases, highest amount of strong acid sites and Brønsted sites promoted HMF formation, accordingly improved the selectivity. Thus, the highest HMF selectivity (81 %) at complete fructose conversion was obtained over SO<sub>4</sub>/ZrO<sub>2</sub>-3. Significant sulfur leaching as well as activity losses were obtained with SO<sub>4</sub>/ZrO<sub>2</sub>-2.5 and SO<sub>4</sub>/ZrO<sub>2</sub>-3.5. Slight sulfur leaching (3.2 %) and 6 % of activity loss after 4<sup>th</sup> reuse was observed over SO<sub>4</sub>/ZrO<sub>2</sub>-3.0.

Among the sulfated catalysts (SO<sub>4</sub>/SiO<sub>2</sub>, SO<sub>4</sub>/AC, SO<sub>4</sub>/TS-6 and SO<sub>4</sub>/Ti-SBA-15), the highest amount of strong and Brønsted acid sites were observed over SO<sub>4</sub>/TS-6 and SO<sub>4</sub>/Ti-SBA-15. This was attributed to the formation of strong chelating bidentate bonds in titania-silicates. They were the most selective catalysts. Over SO<sub>4</sub>/TS-6, 82 % HMF selectivity was observed at 77 % of fructose conversion and over SO<sub>4</sub>/Ti-SBA-6, 74 % HMF selectivity was observed at 75 % of fructose conversion. These HMF selectivities were comparable with the selectivity observed by homogeneous H<sub>2</sub>SO<sub>4</sub> catalyst (82 %). Significant amounts of sulfur leaching were observed over SO<sub>4</sub>/AC and SO<sub>4</sub>/SiO<sub>2</sub>. On the other hand, SO<sub>4</sub>/TS-6 and SO<sub>4</sub>/TiSBA-6 preserved their activities up to 4 times without leaching. This was also related to chelating bond formation.

Increase in Ti content in titania-silicates also increased the total number of the acid sites and Brønsted acidities. Accordingly, HMF selectivity was improved. This was attributed to the octahedral coordination sites of Ti in titania-silicates. These sites are

selective acidic sites and increased with the amount of Ti. The sulfur content of the catalysts increased with the Ti amount loaded which was attributed to more chelating bond formation between sulfur, titanium and silicon. Incorporation of La also enhanced the sulfur content of the catalyst (SO<sub>4</sub>/La-TS-6) which was considered to be due to prevention of sulfur decomposition by La during calcination. This catalyst was the most selective catalyst; 95 % HMF selectivity at 58 % fructose conversion. All sulfated titania-silicates (SO<sub>4</sub>/TS-2, SO<sub>4</sub>/TS-6, SO<sub>4</sub>/La-TS-6 and SO<sub>4</sub>/La-TiSBA-6) exhibited high stabilities without sulfur leaching up to 4 reuse cycles.

The most efficient catalyst (SO<sub>4</sub>/La-TS-6) in DMSO was tested in water, water-MIBK and water-MIBK-butanol and the following information were obtained. Reaction in water gave considerable amounts of rehydration products (LA and FA). Thus, the lowest selectivity (58 % selectivity at 50 % conversion) was obtained in water due to rehydration of HMF. Addition of MIBK to water improved the selectivity by 20 % by lowering the LA and FA formations. This was due to transfer of HMF from water into MIBK. Butanol addition slightly affected the selectivity (by 5 %). It increased the HMF transfer rate to MIBK.

Reusability of SO<sub>4</sub>/La-TS-6 in water-butanol-MIBK at 160 °C exhibited high stability. Similar activities and selectivities were observed after 4<sup>th</sup> use. This may be due to the strong sulfur-metal oxide interaction of these catalysts (chelating bidentate bonds) which prevented the sulfur leaching during the reaction.

Selectivity to HMF was affected significantly by the reaction temperature in water-MIBK-butanol. Increase in reaction temperature from 110 to 160 °C enhanced the HMF selectivity. However, it dropped significantly at 200 °C. The highest selectivity to HMF (97 %) was achieved at 160 °C at 77 % conversion. Side product formation was minimized at this temperature. Catalyst loading also affected the activity and selectivity. Increasing W<sub>Fr</sub>/W<sub>cat</sub> from 0.5 to 2.0, reduced the selectivity to HMF. HMF selectivity of 99 % was achieved at complete conversion for W<sub>Fr</sub>/W<sub>cat</sub>=0.5.

## REFERENCES

- Amarasekara, A. S.; Williams, L. D.; Ebede, C. C. Mechanism of the dehydration of D-fructose to 5- hydroxymethylfurfural in dimethyl sulfoxide at 150 °C. An NMR Study. *Carbohydr. Res.* **2008**, 343, 3021-3024.
- Asghari, F. S.; Yoshida, H. Dehydration of fructose to 5- hydroxymethylfurfural in sub-critical water over heterogeneous zirconium phosphate catalysts. *Carbohydr. Res.* **2006**, 341, 2379-2387.
- Benvenuti, F.; Carlini, C.; Patrono, P.; Galletti, A.M.R.; Sbrana, G.; Massucci, M.A.; Galli, P.; Heterogeneous zirconium and titanium catalysts for the selective synthesis of 5-hydroxymethyl-2-furaldehyde from carbohydrates. *Appl. Catal., A.* **2000**, 193, 147-153.
- Bicker, M.; Hirth, J.; Vogel, H. Dehydration of fructose to hydroxymethylfurfural in sub- and supercritical fluids. *Green Chem.* **2005**, 36, 118-126.
- Brahmkatri, V.; Patel, A.; 12-Tungstophosphoric acid anchored to SBA-15: An efficient, environmentally benign reusable catalysts for biodiesel production by esterification of free fatty acids. *Appl. Catal., A.* **2011**, 403, 161-172.
- Cao, Q.; Guo, X.; Guan, J.; Mu, X.; Zhang, D.; A process for efficient conversion of fructose into 5-hydroxymethylfurfural in ammonium salts. *Appl. Catal., A.* **2011**, 403, 98-103.
- Caratzoulas, S.; Vlachos, D.G. Converting Fructose to 5-Hydroxymethylfurfural: A Quantum Mechanics/Molecular Mechanics Study of the Mechanism and Energetics. *Carbohydrate Research* **2011**, 346, 664–672.
- Carlini, C.; Patrono, P.; Galletti, A. M. R.; Sbrana, G. Heterogeneous catalysts based on vanadyl phosphate for fructose dehydration to 5-hydroxymethyl-2-furaldehyde. *Appl. Catal., A.* **2004**, 275, 111-118.
- Carniti, P.; Gervasini, A.; Marzo, M. Absence of Expected Side-Reactions in the Dehydration Reaction of Fructose to HMF in Water Over Niobic Acid Catalyst. *Catal. Commun.* **2011**, 12, 1122–1126.
- Chareonlimkun, A.; Champreda, V.; Shotipruk, A.; Laosiripojana, N.; Reactions of C5 and C6-sugars, cellulose, and lignocellulose under hot compressed water (HCW) in the presence of heterogeneous acid catalysts. *Fuel.* **2010**, 89, 2873-2880.
- Chedda, J.N.; Leshkov, R.; Dumesic, J.A.; Production of 5-hydroxymethylfurfural and furfural by dehydration of biomass-derived mono- and poly-saccharides. *Green Chem.*, **2007**, 9, 342–350.

- Chen, C.L.; Cheng, S.; Lin, H.P.; Wong, S.T.; Mou, C.Y.; Sulfated zirconia catalyst supported on MCM-41 mesoporous molecular sieve. *Appl. Catal., A*. **2001**, 215, 21-30.
- Dutta, S.; De, S.; Patra, A.K.; Sasidharan, M.; Bhaumik, A.; Saha, B.; Microwave assisted rapid conversion of carbohydrates into 5-hydroxymethylfurfural catalyzed by mesoporous TiO<sub>2</sub> nanoparticles. *Appl. Catal., A*. **2011**, 409-410, 133-139.
- Fan, C.; Guan, H.; Zhang, H.; Wang, J.; Wang, S.; Wang, X. Conversion of Fructose and Glucose into 5-Hydroxymethylfurfural Catalyzed by a Solid Heteropolyacid Salt. *Biomass and Bioenergy* **2011**, 35, 2659-2665.
- Farcasiu, D.; Li, Q.; Cameron, S. Preparation of sulfated zirconia catalysts with improved control of sulfur content II. Effect of sulfur content on physical properties and catalytic activity. *Appl. Catal., A*. **1997**, 154, 173-184.
- Guo, F.; Fang, Z.; Zhou, T. Conversion of Fructose and Glucose into 5-hydroxymethylfurfural with Lignin-derived Carbonaceous Catalyst under Microwave Irradiation in Dimethyl Sulfoxide-ionic Liquid Mixtures. *Bioresour. Technol.* **2012**, 112, 313-318.
- Huang, R.; Qi, W.; Su, R.; He, Z. Integrating enzymatic and acid catalysis to convert glucose into 5-hydroxymethylfurfural. *Chem. Commun.* **2010**, 46, 1115-1117.
- Jin, H.; Wu, Q.; Zhang, P.; Pang, Q. Assembling of tungstovanadogermanic heteropoly acid into mesoporous molecular sieve SBA-15. *Solid State Sciences*. **2005**, 7, 333-337.
- Juan, J. C.; Zhang, J.; Jiang, Y.; Cao, W.; Yarmob, M. A. Zirconium Sulfate Supported on Activated Carbon as Catalyst for Esterification of Oleic Acid by n-Butanol under solvent free conditions. *Cat. Lett.* **2007** 117, 153-158.
- Khayoon, M. S.; Hamedd, B. Acetylation of glycerol to biofuel additives over sulfated activated carbon catalyst. *Bioresour. Technol.* 2011, 102, 9229-9235.
- Leshkov, Y. R.; Chedda, J.N.; Dumesic, J. A. Phase Modifiers Promote Efficient Production of Hydroxymethylfurfural from Fructose. *Science*. **2006**, 312, 1933-1937.
- Li, L.; Liu S.; Xu J.; Yu S.; Liu F.; Xie C.; Ge X.; Ren J. Esterification of itaconic acid using Ln-SO<sub>4</sub><sup>2-</sup>/TiO<sub>2</sub>-SiO<sub>2</sub> (Ln = La<sup>3+</sup>, Ce<sup>4+</sup>, Sm<sup>3+</sup>) as catalysts, *J. Mol. Cat. A: Chem.* **2013**, 368, 24- 30.
- Lourvanij, K.; Rorrer, G.L. Reactions of Aqueous Glucose Solutions over Solid-Acid Y-Zeolite Catalyst at 110-160 °C. *Ind. Eng. Chem. Res.* **1993**, 32, 11-19.

- Lucas, N.; Kokate, G.; Nagpure, A.; Chilukuri, S.; Dehydration of fructose to 5-hydroxymethyl furfural over ordered AlSBA-15 catalysts. *Microporous and Mesoporous Mater.* **2013**, 181, 38-46.
- Moreau, C; Finiels, A; Vanoye, L. Dehydration of fructose and sucrose into 5-hydroxymethylfurfural in the presence of 1-H-3-methyl imidazolium chloride acting both as solvent and catalyst. *J. Mol. Catal. A: Chem.* **2006**, 253, 165–169.
- Ninomiya, W.; Sadakane, M.; Matsuoka, S.; Nakamura, H.; Naitou, Hiroyuki U.; Ueda, W. An efficient synthesis of  $\alpha$ -acyloxyacrylate esters as candidate monomers for bio-based polymers by heteropolyacid-catalyzed acylation of pyruvate esters. *Green Chem.* **2009**, 11, 1666–1674.
- Ordonsky, V.V.; van der Schaaf, J.; Schouten, J.C.; Nijhuis T.A. The Effect of Solvent Addition on Fructose Dehydration to 5-Hydroxymethylfurfural in Biphasic System over Zeolites. *J. Catal.* **2012**, 287, 68–75.
- Perego, C.; Bosetti, A.; Biomass to fuels: The role of zeolite and mesoporous materials. *Microporous and Mesoporous Mater.* **2011**, 144, 28-39.
- Qi, X.; Watanabe, M.; Aida, T. M.; Smith, R., Jr. Sulfated zirconia as a solid acid catalyst for the dehydration of fructose to 5-hydroxymethylfurfural. *Catal. Commun.* **2009**, 10, 1771–1775.
- Rosatella, A. A.; Simeonov, S. P.; Frade, R. F. M.; Afonso, C. A. M. 5-Hydroxymethylfurfural (HMF) as a building block platform: Biological properties, synthesis, and synthetic applications. *Green Chem.* **2011**, 13, 754.
- Shao G. N.; Sheikh R.; Hilonga A.; Lee J. E.; Park Y. H.; Kim H. T.; Biodiesel production by sulfated mesoporous titania–silica catalysts synthesized by the sol–gel process from less expensive precursors *Chem. Eng. Jour.* **2013**, 215-216, 600–607.
- Sharma R. V.; Soni K. K.; Dalai A. K.; Preparation, characterization and application of sulfated Ti-SBA-15 catalyst for oxidation of benzyl alcohol to benzaldehyde, *Cat. Com.* **2012**, 29, 87–91.
- Shimizu, K.; Uozumi, R.; Satsuma, A. Enhanced production of hydroxymethylfurfural from fructose with solid acid catalysts by simple water removal methods. *Catal. Commun.* **2009**, 10, 1849-1853.
- Sun, Y.; Zhu, L.; Lu, H.; Wang, R.; Lin, S.; Jiang, D.; Xiao, F.S.; Sulfated zirconia supported in mesoporous materials. *Appl. Catal., A.* **2002**, 237, 21-31.

- Takagaki, A.; Ohara, M.; Nishimura, S.; Ebitani, K. A one-pot reaction for biorefinery: combination of solid acid and base catalysts for direct production of 5-hydroxymethylfurfural from saccharides. *Chem. Commun.* **2009**, 2009, 6276-6278.
- Tong, X.; Ma, Y.; Li, Y. Biomass into chemicals: Conversion of Sugars to Furan Derivatives by Catalytic Processes. *Appl. Catal., A.* **2010**, 385, 1–13.
- Wang, J.; Xu, W.; Ren, J.; Liu, X.; Lu, G.; Wang, Y. Efficient Catalytic Conversion of Fructose into Hydroxymethylfurfural by a Novel Carbon-Based Solid Acid. *Green Chem.* **2011**, 13, 2678-2681.
- Weingarten R; Tompsett G.A.; Conner W.C.; Huber G.W.; Design of solid acid catalysts for aqueous-phase dehydration of carbohydrates: The role of Lewis and Brønsted acid sites, *J.Catal.*, **2011**, 279, 174-182.
- Yadav G. D.; Murkute A. D.; Preparation of a novel catalyst UDCaT-5: enhancement in activity of acid-treated zirconia-effect of treatment with chlorosulfonic acid vis-à-vis sulfuric acid, *J. Catal.* **2004**, 224, 218–223.
- Yang, F.; Liu, Q.; Bai, X.; Du Y., Conversion of Biomass into 5-hydroxymethylfurfural Using Solid Acid Catalyst. *Bioresour. Technol.* **2011**, 102, 3424–3429.
- Yang, H.; Lu, R.; Zhao, J.; Yang, X.; Shen, L.; Wang, Z. Sulfated binary oxide solid superacids. *Mater. Chem. Phys.* **2003**, 80, 68-72.
- Zhang, J.; Ma Z.; Jiao J.; Yin H.; Yan W.; Hagaman E. W.; Yu B. J.; Dai S.; Surface functionalization of mesoporous silica SBA-15 by liquid-phase grafting of zirconium phosphate. *App. Cat. A: Gen.* **2010**, 379, 141–147.
- Zhu, H.; Cao, Q.; Li, C.; Mu, X.; Acidic resin-catalysed conversion of fructose into furan derivatives in low boiling point solvents. *Carbohydr. Res.* **2011**, 1346, 2016-2018.

# CURRICULUM VITAE

---

## EMRE KILIÇ

Izmir Institute of Technology  
Chemical Engineering Department,  
35430, URLA, İZMİR, TURKEY  
**Phone:** 00 90 232 750 66 80  
**Mobile Phone:** 00 90 555 678 95 98  
**E-mail:** [ekilic21@gmail.com](mailto:ekilic21@gmail.com)  
[emrekilic@iyte.edu.tr](mailto:emrekilic@iyte.edu.tr)



### EDUCATION

---

Philosophy of Doctorate, 2016  
Izmir Institute of Technology  
Chemical Engineering Department  
Specialization: Reaction and Catalysis Engineering

Research, 2013-2014  
Technical University of Eindhoven  
Chemical Engineering and Chemistry Department  
Specialization: Reaction and Catalysis Engineering

Master of Science, 2010  
Izmir Institute of Technology  
Chemical Engineering Department  
Specialization: Reaction and Catalysis Engineering

Bachelor of Science, 2007  
Izmir Institute of Technology  
Major: Chemical Engineering

### TEACHING EXPERIENCE

---

- ✓ Chemical Reaction Engineering
- ✓ Solution Thermodynamics
- ✓ Heat and Mass Transfer
- ✓ Separation Process
- ✓ Engineering Economics and Design
- ✓ Introduction to Chemical Engineering
- ✓ Material and Energy Balances in Chemical Engineering

### PUBLICATIONS (ARTICLES)

---

Kilic E., Yilmaz S. "Effect of Reaction Conditions in Fructose Conversion to 5-Hydroxymethylfurfural over Sulfated Catalysts" App. Catal:Gen. To be Prepared in 2016

Kilic E., Yilmaz S. "Fructose Dehydration over Sulfated Titania Silicates Catalysts in Different Solvent Systems" App. Catal:Gen. To be Prepared in 2016

Kilic E., Yilmaz S. "Fructose Dehydration to 5-Hydroxymethylfurfural over Sulfated  $\text{TiO}_2\text{-SiO}_2$ , Ti-SBA-15,  $\text{ZrO}_2$ ,  $\text{SiO}_2$ , and Activated Carbon Catalysts" Ind. Eng. Chem. Res. (2015) 54 5220–5225.

Kilic E., Yilmaz S. "Effect of different acidity modifications on the activity and selectivity on H-ZSM5 zeolites in n-butene isomerization" Reac. Kinet. Mech. Cat. (2014) 112:283–294.

Kilic E., Yilmaz S. "HZSM-5 and Ferrierite Acidity Modification by Silylation and Their Activities in n-Butene Isomerisation" Int. J. Chem. Reactor Eng. (2010) Volume 8, Issue 1.

### RESEARCH EXPERIENCE

---

- ✓ Skeletal isomerization of n-butene (Ms Thesis)
- ✓ Dehydration of fructose over different catalysts and different solvent systems (PhD Thesis)
- ✓ Biomass conversion
- ✓ Catalytic conversion of glucose to valuable chemicals
- ✓ Zeolite synthesis
- ✓ Modification of zeolites (silylation, dealumination, alkylation)
- ✓ Acid modifications of catalysts
- ✓ Sol-gel synthesis of metallic catalysts
- ✓ Synthesis of mesoporous silica
- ✓ Esterification of Glycerol with oleic acid to mono-, di-, triglycerides
- ✓ Gas Chromatography
- ✓ High Performance Liquid Chromatography
- ✓ Pyridine-FT-IR
- ✓ Temperature Program Desorption of Ammonia